The evolution and merger of (binary) black holes

Enrico Barausse

Institut d'astrophysique de Paris/CNRS, France

H2020-MSCA-RISE-2015 StronGrHEP-690904

The first direct observation of GWs and … BHs!

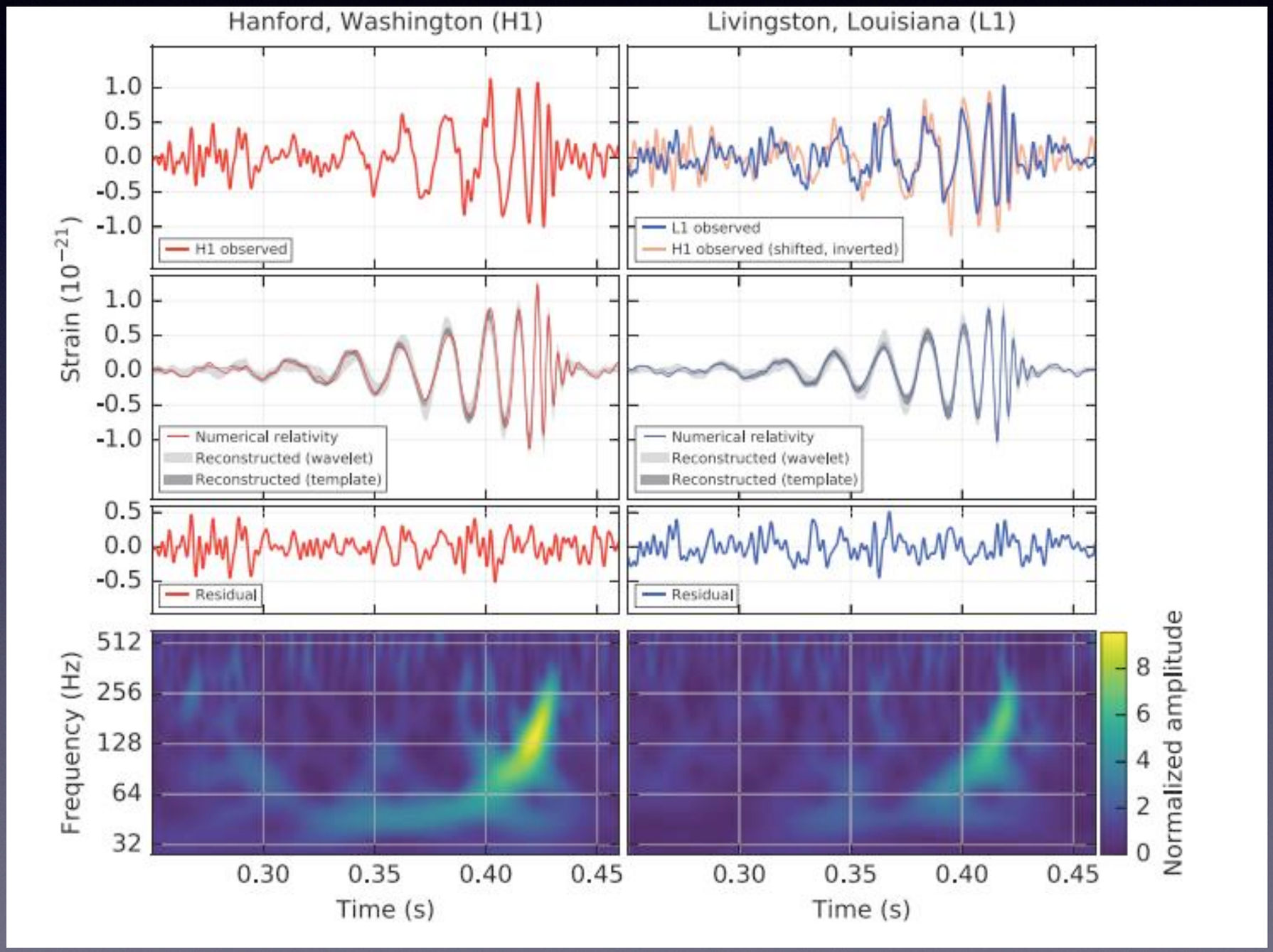

LSC collaboration 2015

GWs from binary BHs

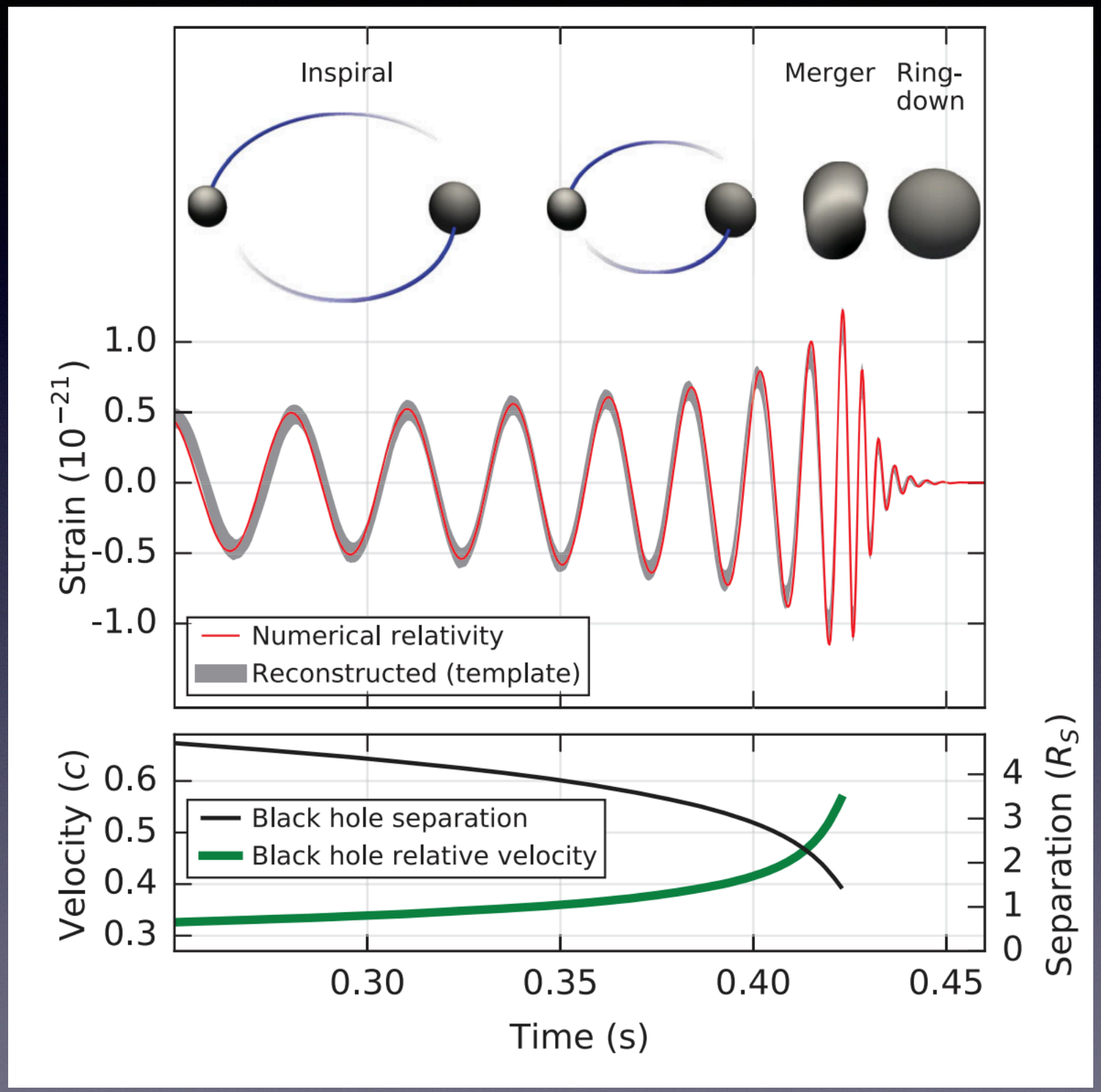

LSC collaboration 2015

Lectures outline

- The GW signal from two BHs (inspiral+ merger/ ringdown)
- The LIGO/Virgo detections (data analysis, physics, astrophysics)
- Supermassive BH binaries (LISA and pulsar timing arrays)

General relativity in a nutshell

$$G_{\mu\nu} \equiv R_{\mu\nu} - \frac{1}{2} g_{\mu\nu} R = 8\pi T_{\mu\nu}$$

$$\nabla^2 \phi = 4\pi G \rho.$$

$$T^{\mu\nu} = (\epsilon + p) u^\mu u^\nu + p g^{\mu\nu}$$

(perfect fluid)

$$\nabla_\nu G^{\mu\nu} = 0$$

$$\nabla_\nu T^{\mu\nu} = 0$$

$$a^\mu = -\frac{(g^{\mu\nu} + u^\mu u^\nu)\partial_\mu p}{p + \epsilon}$$

$$u^\mu \partial_\mu \epsilon = -(p + \epsilon) \nabla_\mu u^\mu$$

For dust (p=0) Euler equation gives geodesic equation

$$a^\mu \equiv \frac{du^\mu}{d\tau} + \Gamma^\mu_{\alpha\beta} u^\alpha u^\beta = 0$$

BHs in GR (or BHs have no hair)

$$G^{\mu\nu} = 0$$

$$ds^2 = -\left(1 - \frac{2M}{r}\right) dt^2 + \left(1 - \frac{2M}{r}\right)^{-1} dr^2 + r^2 d\Omega^2$$

$$d\Omega^2 = d\theta^2 + \sin^2\theta d\varphi^2$$

Schwarzschild BH (parametrized by mass alone)

$$\begin{aligned} ds^2 &= -\frac{\left(\Delta - a^2\sin^2\theta\right)}{\Sigma} dt^2 - 2a\sin^2\theta \frac{\left(r^2 + a^2 - \Delta\right)}{\Sigma} dt\, d\phi \\ &+ \left(\frac{\left(r^2 + a^2\right)^2 - \Delta a^2 \sin^2\theta}{\Sigma}\right) \sin^2\theta d\phi^2 + \frac{\Sigma}{\Delta} dr^2 + \Sigma d\theta^2 \end{aligned}$$

$$\begin{aligned} \Sigma &= r^2 + a^2\cos^2\theta \\ \Delta &= r^2 - 2Mr + a^2 \end{aligned}$$

$$a = \frac{J}{M}$$

Kerr BH (parametrized by mass and spin)

Electrically charged BHs (Reissner-Nordström, Kerr-Newman) probably irrelevant astrophysical

Geodesics in Schwarzschild

Metric is static and spherically symmetric

Conserved energy and orbital angular momentum (per unit particle mass) E and L

$$\theta = \frac{\pi}{2}$$

$$\epsilon = -g_{\mu\nu}\frac{dx^\mu}{d\lambda}\frac{dx^\nu}{d\lambda}$$

$$\left(1 - \frac{2GM}{r}\right)\frac{dt}{d\lambda} = E\ ,$$

$$r^2\frac{d\phi}{d\lambda} = L\ .$$

$$\frac{1}{2}\left(\frac{dr}{d\lambda}\right)^2 + V(r) = \frac{1}{2}E^2\ ,$$

$$V(r) = \frac{1}{2}\epsilon - \epsilon\frac{GM}{r} + \frac{L^2}{2r^2} - \frac{GML^2}{r^3}$$

Motion in 1D potential (Newtonian + corrections!)

Geodesics in Schwarzschild

Massive particles

$$\frac{1}{2}\left(\frac{dr}{d\lambda}\right)^2 + V(r) = \frac{1}{2}E^2 \ ,$$

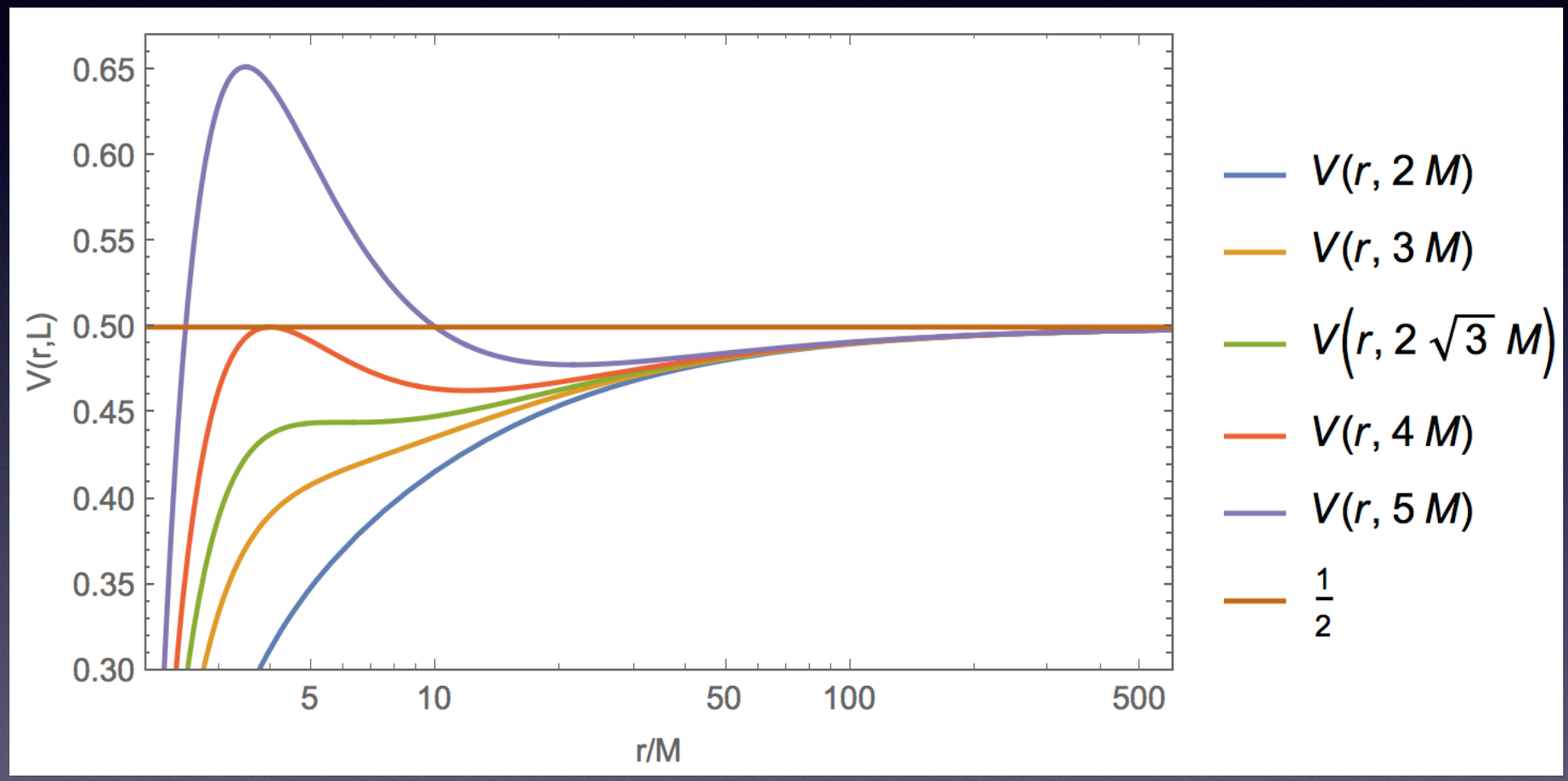

- Innermost stable circular orbit (ISCO) at r=6M
- Marginally bound orbit at r=4M
- Different than in Newtonian gravity

(circular orbits all the way down to r=0)

Geodesics in Schwarzschild

Dynamics of massless particles only depends on b=L/E

$$\frac{1}{E^2}\left(\frac{dr}{d\lambda}\right)^2 = -V = 1 - \frac{b^2}{r^2}\left(1 - \frac{2GM}{r}\right)$$

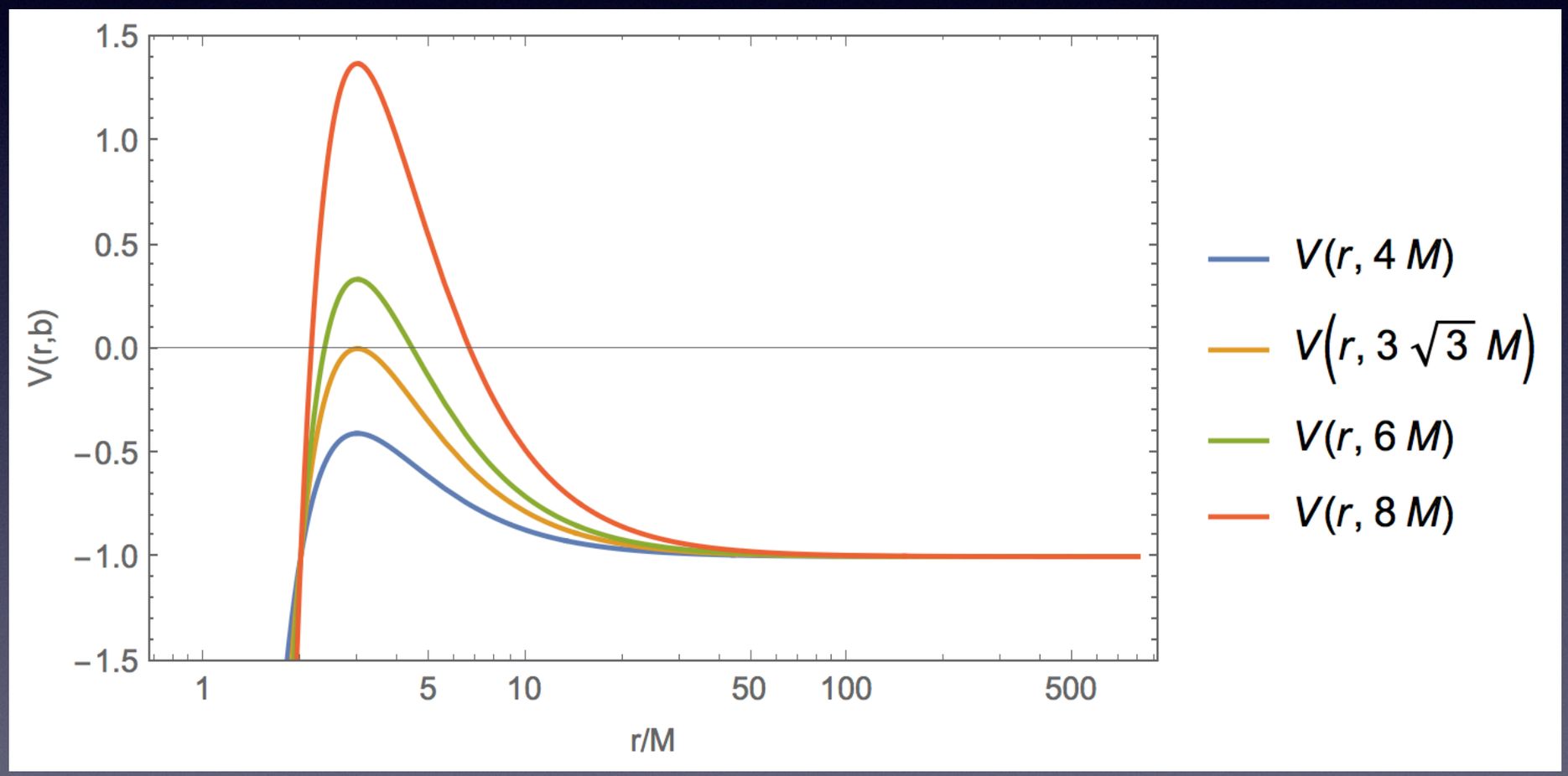

(Unstable) circular photon orbit (“light ring”) at r=3M

Peak of “potential barrier” at r=3M

Geodesics in Schwarzschild

Dynamics of massless particles only depends on b=L/E

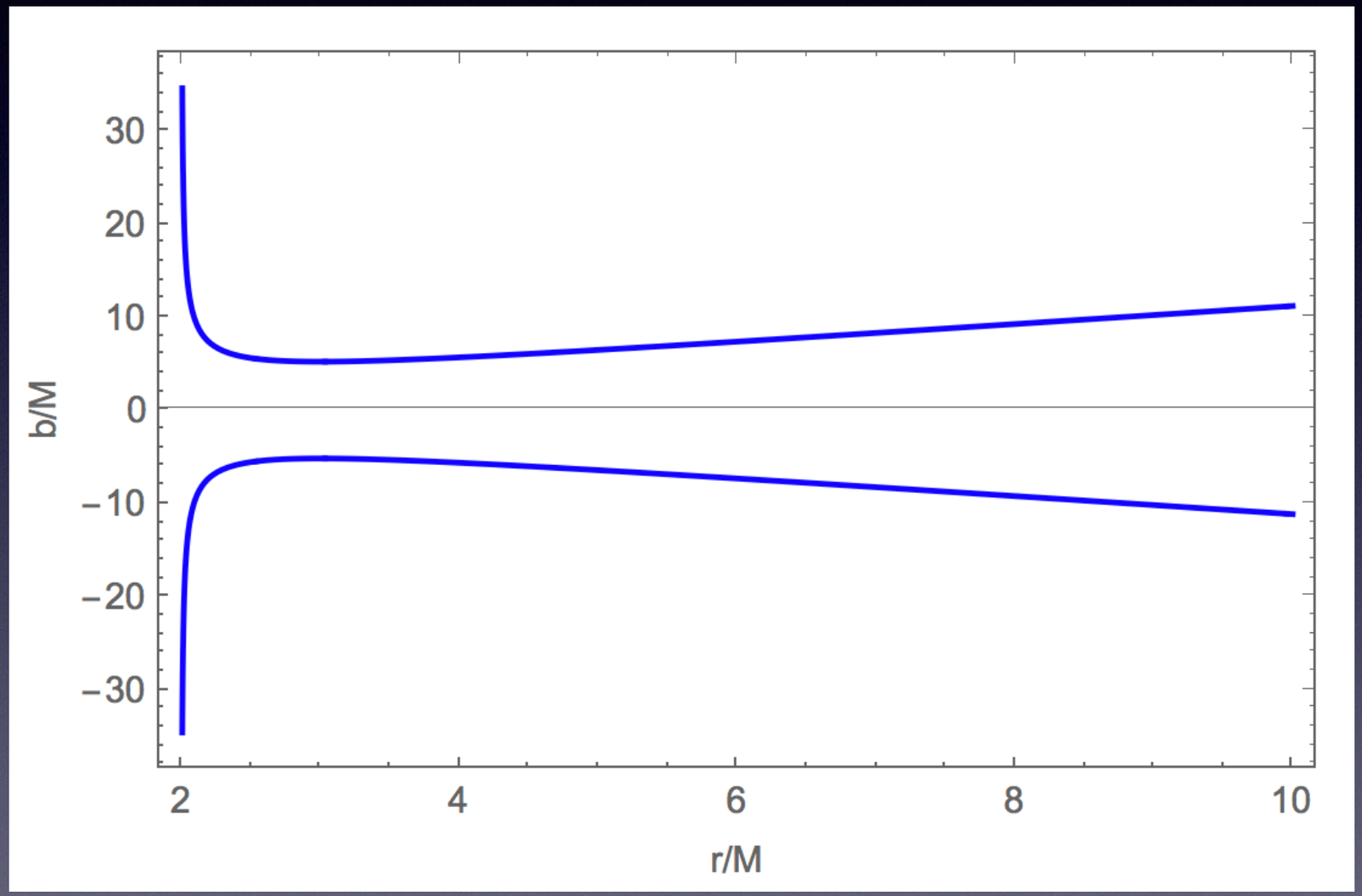

Below critical impact parameter $b = 3\sqrt{3}M$ photons fall into BH

Geodesics in Kerr

- "Separability" of geodesics equations not trivial, but possible due to presence of "hidden symmetry" that gives Carter constant Q

$$\left(\mu\frac{dr}{d\lambda}\right)^2 = V_r(r), \qquad \mu\frac{dt}{d\lambda} = V_t(r,\theta),$$
$$\left(\mu\frac{d\theta}{d\lambda}\right)^2 = V_\theta(\theta), \qquad \mu\frac{d\phi}{d\lambda} = V_\phi(r,\theta)\ ,$$

$$\Sigma \equiv r^2 + a^2\cos^2\theta, \qquad \Delta \equiv r^2 - 2Mr + a^2$$

$$\varpi^2 \equiv r^2 + a^2$$

$$V_t(r,\theta) \equiv E\left(\frac{\varpi^4}{\Delta} - a^2\sin^2\theta\right) + aL_z\left(1 - \frac{\varpi^2}{\Delta}\right),$$

$$V_r(r) \equiv \left(E\varpi^2 - aL_z\right)^2 - \Delta\left[\mu^2 r^2 + (L_z - aE)^2 + Q\right]$$

$$V_\theta(\theta) \equiv Q - L_z^2\cot^2\theta - a^2(\mu^2 - E^2)\cos^2\theta,$$
$$V_\phi(r,\theta) \equiv L_z\csc^2\theta + aE\left(\frac{\varpi^2}{\Delta} - 1\right) - \frac{a^2 L_z}{\Delta},$$

- Qualitatively same dynamics as in Schwarzschild ("light ring", ISCO, marginally bound orbits), but details depend on whether motion is prograde/retrograde

The effect of BH spins: frame-dragging in isolated BHs

Spin affects motion around BHs ("frame dragging")

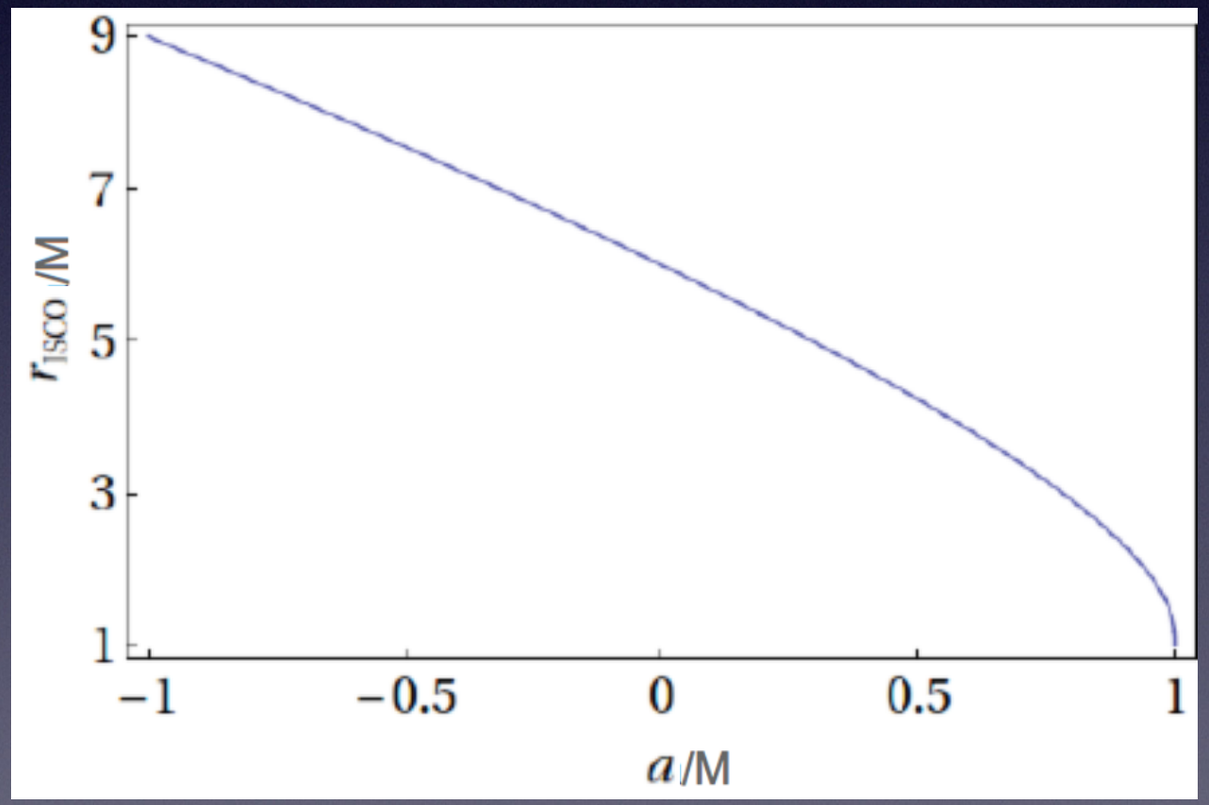

Innermost Stable Circular Orbit
(i.e. inner edge of thin disks)

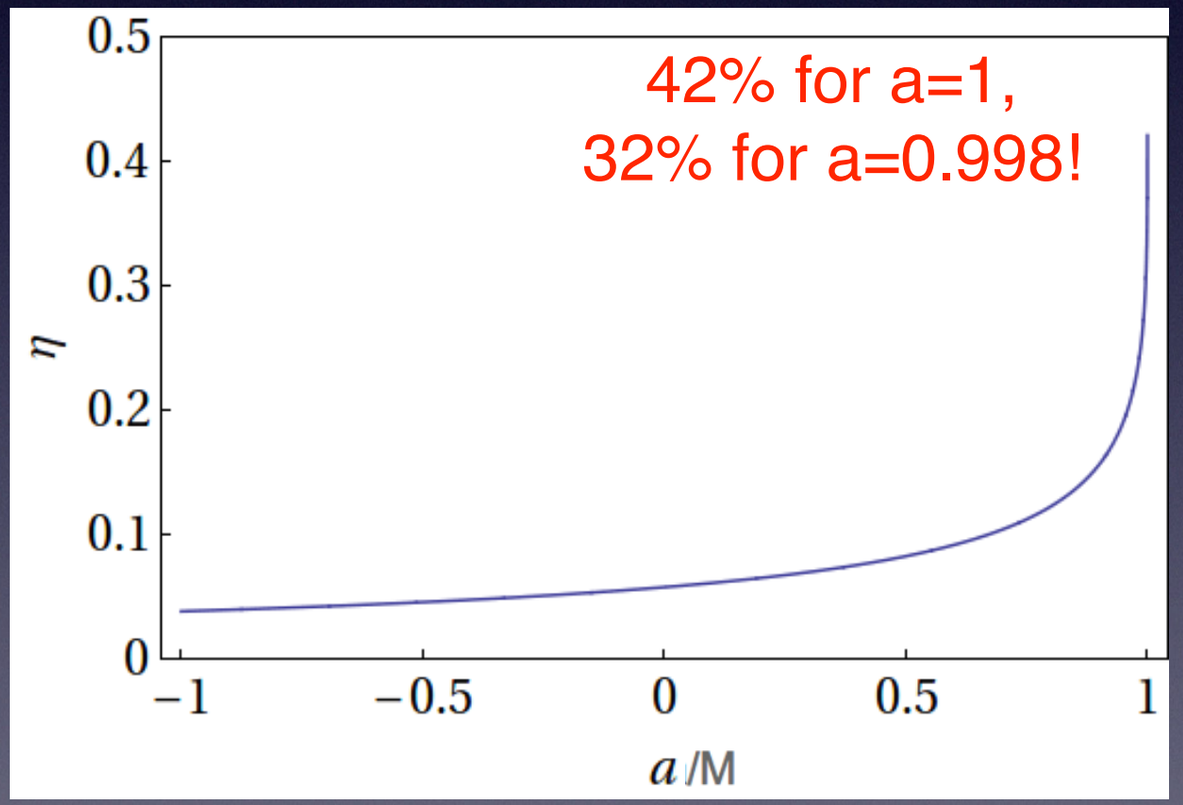

Efficiency of EM
emission from thin disks

The effect of BH spins: frame-dragging in isolated BHs

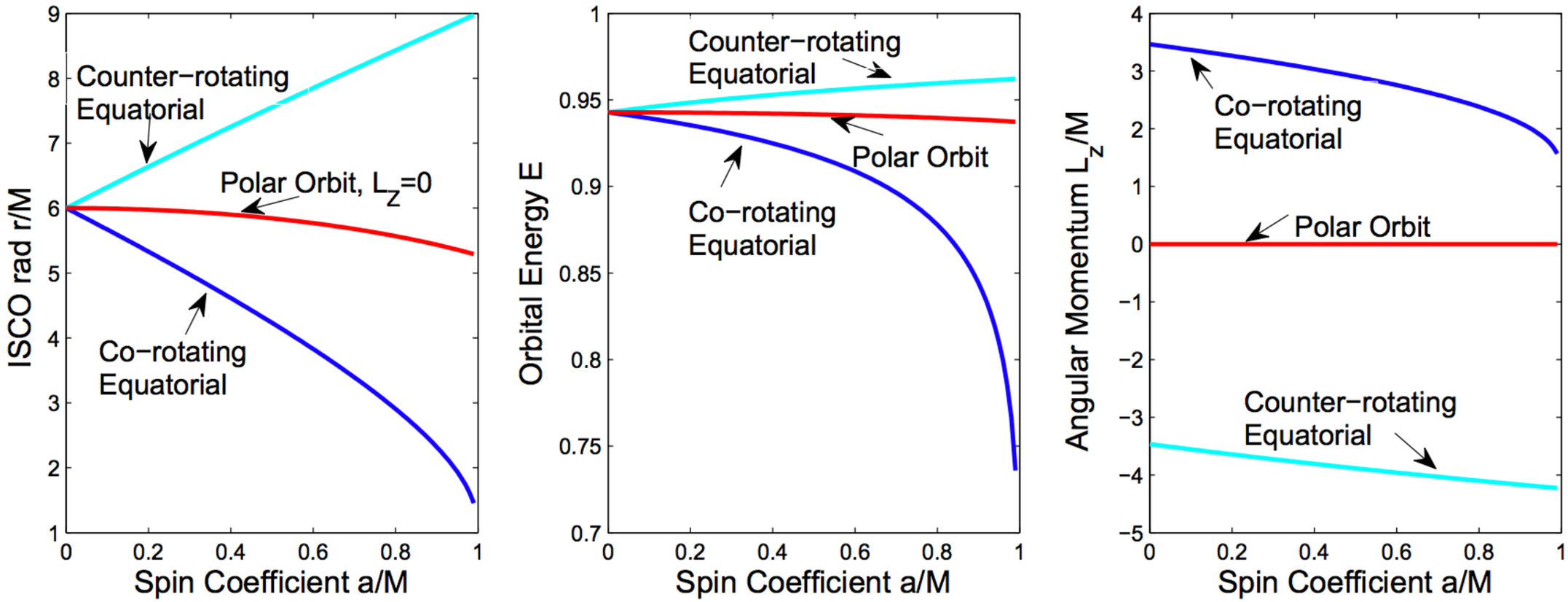

Figure from Mino & Brink 2008

EM BH spin measurements

Continuum fitting/iron-Kα lines

Binary System	$M/M_\odot$	a	Reference
4U 1543-47	9.4 ± 1.0	$0.75 - 0.85$	Shafee et al. (2006)
GRO J1655-40	6.30 ± 0.27	$0.65 - 0.75$	Shafee et al. (2006)
GRS 1915+105	14.0 ± 4.4	> 0.98	McClintock et al. (2006)
LMC X-3	$5 - 11$	< 0.26	Davis et al. (2006)
M33 X-7	15.65 ± 1.45	0.84 ± 0.05	Liu et al. (2008, 2010)
LMC X-1	10.91 ± 1.41	$0.92^{+0.05}_{-0.07}$	Gou et al. (2009)
XTE J1550-564	9.10 ± 0.61	$0.34^{+0.20}_{-0.28}$	Steiner et al. (2010b)

Stellar-mass BH spins

Object name	Galaxy type	z	L_X[erg s^{-1}]	$f_{\rm Edd}$	$\log(M_{\rm bh}[M_\odot])$	spin
1H0707-495	–	0.0411	3.7×10^{43}	1.0	6.70 ± 0.4	> 0.97
Mrk1018	S0	0.043	9.0×10^{43}	0.01	8.15	$0.58^{+0.36}_{-0.74}$
NGC4051	SAB(rs)bc	0.0023	3.0×10^{42}	0.03	6.28	> 0.99
NGC3783	SB(r)ab	0.0097	1.8×10^{44}	0.06	7.47 ± 0.08	> 0.88
1H0419-577	–	0.104	1.8×10^{44}	0.04	8.18 ± 0.05	> 0.89
3C120	S0	0.033	2.0×10^{44}	0.31	$7.74^{+0.20}_{-0.22}$	> 0.95
MCG-6-30-15	E/S0	0.008	1.0×10^{43}	0.4	6.65 ± 0.17	> 0.98
Ark564	SB	0.0247	1.4×10^{44}	0.11	< 6.90	$0.96^{+0.01}_{-0.06}$
TonS180	–	0.062	3.0×10^{44}	2.15	$7.30^{+0.60}_{-0.40}$	$0.91^{+0.02}_{-0.09}$
RBS1124	–	0.208	1.0×10^{45}	0.15	8.26	> 0.97
Mrk110	–	0.0355	1.8×10^{44}	0.16	7.40 ± 0.09	> 0.89
Mrk841	E	0.0365	8.0×10^{43}	0.44	7.90	> 0.52
Fairall9	Sc	0.047	3.0×10^{44}	0.05	8.41 ± 0.11	$0.52^{+0.19}_{-0.15}$
SWIFTJ2127.4+5654	SB0/a(s)	0.0147	1.2×10^{43}	0.18	7.18 ± 0.07	0.6 ± 0.2
Mrk79	SBb	0.0022	4.7×10^{43}	0.05	7.72 ± 0.14	0.7 ± 0.1
Mrk335	S0a	0.026	5.0×10^{43}	0.25	7.15 ± 0.13	$0.83^{+0.09}_{-0.13}$
Ark120	Sb/pec	0.0327	3.0×10^{45}	1.27	8.18 ± 0.12	$0.64^{+0.19}_{-0.11}$
Mrk359	pec	0.0174	6.0×10^{42}	0.25	6.04	$0.66^{+0.30}_{-0.54}$
IRAS13224-3809	–	0.0667	7.0×10^{43}	0.71	7.00	> 0.987
NGC1365	SB(s)b	0.0054	2.7×10^{42}	0.06	$6.60^{+1.40}_{-0.30}$	$0.97^{+0.01}_{-0.04}$

Compilations (Reynolds, Brenneman,...) of massive BH spins

The effect of BH spins: frame-dragging in binaries

- For large spins aligned with L, effective ISCO moves inward …

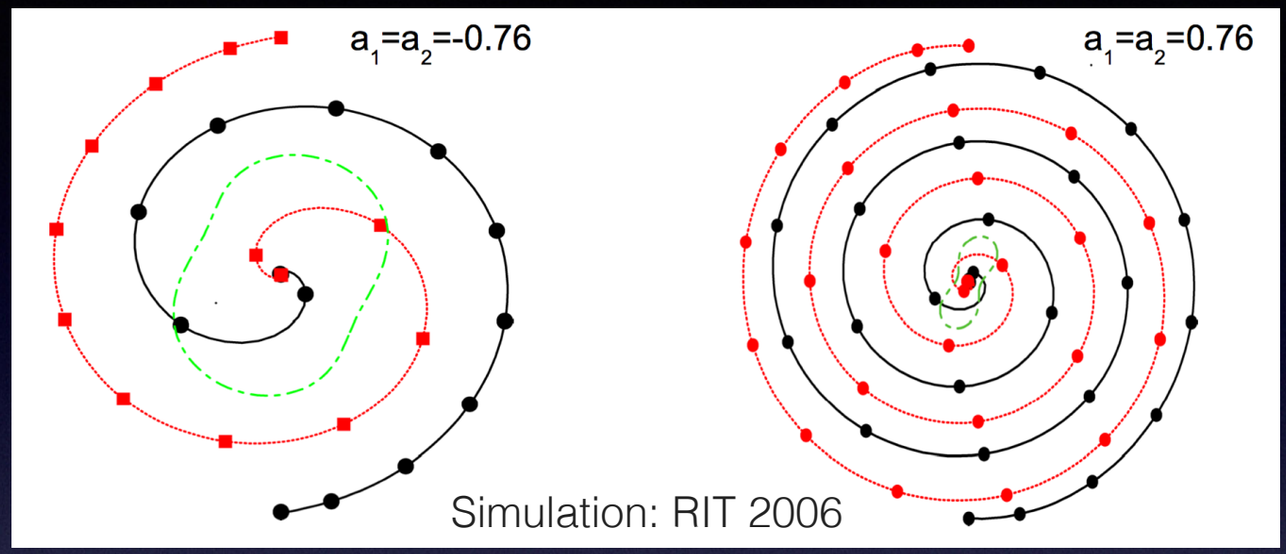

- ... and GW “efficiency” gets larger

Spins increase GW amplitudes

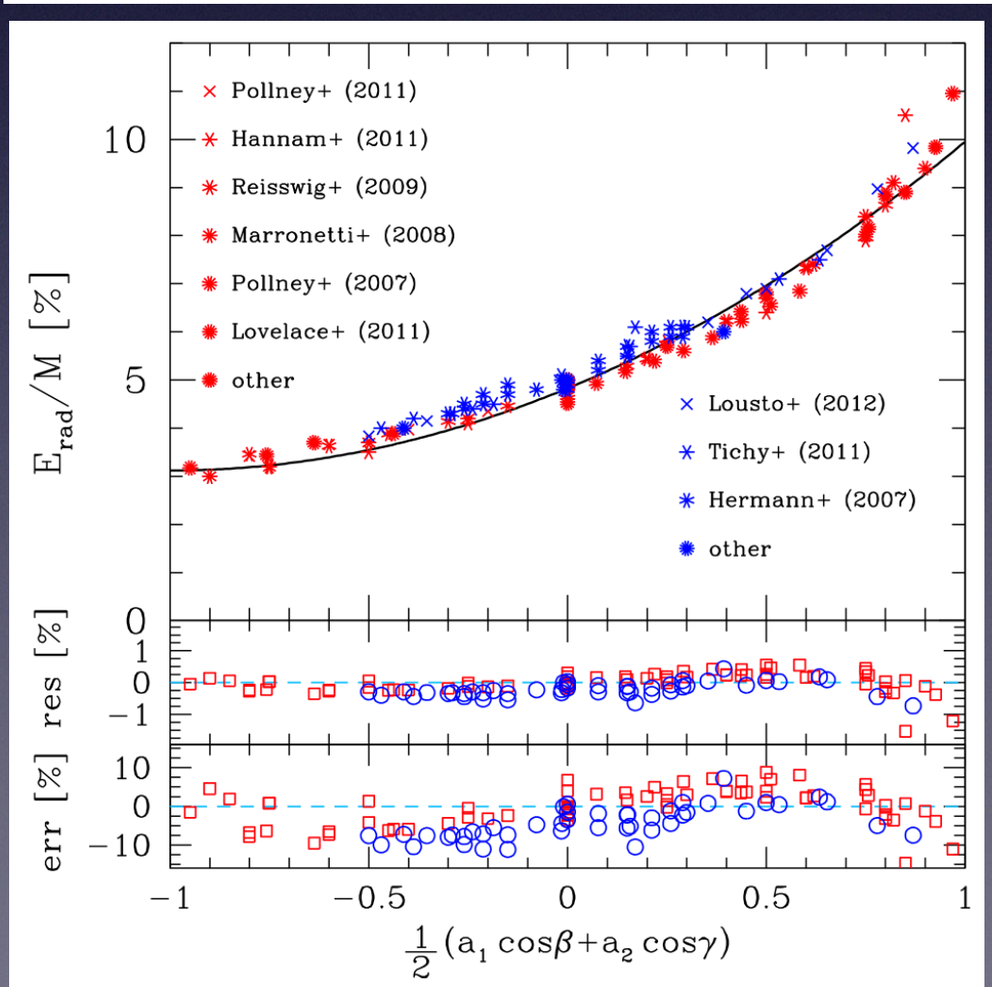

EB, Morozova & Rezzolla (2012)

The effect of BH spins: frame-dragging in isolated BHs

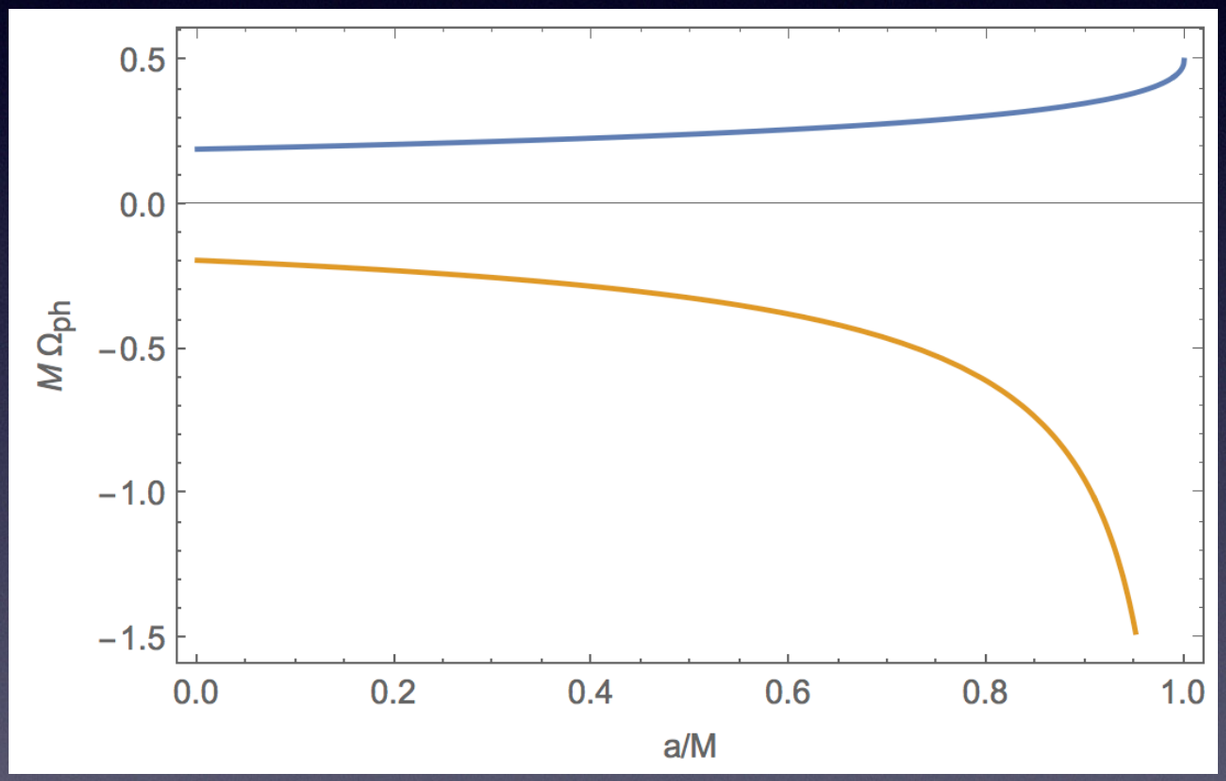

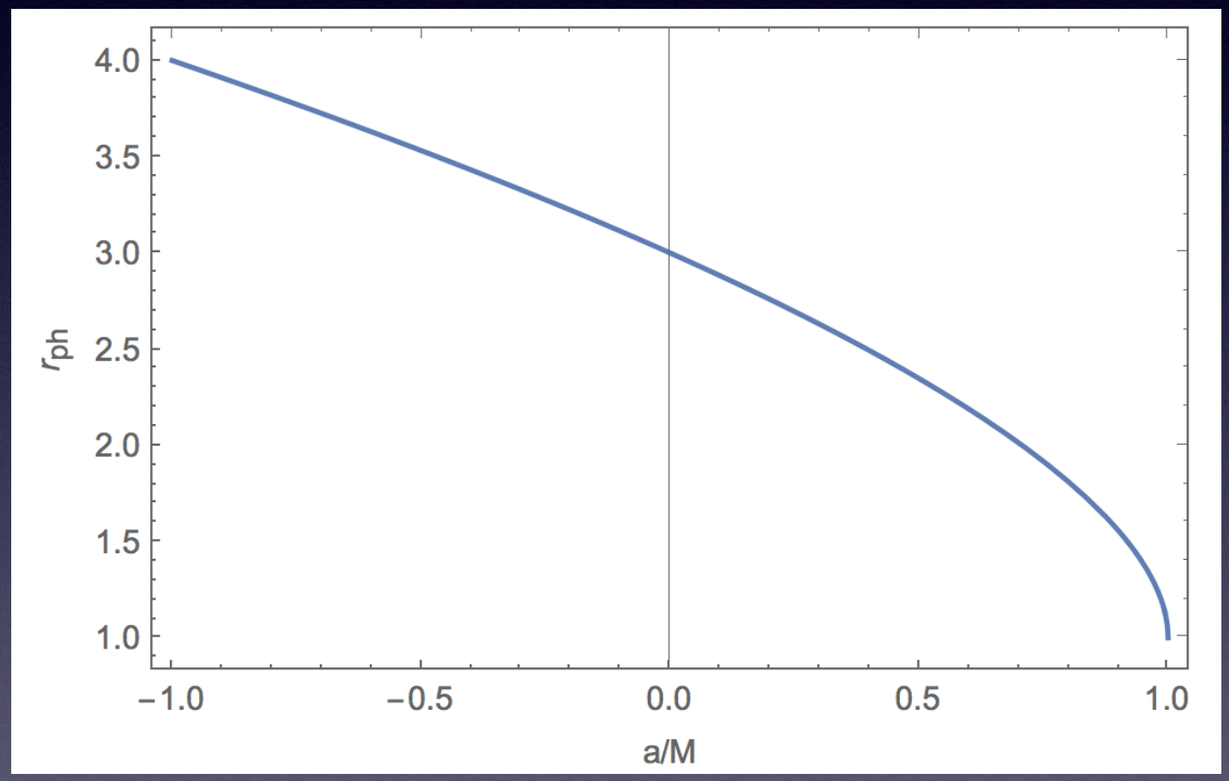

Orbital frequency of prograde circular photon orbit matches horizon's when a=M

BH shadows

Event Horizon Telescope
will image SgrA* and M87
via VLBI radio (mm wavelength)
observations

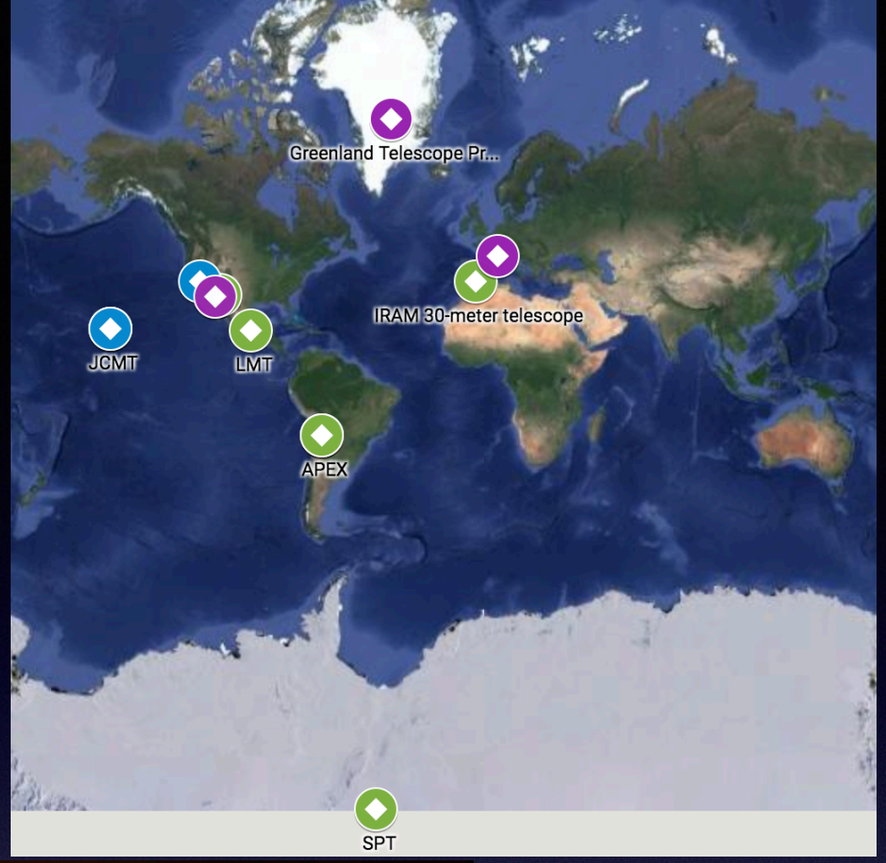

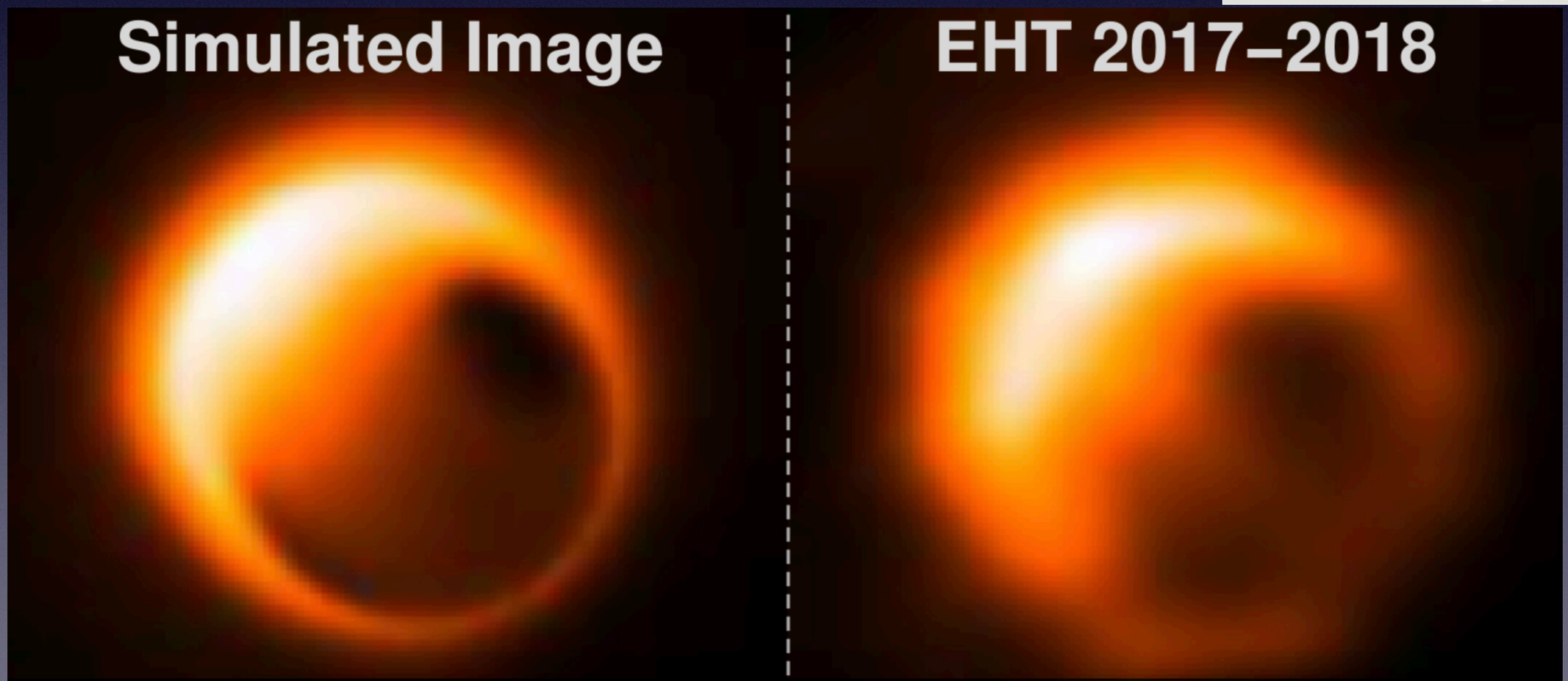

Imaging a Black Hole. At left is a model image for Sgr A* using a semi-analytic accretion flow (Broderick et al. 2011). Light is gravitationally lensed by the black hole to form a distinctive “ring” encircling the black hole’s “shadow” (Falcke et al. 2000). The ring diameter is ~5 Schwarzschild radii . The image is bright on the approaching side of the accretion disk and faint on the receding side because of Doppler effects. At right, a sample image shows expected EHT performance in 2017-2018 (Fish, Johnson, et al. 2014).

BH binary dynamics

- We can rewrite geodesic motion in Schwarzschild/Kerr as Hamiltonian/Lagrangian

$$H = \beta^i P_i + \alpha \sqrt{m^2 + \gamma^{ij} P_i P_j} \,,$$

$$\begin{aligned} \alpha &= \frac{1}{\sqrt{-g^{tt}}} \,, \\ \beta^i &= \frac{g^{ti}}{g^{tt}} \,, \\ \gamma^{ij} &= g^{ij} - \frac{g^{ti} g^{tj}}{g^{tt}} \,, \end{aligned}$$

- How to go from test-particle limit to BH binary?
- In Newtonian gravity, one can go to center of mass frame and replace test-particle mass by binary's reduced mass
- At post-Newtonian orders ($O(v/c)^{2n}$ beyond Newton) things are more involved

The post-Newtonian Hamiltonian

$$H = m_1c^2 + m_2c^2 + H_N + H_{1PN} + H_{2PN} + H_{3PN} + \dots$$

$$\hat{H} = (H - Mc^2)/\mu \qquad M = m_1 + m_2$$

$$\mu = m_1m_2/M \qquad \nu = \mu/M$$

$$p_r = (\mathbf{n}\cdot\mathbf{p}),\ \mathbf{q} = (\mathbf{x}_1 - \mathbf{x}_2)/GM,$$

$$\mathbf{p} = \mathbf{p}_1/\mu,\ r = r_{12} = |\mathbf{x}_1 - \mathbf{x}_2|,$$

$$\mathbf{n} = \mathbf{q}/|\mathbf{q}| \qquad \mathbf{p}_1 + \mathbf{p}_2 = 0$$

$$H^{1PN}_{S_1S_2} = \frac{G}{c^2}\sum_a\sum_{b\neq a}\frac{1}{2r^3_{ab}}\left[3(\mathbf{S}_a\cdot\mathbf{n}_{ab})(\mathbf{S}_b\cdot\mathbf{n}_{ab}) - (\mathbf{S}_a\cdot\mathbf{S}_b)\right]$$

$$H^{1PN}_{SO} = \frac{G}{c^2}\sum_a\sum_{b\neq a}\frac{1}{r^2_{ab}}(\mathbf{S}_a\times\mathbf{n}_{ab})\cdot\left[\frac{3m_b}{2m_a}\mathbf{p}_a - 2\mathbf{p}_b\right]$$

$$\hat{H}_N = \frac{p^2}{2} - \frac{1}{q},$$

$$c^2\hat{H}_{1PN} = \frac{1}{8}(3\nu-1)p^4 - \frac{1}{2}[(3+\nu)p^2 + \nu p_r^2]\frac{1}{q} + \frac{1}{2q^2},$$

$$c^4\hat{H}_{2PN} = \frac{1}{16}(1-5\nu+5\nu^2)p^6 + \frac{1}{8}[(5-20\nu-3\nu^2)p^4 - 2\nu^2p_r^2p^2 - 3\nu^2p_r^4]\frac{1}{q} + \frac{1}{2}[(5+8\nu)p^2 + 3\nu p_r^2]\frac{1}{q^2} - \frac{1}{4}(1+3\nu)\frac{1}{q^3},$$

$$c^6\hat{H}_{3PN} = \frac{1}{128}(-5+35\nu-70\nu^2+35\nu^3)p^8 + \frac{1}{16}\left[(-7+42\nu-53\nu^2-5\nu^3)p^6 + (2-3\nu)\nu^2p_r^2p^4 + 3(1-\nu)\nu^2p_r^4p^2 - 5\nu^3p_r^6\right]\frac{1}{q} + \left[\frac{1}{16}(-27+136\nu+109\nu^2)p^4 + \frac{1}{16}(17+30\nu)\nu p_r^2p^2 + \frac{1}{12}(5+43\nu)\nu p_r^4\right]\frac{1}{q^2} + \left[\left(-\frac{25}{8} + \left(\frac{1}{64}\pi^2 - \frac{335}{48}\right)\nu - \frac{23}{8}\nu^2\right)p^2 + \left(-\frac{85}{16} - \frac{3}{64}\pi^2 - \frac{7}{4}\nu\right)\nu p_r^2\right]\frac{1}{q^3} + \left[\frac{1}{8} + \left(\frac{109}{12} - \frac{21}{32}\pi^2\right)\nu\right]\frac{1}{q^4}.$$

The EOB formalism (Damour & Buonanno 1999)

- PN Hamiltonian is complicated, can we make sense of it?
- Newtonian binaries can be mapped to non-spinning test-particle with mass $\mu = m_1 m_2/M$ around mass $M=m_1+m_2$
- Energy levels of positronium (e^+ - e^-) can be mapped to those of hydrogen through

$$\frac{E_{\rm H}}{\mu c^2} = \frac{E_{\rm pos}^2 - m_1^2 c^4 - m_2^2 c^4}{2 m_1 m_2 c^4}$$

$m_1=m_2=m_e$

- Particle with mass $\mu = m_1 m_2/M$ around *deformed* Schwarzschild BH with $M=m_1+m_2$ (“effective one body'') has Hamiltonian related to PN Hamiltonian by

$$\frac{H_{\rm eff}}{\mu c^2} = \frac{H_{\rm PN}^2 - m_1^2 c^4 - m_2^2 c^4}{2 m_1 m_2 c^4}$$

(up to 3PN order)

EOB can be generalized to include BH spins
and produce GW waveforms

PN/EOB ISCO

Qualitatively the same as Schwarzschild/Kerr

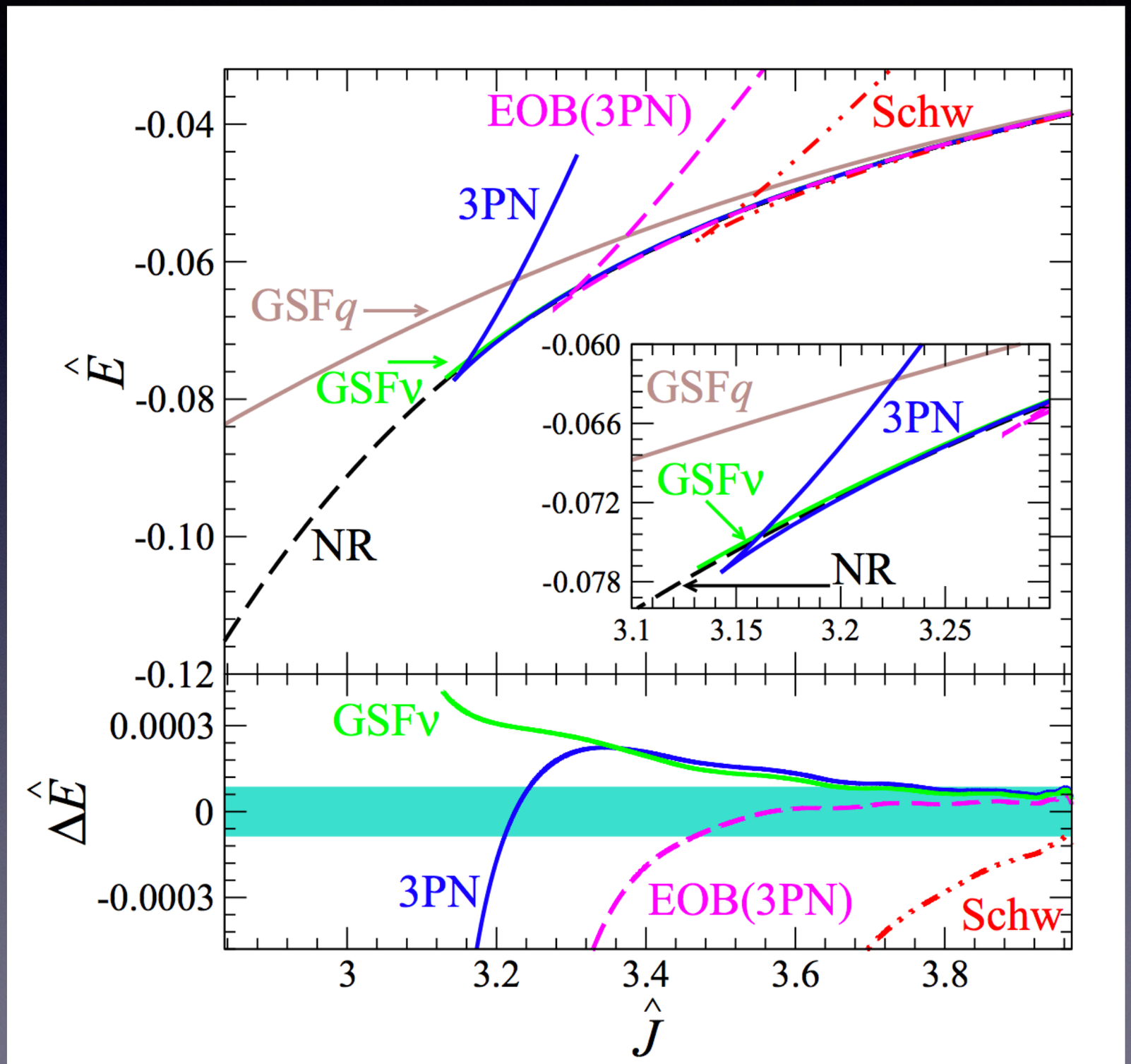

Le Tiec, EB, Buonanno 2011

BH spin precession

- Spin precesses around total angular momentum $J=L+S_1+S_2$
- Precession-induced modulations observable with GW detectors:

  - Increase SNR and improve measurements of binary parameters (e.g. luminosity distance and sky localization)

  - Allow measurements of angle between spins

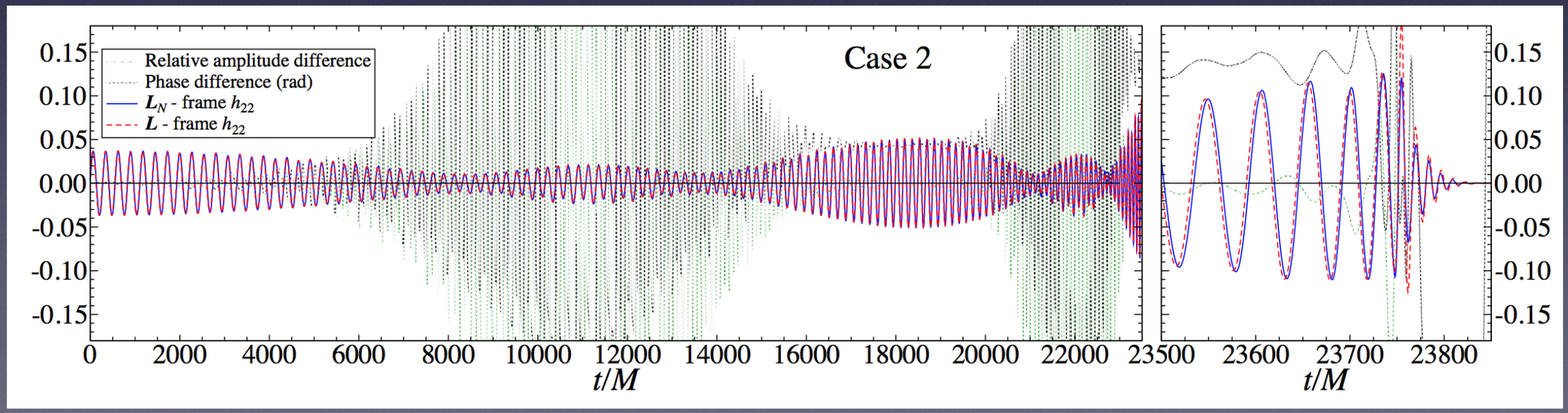

EOB waveforms for BH binary with mass ratio 1:6 and spins 0.6 and 0.8, from Pan et al (2013) [using spin-EOB model of EB & Buonanno 2010, 2011]

The PN formalism

Main idea: expand dynamics in powers of 1/c [i.e. of v/c, ∂_t/c GM/(r c^2)]:

$$g_{00} = -\left(1 + 2\frac{\phi}{c^2}\right),$$
$$g_{0i} = \frac{\hat{\omega}_i}{c^3},$$
$$g_{ij} = \left(1 - 2\frac{\psi}{c^2}\right)\delta_{ij} + \frac{\hat{\chi}_{ij}}{c^2},$$

$$\hat{\omega}_i = \partial_i \omega + \omega_i,$$

$$\hat{\chi}_{ij} = \left(\partial_{ij} - \frac{1}{3}\delta_{ij}\nabla^2\right)\chi + \partial_{(i}\chi_{j)} + \chi_{ij},$$

$$\partial_i \omega^i = \partial_i \chi^i = \partial_i \chi^{ij} = \chi^i_i = 0.$$

$$\omega = \chi = \chi_i = 0.$$

$$\partial_i \hat{\omega}^i = \partial_i \hat{\chi}^{ij} = 0$$

"Poisson gauge"

$$g_{00} = -\left(1 + 2\frac{\phi}{c^2}\right),$$
$$g_{0i} = \frac{\omega_i}{c^3},$$
$$g_{ij} = \left(1 - 2\frac{\psi}{c^2}\right)\delta_{ij} + \frac{\chi_{ij}}{c^2},$$

Einstein equations

$$\nabla^2\phi = \ldots$$
$$\nabla^2\phi = \ldots$$
$$\nabla^2\omega_i = \ldots$$

$$\Box\chi_{ij} = \ldots$$

The PN formalism

Expand Einstein eqs+perfect fluid in 1/c, over flat space:

$$\psi \equiv \phi + \frac{\delta\psi}{c^2}$$

$$\nabla^2\phi = 4\pi\left(3\frac{p}{c^2}+\rho\right) + \frac{2}{c^2}\phi_{,i}\phi_{,i} + 8\pi\rho\left(\frac{v}{c}\right)^2 - \frac{3}{c^2}\phi_{,tt}$$
$$+\frac{1}{c^4}\Big[-16\pi\rho\phi^2 - 8\pi\rho\delta\psi + \phi_{,i}\delta\psi_{,i} + \phi_{,i}\omega^i{}_{,t} - \frac{1}{2}\omega^i{}_{,j}\omega^i{}_{,j}$$
$$+\frac{1}{2}\omega^i{}_{,j}\omega^j{}_{,i} + 8\pi(p-4\rho\phi)v^2 + 8\pi\rho v^4 + \phi_{,ij}\chi^{ij}$$
$$-3\delta\psi_{,tt}\Big] + \mathcal{O}\left(\frac{1}{c^6}\right),$$

$$\nabla^2\delta\psi = -12p\pi - 16\pi\rho\phi - \frac{7}{2}\phi_{,j}\phi_{,j}$$
$$- 4\pi\rho v^2 + 3\phi_{,tt} + \mathcal{O}\left(\frac{1}{c^2}\right).$$

$$\nabla^2\omega^i = 4(4\pi\rho v^i + \phi_{,ti}) + \frac{2}{c^2}\Big[\phi_{,j}\omega^j{}_{,i} - \phi_{,ij}\omega^j$$
$$+2\left(\phi_{,t}\phi_{,i} + \delta\psi_{,it} + 4p\pi v^i - 16\pi\rho\phi v^i + 4\pi\rho v^2 v^i + 2\pi\rho\omega^i\right)\Big]$$
$$+\mathcal{O}\left(\frac{1}{c^4}\right).$$

The PN formalism

Expand Einstein eqs+perfect fluid in 1/c, over flat space:

$$\psi \equiv \phi + \frac{\delta\psi}{c^2}$$

$$\nabla^2\phi = 4\pi\left(3\frac{p}{c^2} + \rho\right) + \frac{2}{c^2}\phi_{,i}\phi_{,i} + 8\pi\rho\left(\frac{v}{c}\right)^2 - \frac{3}{c^2}\phi_{,tt}$$
$$+\frac{1}{c^4}\Big[-16\pi\rho\phi^2 - 8\pi\rho\delta\psi + \phi_{,i}\delta\psi_{,i} + \phi_{,i}\omega^i{}_{,t} - \frac{1}{2}\omega^i{}_{,j}\omega^i{}_{,j}$$
$$+\frac{1}{2}\omega^i{}_{,j}\omega^j{}_{,i} + 8\pi(p - 4\rho\phi)v^2 + 8\pi\rho v^4 + \phi_{,ij}\chi^{ij}$$
$$-3\delta\psi_{,tt}\Big] + \mathcal{O}\left(\frac{1}{c^6}\right),$$

$$\nabla^2\delta\psi = -12p\pi - 16\pi\rho\phi - \frac{7}{2}\phi_{,j}\phi_{,j}$$
$$- 4\pi\rho v^2 + 3\phi_{,tt} + \mathcal{O}\left(\frac{1}{c^2}\right).$$

a=a_N

$$\nabla^2\omega^i = 4(4\pi\rho v^i + \phi_{,ti}) + \frac{2}{c^2}\Big[\phi_{,j}\omega^j{}_{,i} - \phi_{,ij}\omega^j$$
$$+2\left(\phi_{,t}\phi_{,i} + \delta\psi_{,it} + 4p\pi v^i - 16\pi\rho\phi v^i + 4\pi\rho v^2 v^i + 2\pi\rho\omega^i\right)\Big]$$
$$+\mathcal{O}\left(\frac{1}{c^4}\right).$$

The PN formalism

Expand Einstein eqs+perfect fluid in 1/c, over flat space:

$$\psi \equiv \phi + \frac{\delta\psi}{c^2}$$

$$\nabla^2\phi = 4\pi\left(3\frac{p}{c^2}+\rho\right)+\frac{2}{c^2}\phi_{,i}\phi_{,i}+8\pi\rho\left(\frac{v}{c}\right)^2-\frac{3}{c^2}\phi_{,tt}$$
$$+\frac{1}{c^4}\Big[-16\pi\rho\phi^2-8\pi\rho\delta\psi+\phi_{,i}\delta\psi_{,i}+\phi_{,i}\omega^i{}_{,t}-\frac{1}{2}\omega^i{}_{,j}\omega^i{}_{,j}$$
$$+\frac{1}{2}\omega^i{}_{,j}\omega^j{}_{,i}+8\pi(p-4\rho\phi)v^2+8\pi\rho v^4+\phi_{,ij}\chi^{ij}$$
$$-3\delta\psi_{,tt}\Big]+\mathcal{O}\left(\frac{1}{c^6}\right),$$

$$\nabla^2\delta\psi = -12p\pi-16\pi\rho\phi-\frac{7}{2}\phi_{,j}\phi_{,j}$$
$$-4\pi\rho v^2+3\phi_{,tt}+\mathcal{O}\left(\frac{1}{c^2}\right).$$

$$\nabla^2\omega^i = 4(4\pi\rho v^i+\phi_{,ti})+\frac{2}{c^2}\Big[\phi_{,j}\omega^j{}_{,i}-\phi_{,ij}\omega^j$$
$$+2\left(\phi_{,t}\phi_{,i}+\delta\psi_{,it}+4p\pi v^i-16\pi\rho\phi v^i+4\pi\rho v^2 v^i+2\pi\rho\omega^i\right)\Big]$$
$$+\mathcal{O}\left(\frac{1}{c^4}\right).$$

$a=a_N(1+1PN/c^2$

The PN formalism

Expand Einstein eqs+perfect fluid in 1/c, over flat space:

$$\psi \equiv \phi + \frac{\delta\psi}{c^2}$$

$$\nabla^2\phi = 4\pi\left(3\frac{p}{c^2}+\rho\right)+\frac{2}{c^2}\phi_{,i}\phi_{,i}+8\pi\rho\left(\frac{v}{c}\right)^2-\frac{3}{c^2}\phi_{,tt}$$
$$+\frac{1}{c^4}\Big[-16\pi\rho\phi^2-8\pi\rho\delta\psi+\phi_{,i}\delta\psi_{,i}+\phi_{,i}\omega^i{}_{,t}-\frac{1}{2}\omega^i{}_{,j}\omega^i{}_{,j}$$
$$+\frac{1}{2}\omega^i{}_{,j}\omega^j{}_{,i}+8\pi(p-4\rho\phi)v^2+8\pi\rho v^4+\phi_{,ij}\chi^{ij}$$
$$-3\delta\psi_{,tt}\Big]+\mathcal{O}\left(\frac{1}{c^6}\right),$$

$$\nabla^2\delta\psi = -12p\pi-16\pi\rho\phi-\frac{7}{2}\phi_{,j}\phi_{,j}$$
$$-4\pi\rho v^2+3\phi_{,tt}+\mathcal{O}\left(\frac{1}{c^2}\right).$$

$$\nabla^2\omega^i = 4(4\pi\rho v^i+\phi_{,ti})+\frac{2}{c^2}\Big[\phi_{,j}\omega^j{}_{,i}-\phi_{,ij}\omega^j$$
$$+2\left(\phi_{,t}\phi_{,i}+\delta\psi_{,it}+4p\pi v^i-16\pi\rho\phi v^i+4\pi\rho v^2 v^i+2\pi\rho\omega^i\right)\Big]$$
$$+\mathcal{O}\left(\frac{1}{c^4}\right).$$

$a=a_N(1+1PN/c^2+2PN/c^4+\ldots)$

PN effects are not only relevant for BH binaries

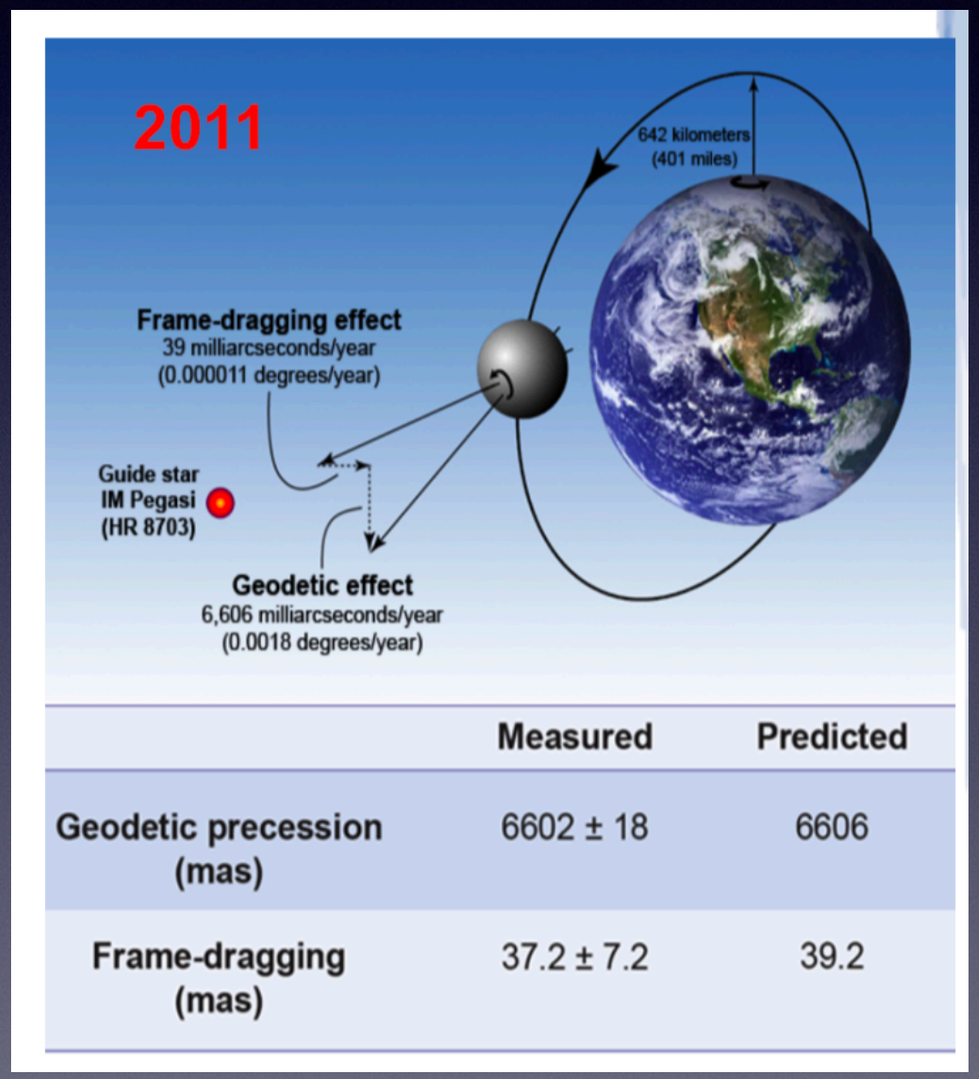

	Measured	Predicted
Geodetic precession (mas)	6602 ± 18	6606
Frame-dragging (mas)	37.2 ± 7.2	39.2

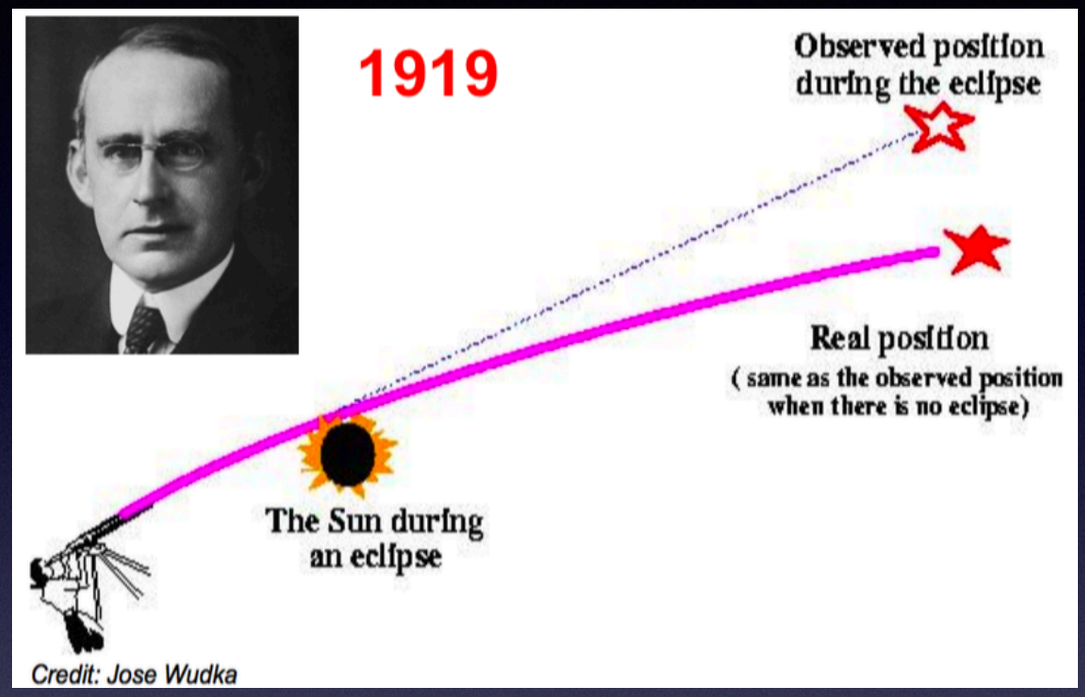

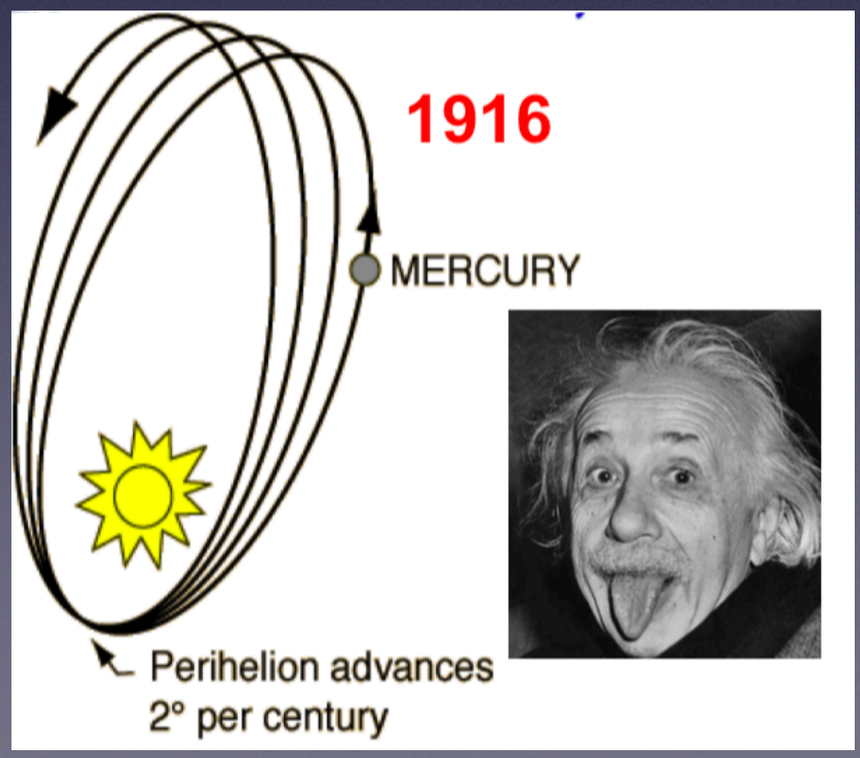

How about the TT term?

Keep time derivatives even though
they carry factor 1/c, because for GWs $\partial_t/c \sim \partial_x$)

$$\Box\chi_{ij} \approx -16\pi\sigma_{ij}$$

$$\sigma_{ij} = P_i^k P_j^l T_{kl} - P_{ij}P^{kl}T_{kl}/2$$

$$P_{ij} = \delta_{ij} - \frac{\partial_i\partial_j}{\nabla^2}$$

$$\chi_{ij} = -16\pi\Box^{-1}\sigma_{ij} = -16\pi\Box^{-1}\left(P_i^k P_j^l - \frac{1}{2}P_{ij}P^{kl}\right)T_{kl}$$

$$= -16\pi\left(P_i^k P_j^l - \frac{1}{2}P_{ij}P^{kl}\right)\Box^{-1}T_{kl}$$

$$= 4\left(P_i^k P_j^l - \frac{1}{2}P_{ij}P^{kl}\right)\int\frac{T_{ij}\left(t-|\boldsymbol{x}-\boldsymbol{x}'|,\boldsymbol{x}'\right)}{|\boldsymbol{x}-\boldsymbol{x}'|}\mathrm{d}^3x'$$

$$\approx \frac{4}{r}\left(P_i^k P_j^l - \frac{1}{2}P_{ij}P^{kl}\right)\int T_{ij}(t-r,\boldsymbol{x}')\mathrm{d}^3x'$$

How about the TT term?

Keep time derivatives even though
they carry factor 1/c, because for GWs $\partial_t/c \sim \partial_x$)

$$\Box\chi_{ij} \approx -16\pi\sigma_{ij}$$

$$\sigma_{ij} = P_i^k P_j^l T_{kl} - P_{ij}P^{kl}T_{kl}/2$$

$$P_{ij} = \delta_{ij} - \frac{\partial_i\partial_j}{\nabla^2}$$

$$\chi_{ij} = -16\pi\Box^{-1}\sigma_{ij} = -16\pi\Box^{-1}\left(P_i^k P_j^l - \frac{1}{2}P_{ij}P^{kl}\right)T_{kl}$$

$$= -16\pi\left(P_i^k P_j^l - \frac{1}{2}P_{ij}P^{kl}\right)\Box^{-1}T_{kl}$$

$$= 4\left(P_i^k P_j^l - \frac{1}{2}P_{ij}P^{kl}\right)\int\frac{T_{ij}\left(t-|\boldsymbol{x}-\boldsymbol{x}'|,\boldsymbol{x}'\right)}{|\boldsymbol{x}-\boldsymbol{x}'|}\mathrm{d}^3x'$$

$$\approx \frac{4}{r}\left(P_i^k P_j^l - \frac{1}{2}P_{ij}P^{kl}\right)\int T_{ij}(t-r,\boldsymbol{x}')\mathrm{d}^3x'$$

The quadrupole formula

$$\partial_t^2 \left(T^{tt} x^i x^j\right) = \partial_k \partial_l \left(T^{kl} x^i x^j\right) - 2\partial_k \left(T^{ik} x^j + T^{kj} x^i\right) + 2T^{ij}$$

$$\frac{4}{r}\int d^3x'\, T_{ij} = \frac{4}{r}\int d^3x' \left[\frac{1}{2}\partial_t^2 \left(T^{tt} x'^i x'^j\right) + \partial_k \left(T^{ik} x'^j + T^{kj} x'^i\right) - \frac{1}{2}\partial_k \partial_l \left(T^{kl} x'^i x'^j\right)\right]$$

$$= \frac{2}{r}\int d^3x'\, \partial_t^2 \left(T^{tt} x'^i x'^j\right) = \frac{2}{r}\frac{\partial^2}{\partial t^2}\int d^3x'\, \rho\, x'^i x'^j = \frac{2}{r}\frac{d^2 I_{ij}(t-r)}{dt^2}$$

$$I_{ij}(t) = \int d^3x'\, \rho(t, \mathbf{x}')\, x'^i x'^j$$

$$\chi_{ij} \approx \frac{4}{r}\left(P_i^k P_j^l - \frac{1}{2}P_{ij}P^{kl}\right)\int T_{ij}(t-r, \boldsymbol{x}')\mathrm{d}^3x'$$

$$= \frac{2}{r}\frac{d^2\mathcal{I}_{kl}(t-r)}{dt^2}\left[P_{ik}(\mathbf{n})P_{jl}(\mathbf{n}) - \frac{1}{2}P_{kl}(\mathbf{n})P_{ij}(\mathbf{n})\right]\frac{G}{c^4}$$

$$P_{ij} = \delta_{ij} - n_i n_j \qquad \mathcal{I}_{ij} = I_{ij} - \frac{1}{3}\delta_{ij} I,$$

Quadrupole tensor

small number!

The quadrupole formula

Binary moving on circular orbit on x,y plane with orbital frequency Ω, GW traveling along z

$$\chi_{ij} = h \times \begin{bmatrix} \cos 2\Omega t & \sin 2\Omega t & 0 \\ \sin 2\Omega t & -\cos 2\Omega t & 0 \\ 0 & 0 & 0 \end{bmatrix}$$

$$h = \frac{4\mu\Omega^2 R^2}{r} = \frac{4\mu(M\Omega)^{2/3}}{r} = \frac{4M_c^{5/3}\Omega^{2/3}}{r} \qquad M_c = M\nu^{3/5} \quad \nu = \frac{\mu}{M}$$

$$h \approx 1.9 \times 10^{-21} \left(\frac{f_{\rm gw}}{100Hz}\right)^{2/3} \left(\frac{M_{c,z}}{30M_\odot}\right)^{5/3} \left(\frac{400{\rm Mpc}}{d_L}\right)$$

$$\approx 3.5 \times 10^{-18} \left(\frac{f_{\rm gw}}{10{\rm mHz}}\right)^{2/3} \left(\frac{M_{c,z}}{10^6 M_\odot}\right)^{5/3} \left(\frac{16{\rm Gpc}}{d_L}\right)$$

$h_{Sun} \sim G\, M_{sun}/R_{sun}\, c^2$
$\sim 2 \times 10^{-6}$

$$M_{c,z} = M_c(1+z) \qquad f_{\rm gw} = \frac{2f_{\rm orb}}{1+z} = \frac{\Omega}{\pi(1+z)} \qquad d_L(z=2) \approx 16\ {\rm Gpc}$$

GW detectors

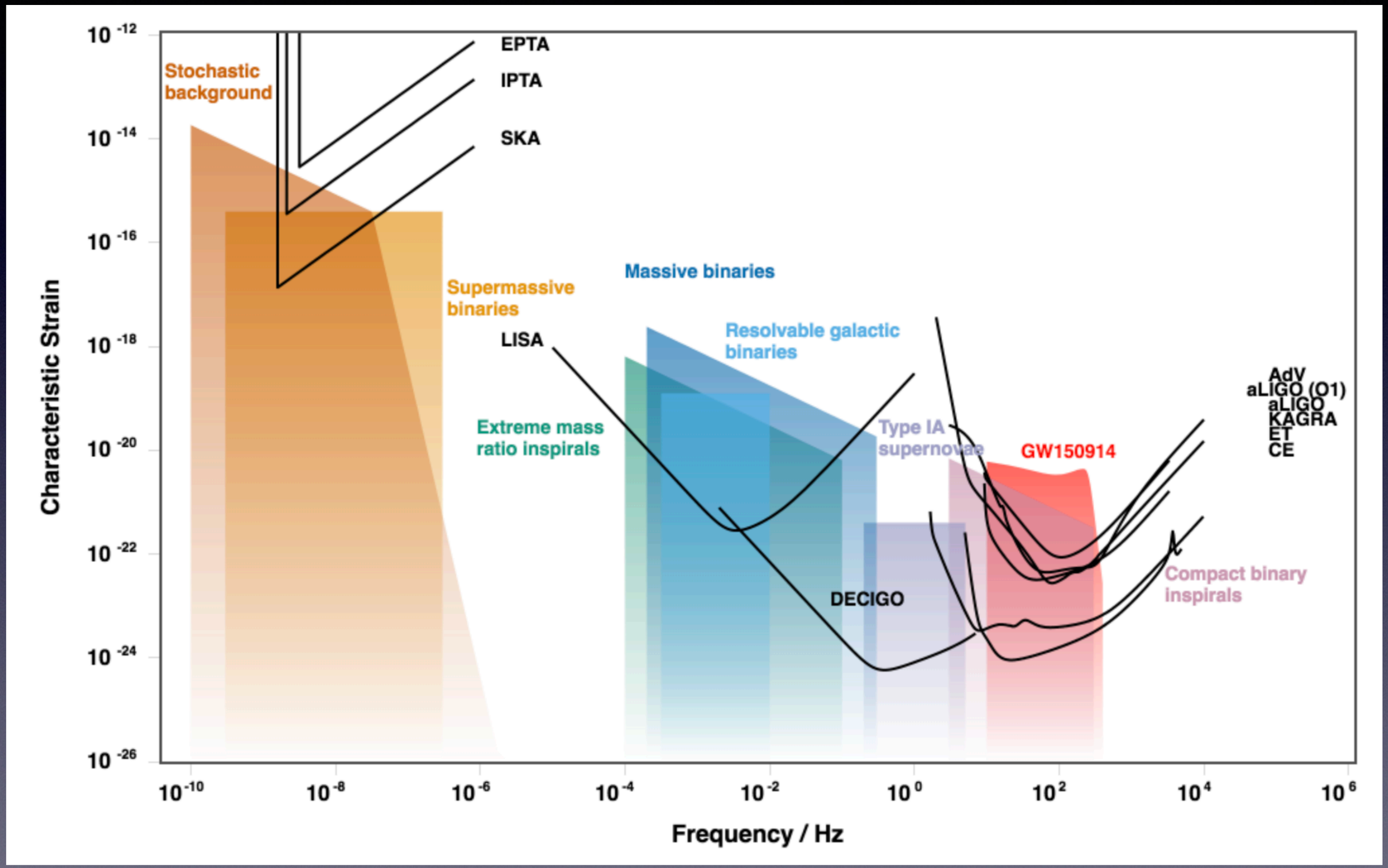

Figure generated by http://gwplotter.com/

Wrong+wrong=right

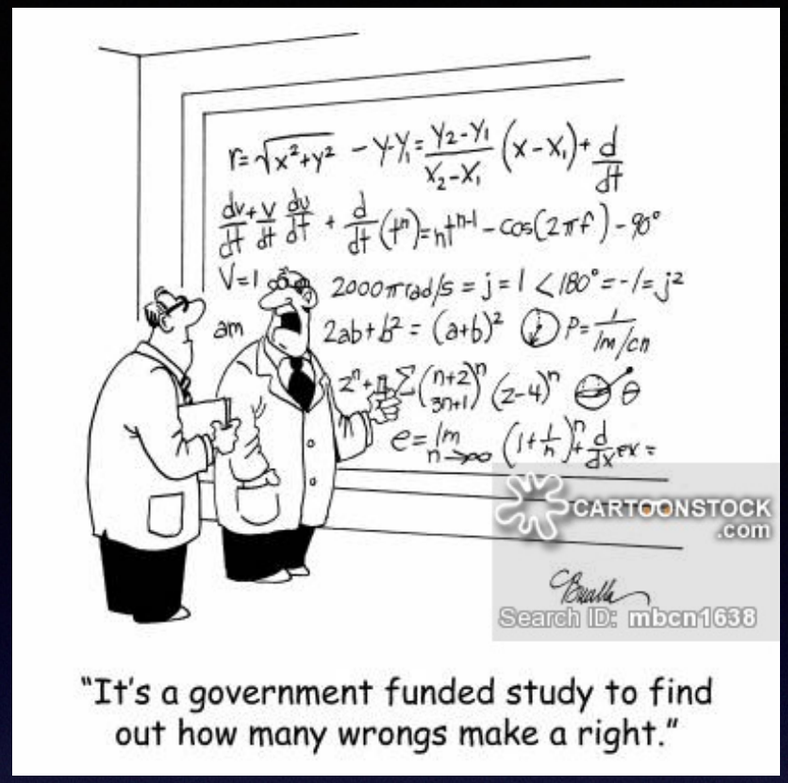

- We have started from linearized theory over Minkowski
- This implies that stress energy tensor is conserved wrt to Minkowski metric ...
- … and that is used to go from ”Green formula” to ”quadrupole formula”
- This is inconsistent as a binary system in GW-dominated regimes does NOT move on Minkowski geodesics (i.e. straight lines)
- Exercise: compute GWs from Green formula for a system of two unequal masses on Keplerian orbits one around the other and verify that the GW amplitudes differ by a factor 2 (assume propagation along z axis)
- Which one is correct? Quadrupole or Green?
- One would expect Green, but actually the quadrupole formula is the correct one

A (more) correct derivation

$$\bar{H}^{\mu\nu} \equiv \eta^{\mu\nu} - (-g)^{1/2} g^{\mu\nu} \qquad \partial_\beta \bar{H}^{\alpha\beta} = 0 \qquad \text{harmonic gauge}$$

$$\Longrightarrow \quad \Box_{\rm flat} \bar{H}^{\alpha\beta} = -16\pi\tau^{\alpha\beta} \qquad \tau^{\alpha\beta} = (-g)T^{\alpha\beta} + (16\pi)^{-1}\Lambda^{\alpha\beta}$$

Full Einstein equations!

$$\Lambda^{\alpha\beta} = 16\pi(-g)t_{\rm LL}^{\alpha\beta} + (\bar{H}^{\alpha\mu}{}_{,\nu}\,\bar{H}^{\beta\nu}{}_{,\mu} - \bar{H}^{\alpha\beta}{}_{,\mu\nu}\,\bar{H}^{\mu\nu})$$

$$16\pi(-g)t_{\rm LL}^{\alpha\beta} \equiv g_{\lambda\mu}g^{\nu\rho}\bar{H}^{\alpha\lambda}_{,\nu}\bar{H}^{\beta\mu}_{,\rho}$$
$$+\frac{1}{2}g_{\lambda\mu}g^{\alpha\beta}\bar{H}^{\lambda\nu}_{,\rho}\bar{H}^{\rho\mu}_{,\nu} - 2g_{\mu\nu}g^{\lambda(\alpha}\bar{H}^{\beta)\nu}_{,\rho}\bar{H}^{\rho\mu}_{,\lambda}$$
$$+\frac{1}{8}(2g^{\alpha\lambda}g^{\beta\mu} - g^{\alpha\beta}g^{\lambda\mu})(2g_{\nu\rho}g_{\sigma\tau} - g_{\rho\sigma}g_{\nu\tau})\bar{H}^{\nu\tau}_{,\lambda}\bar{H}^{\rho\sigma}_{,\mu}$$

From gauge condition,

$$\tau^{\alpha\beta}{}_{,\beta} = 0$$

= geodesic motion in curved metric *g*

$$\bar{H}^{\mu\nu} \approx \bar{h}^{\mu\nu} \equiv h^{\mu\nu} - \frac{1}{2}h\eta^{\mu\nu}$$

Proceed as before but with T replaced by τ

A (more) correct derivation

$$
\begin{aligned}
g_{00} &= -1 - 2\frac{\phi}{c^2} + O(1/c^4) & \tau^{00} &= T^{00} + O(1/c^0) \\
g_{0i} &= O(1/c^3) & \tau^{0i} &= T^{0i} + O(1/c^1) \\
g_{ij} &= \left(1 - 2\frac{\phi}{c^2}\right)\delta_{ij} + O(1/c^4) & \tau^{ij} &= T^{ij} + \frac{1}{4\pi G}\left(\partial^i\phi\partial^j\phi - \frac{1}{2}\delta^{ij}\partial_k\phi\partial^k\phi\right) + O(1/c^2),
\end{aligned}
$$

- Non-linear terms are important in τ_{ij} but not τ_{00}
- Non-linear terms in Green formula account for discrepancy with quadrupole formula for circular Keplerian binaries
- Quadrupole formula is correct, Green's is not

BH binary inspirals

- Quadruple formula (or quadrupole+octupole) often a decent approximation for GW signal during inspiral
- Often used in combination with geodetic motion in Kerr to produce “kludge” waveforms for Extreme Mass Ratio Inspirals (stellar origin BH + massive BH)

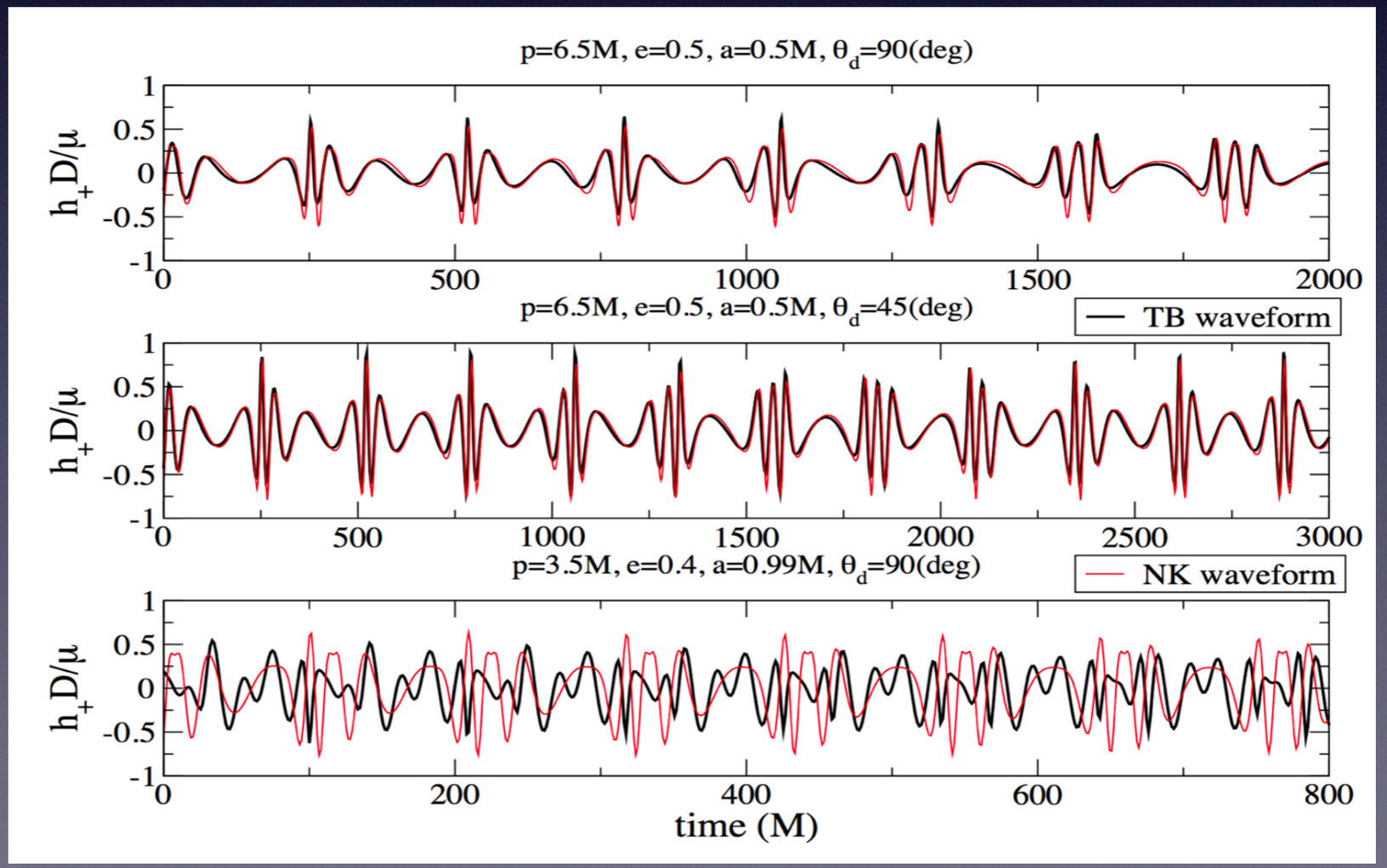

Figure from Babak et al 2007

GW "backreact" on geometry at second order

Figure from Kip Thorne's website

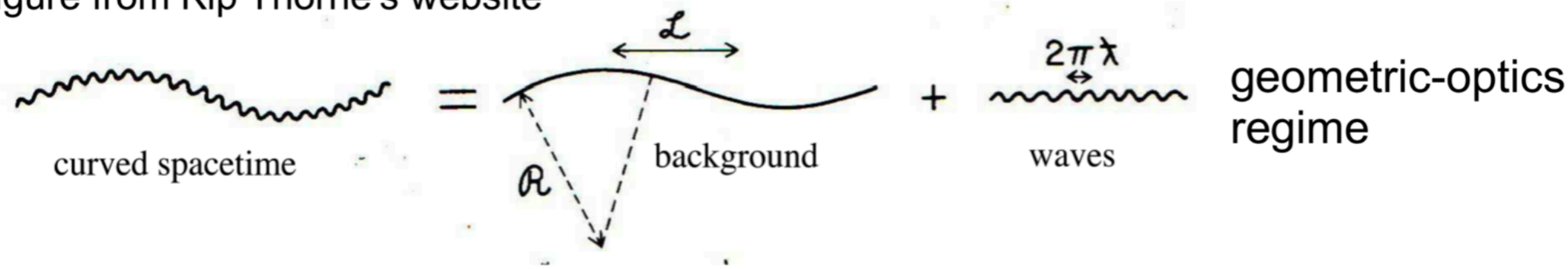

geometric-optics regime

$$g^{\rm B}_{\alpha\beta} \equiv \langle g_{\alpha\beta}\rangle \qquad g_{\alpha\beta} = g^{\rm B}_{\alpha\beta} + \varepsilon h_{\alpha\beta} + \varepsilon^2 j_{\alpha\beta} + O(\varepsilon^3)$$

$$\begin{aligned} 0 &= G_{\alpha\beta} \\ &= G_{\alpha\beta}[g^{\rm B}_{cd}] + \varepsilon G^{(1)}_{\alpha\beta}[h_{cd}; g^{\rm B}_{ef}] + \varepsilon^2 G^{(1)}_{\alpha\beta}[j_{cd}; g^{\rm B}_{ef}] + \varepsilon^2 G^{(2)}_{\alpha\beta}[h_{cd}; g^{\rm B}_{ef}] \\ &\quad + O(\varepsilon^3)\ . \end{aligned}$$

$$G_{\alpha\beta}[g^{\rm B}_{cd}] = 0, \qquad G^{(1)}_{\alpha\beta}[h_{cd}; g^{\rm B}_{ef}] = 0\ , \qquad G^{(1)}_{\alpha\beta}[j_{cd}; g^{\rm B}_{ef}] = -G^{(2)}_{\alpha\beta}[h_{cd}; g^{\rm B}_{ef}]$$

GWs carry energy and momentum

Average Einstein equations on scale >> λ and << L

$$\Delta j_{\alpha\beta} = j_{\alpha\beta} - \langle j_{\alpha\beta} \rangle$$

$$G^{(1)}_{\alpha\beta}[\langle j_{cd} \rangle; g^{\rm B}_{ef}] = -\langle G^{(2)}_{\alpha\beta}[h_{cd}; g^{\rm B}_{ef}] \rangle$$

$$G^{(1)}_{\alpha\beta}[\Delta j_{cd}] = -G^{(2)}_{\alpha\beta}[h_{cd}; g^{\rm B}_{ef}] + \langle G^{(2)}_{\alpha\beta}[h_{cd}; g^{\rm B}_{ef}] \rangle$$

$$G_{\alpha\beta}[g^{\rm B}_{cd} + \varepsilon^2 \langle j_{cd} \rangle] = 8\pi G\, T^{\rm GW,eff}_{\alpha\beta} + O(\varepsilon^3) \qquad T^{\rm GW,eff}_{\alpha\beta} = -\frac{1}{8\pi G} \langle G^{(2)}_{\alpha\beta}[h_{cd}; g^{\rm B}_{ef}] \rangle$$

Using gauge freedom and integrating by parts:

$$T^{\rm GW,eff}_{\alpha\beta} = \frac{1}{32\pi G} \left\langle \nabla^{\rm B}_{\alpha} h^{\rm TT}_{\rho\sigma}\, \nabla^{\rm B}_{\beta} h^{\rho\sigma}_{\rm TT} \right\rangle$$

$$L_{\text{mass quadrupole}} \equiv \frac{1}{5} \frac{G}{c^5} \langle \dddot{I} \rangle^2 = \frac{1}{5} \frac{G}{c^5} \langle \dddot{\mathcal{I}}_{jk} \dddot{\mathcal{I}}_{jk} \rangle^2$$

$$\dddot{\mathcal{I}}_{jk} \sim \frac{(\text{mass of the system in motion}) \times (\text{size of the system})^2}{(\text{time scale})^3} \sim \frac{MR^2}{\tau^3} \sim \frac{Mv^2}{\tau}$$

BH binaries inspiral till (effective) ISCO

From energy balance:

$$\frac{\dot{P}_b}{P_b} = -\frac{3}{2}\frac{\dot{E}_b}{E_b}$$

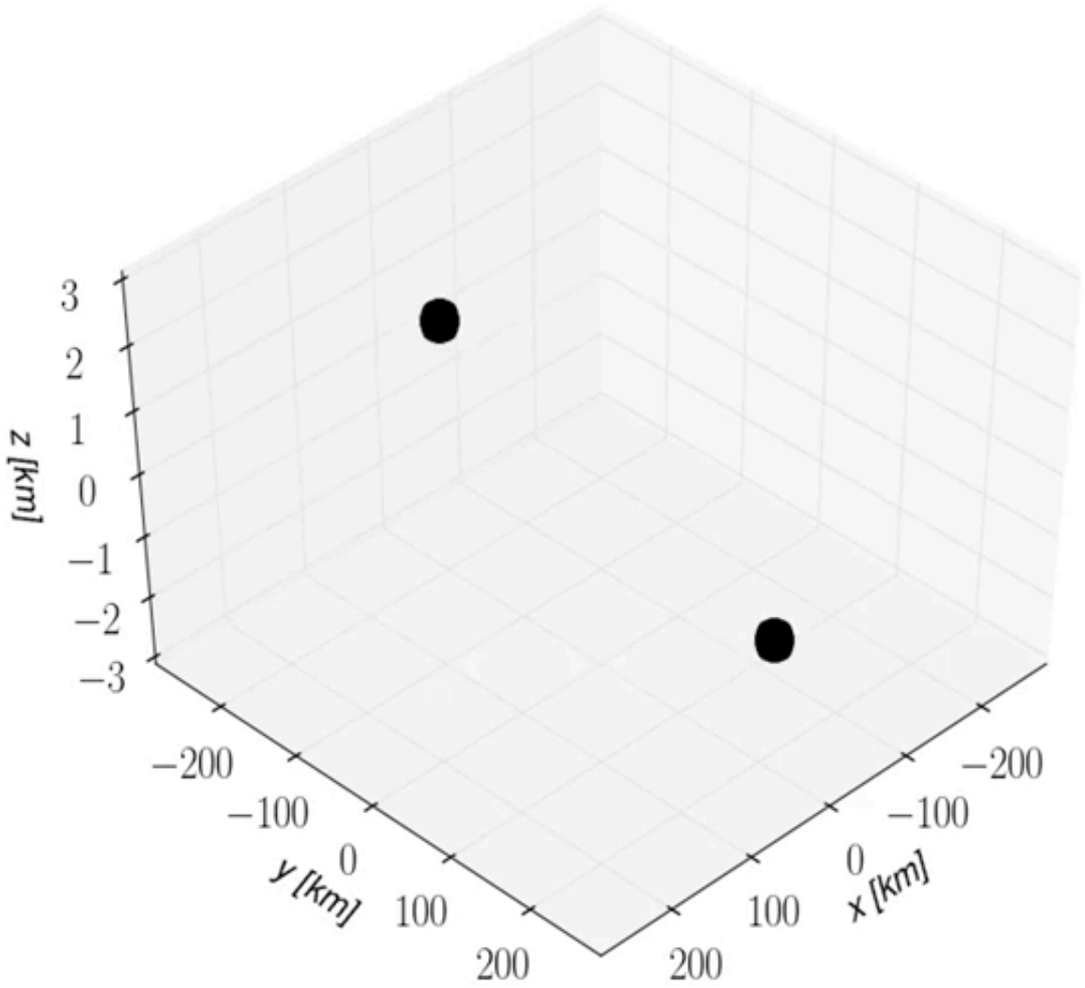

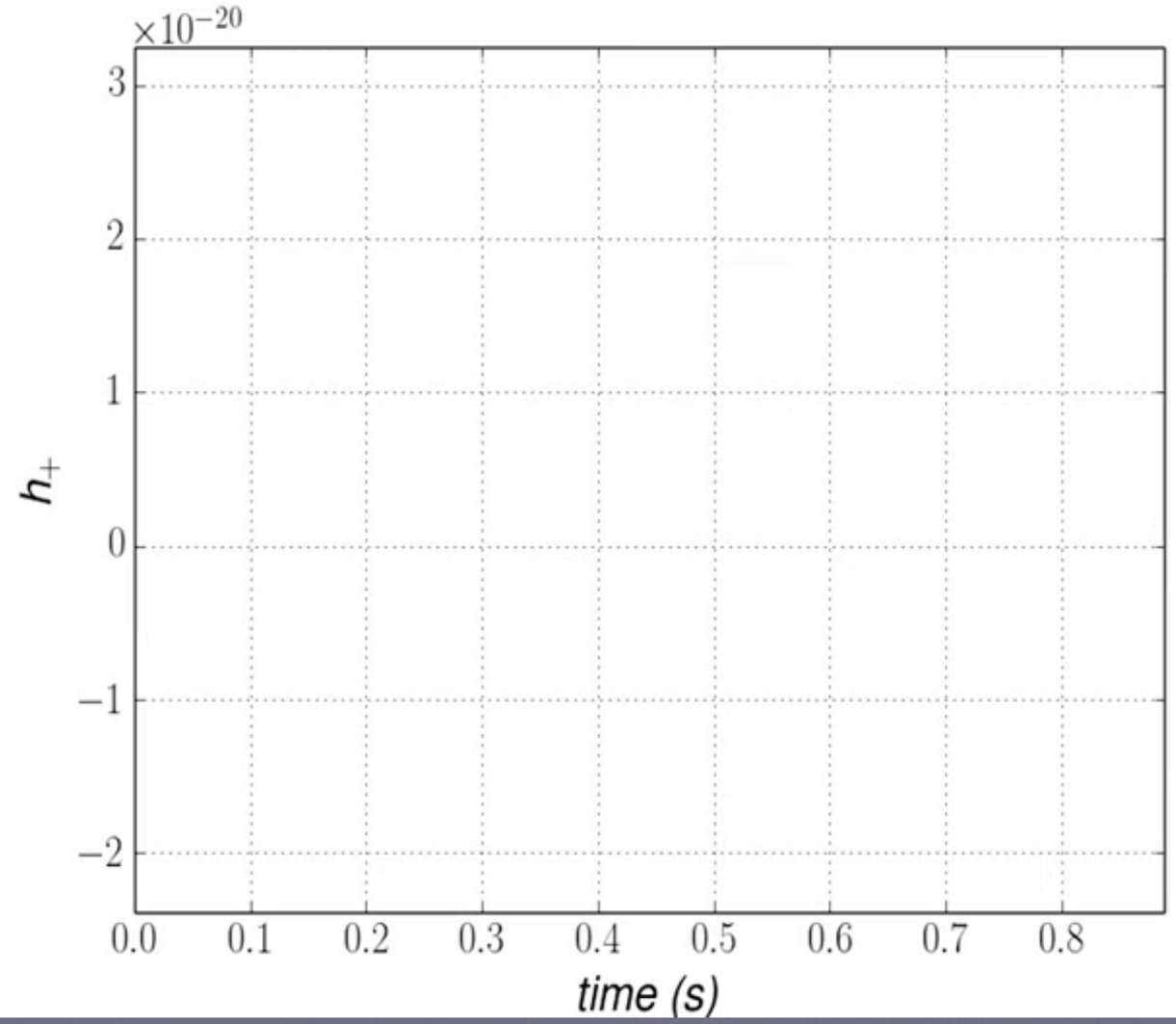

GWs from binary BHs

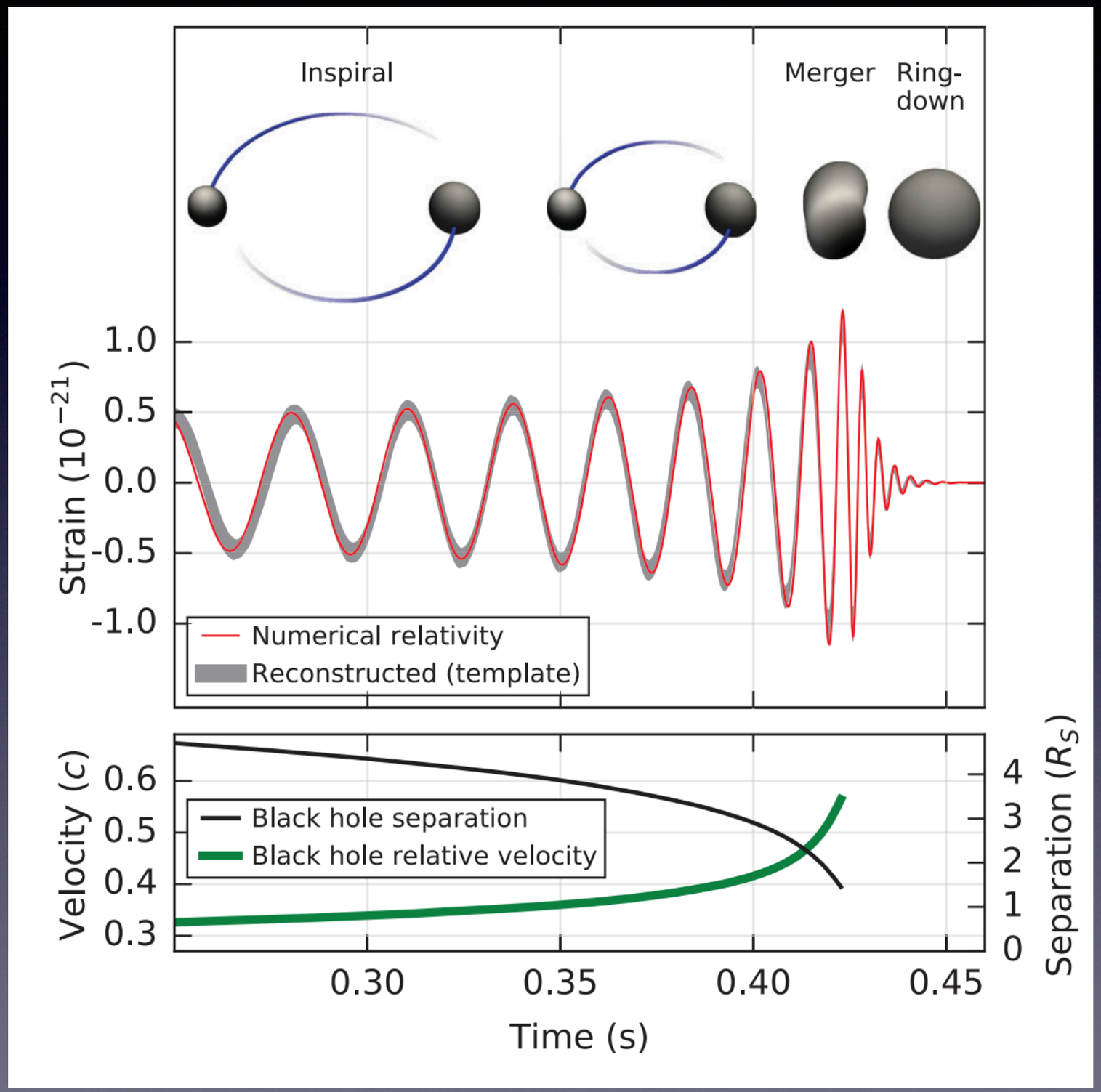

LSC collaboration 2015

GWs from binary BHs

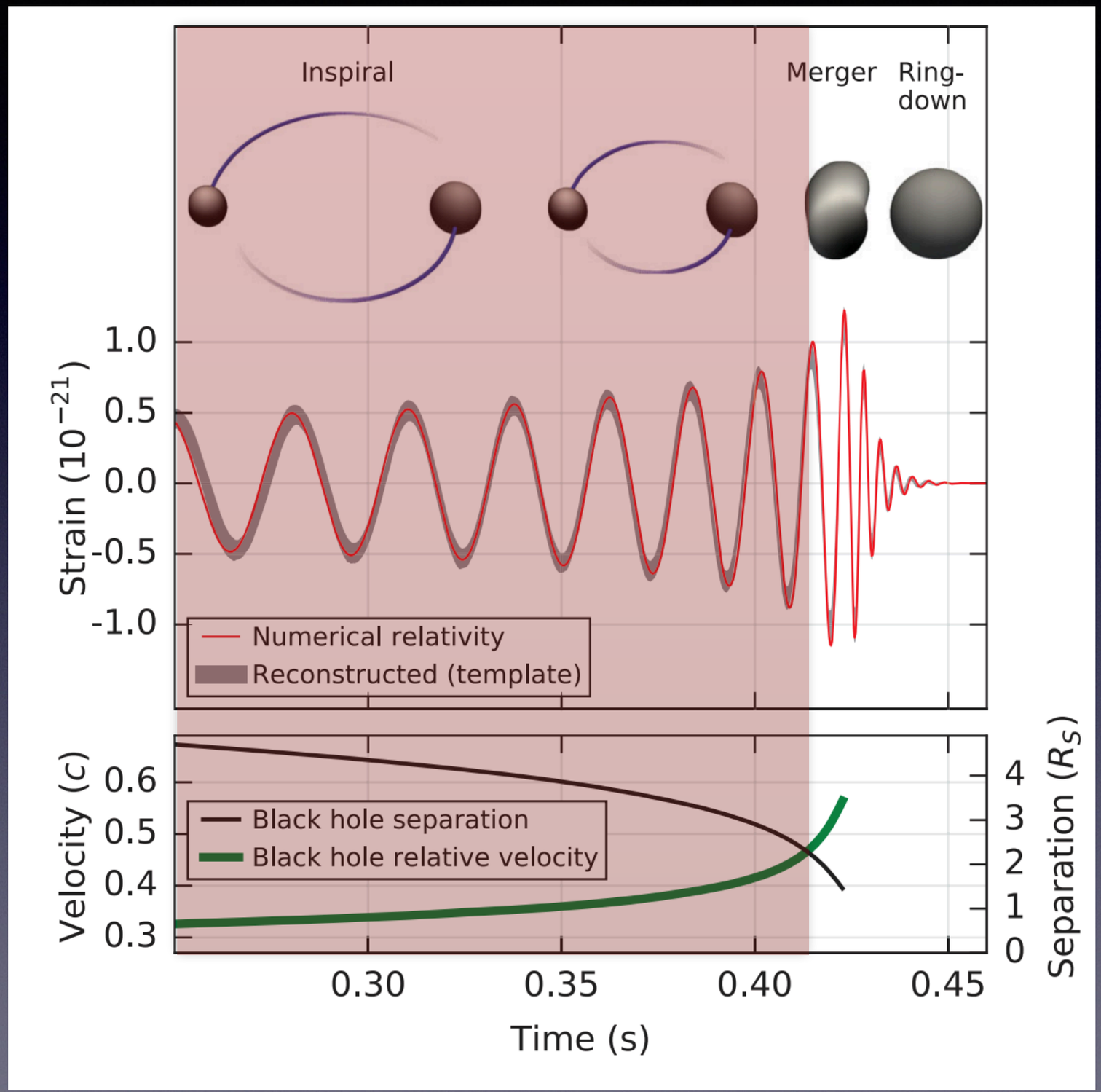

LSC collaboration 2015

Extracting the BH masses

$$\mathcal{M} = \frac{(m_1 m_2)^{3/5}}{(m_1 + m_2)^{1/5}} = \frac{c^3}{G}\left[\frac{5}{96}\pi^{-8/3} f^{-11/3} \dot{f}\right]^{3/5}$$

$$\mathcal{M} \simeq 30 M_\odot$$

$$M = m_1 + m_2 \gtrsim 70 M_\odot$$

$$2GM/c^2 \gtrsim 210 \text{ km}$$

f_{gw}~ 75 Hz corresponds to r_{12}~350 km

Objects in GW150914 must be BHs (not WDs or NSs)

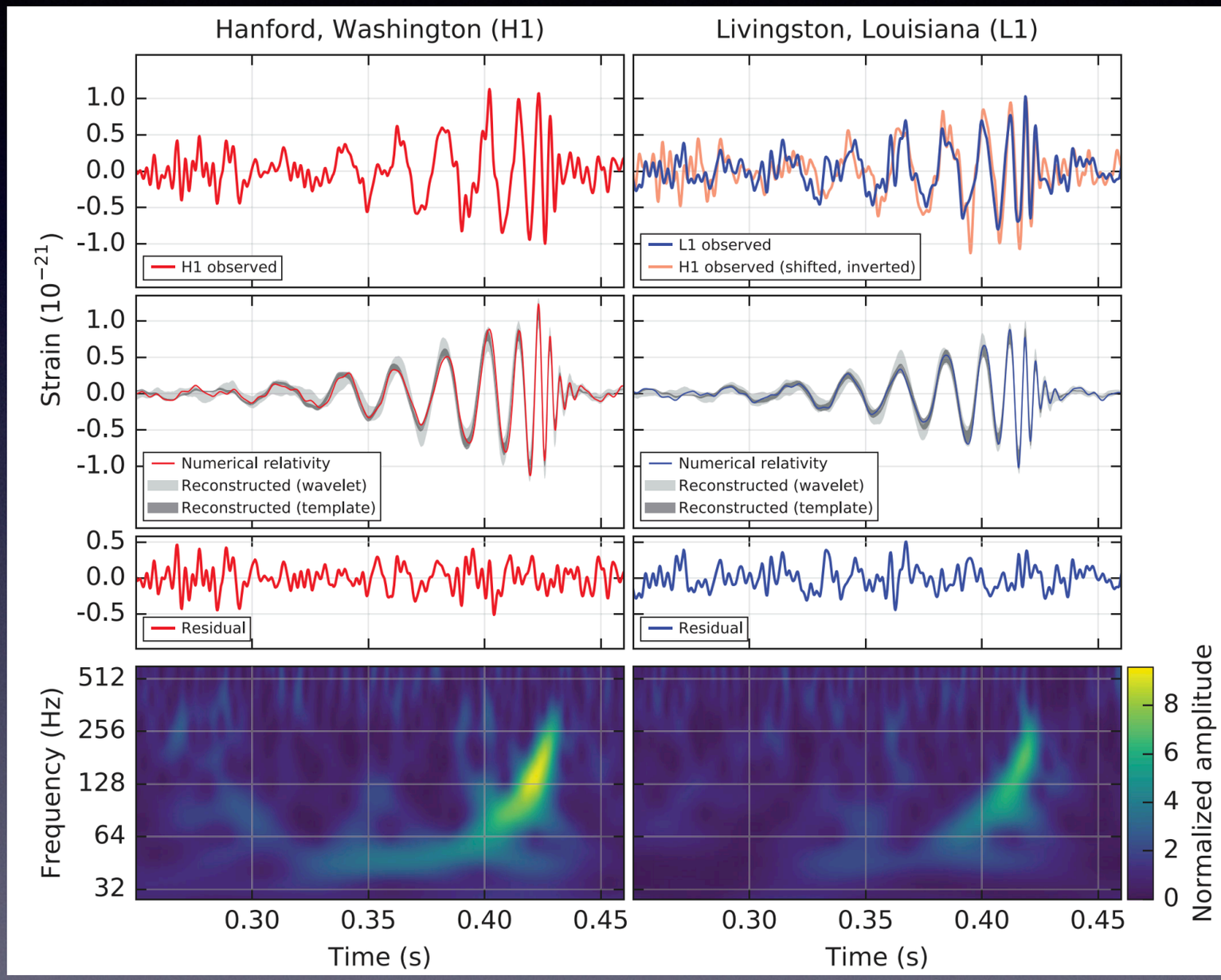

LSC collaboration 2015

Extracting the BH masses

Event	$m_1/M_\odot$	$m_2/M_\odot$	$\mathcal{M}/M_\odot$	$\chi_{\rm eff}$	$M_{\rm f}/M_\odot$	$a_{\rm f}$	$E_{\rm rad}/(M_\odot c^2)$	$\ell_{\rm peak}/({\rm erg\,s^{-1}})$	$d_L/{\rm Mpc}$	z	$\Delta\Omega/{\rm deg}^2$
GW150914	$35.6^{+4.8}_{-3.0}$	$30.6^{+3.0}_{-4.4}$	$28.6^{+1.6}_{-1.5}$	$-0.01^{+0.12}_{-0.13}$	$63.1^{+3.3}_{-3.0}$	$0.69^{+0.05}_{-0.04}$	$3.1^{+0.4}_{-0.4}$	$3.6^{+0.4}_{-0.4}\times10^{56}$	430^{+150}_{-170}	$0.09^{+0.03}_{-0.03}$	179
GW151012	$23.3^{+14.0}_{-5.5}$	$13.6^{+4.1}_{-4.8}$	$15.2^{+2.0}_{-1.1}$	$0.04^{+0.28}_{-0.19}$	$35.7^{+9.9}_{-3.8}$	$0.67^{+0.13}_{-0.11}$	$1.5^{+0.5}_{-0.5}$	$3.2^{+0.8}_{-1.7}\times10^{56}$	1060^{+540}_{-480}	$0.21^{+0.09}_{-0.09}$	1555
GW151226	$13.7^{+8.8}_{-3.2}$	$7.7^{+2.2}_{-2.6}$	$8.9^{+0.3}_{-0.3}$	$0.18^{+0.20}_{-0.12}$	$20.5^{+6.4}_{-1.5}$	$0.74^{+0.07}_{-0.05}$	$1.0^{+0.1}_{-0.2}$	$3.4^{+0.7}_{-1.7}\times10^{56}$	440^{+180}_{-190}	$0.09^{+0.04}_{-0.04}$	1033
GW170104	$31.0^{+7.2}_{-5.6}$	$20.1^{+4.9}_{-4.5}$	$21.5^{+2.1}_{-1.7}$	$-0.04^{+0.17}_{-0.20}$	$49.1^{+5.2}_{-3.9}$	$0.66^{+0.08}_{-0.10}$	$2.2^{+0.5}_{-0.5}$	$3.3^{+0.6}_{-0.9}\times10^{56}$	960^{+430}_{-410}	$0.19^{+0.07}_{-0.08}$	924
GW170608	$10.9^{+5.3}_{-1.7}$	$7.6^{+1.3}_{-2.1}$	$7.9^{+0.2}_{-0.2}$	$0.03^{+0.19}_{-0.07}$	$17.8^{+3.2}_{-0.7}$	$0.69^{+0.04}_{-0.04}$	$0.9^{+0.0}_{-0.1}$	$3.5^{+0.4}_{-1.3}\times10^{56}$	320^{+120}_{-110}	$0.07^{+0.02}_{-0.02}$	396
GW170729	$50.6^{+16.6}_{-10.2}$	$34.3^{+9.1}_{-10.1}$	$35.7^{+6.5}_{-4.7}$	$0.36^{+0.21}_{-0.25}$	$80.3^{+14.6}_{-10.2}$	$0.81^{+0.07}_{-0.13}$	$4.8^{+1.7}_{-1.7}$	$4.2^{+0.9}_{-1.5}\times10^{56}$	2750^{+1350}_{-1320}	$0.48^{+0.19}_{-0.20}$	1033
GW170809	$35.2^{+8.3}_{-6.0}$	$23.8^{+5.2}_{-5.1}$	$25.0^{+2.1}_{-1.6}$	$0.07^{+0.16}_{-0.16}$	$56.4^{+5.2}_{-3.7}$	$0.70^{+0.08}_{-0.09}$	$2.7^{+0.6}_{-0.6}$	$3.5^{+0.6}_{-0.9}\times10^{56}$	990^{+320}_{-380}	$0.20^{+0.05}_{-0.07}$	340
GW170814	$30.7^{+5.7}_{-3.0}$	$25.3^{+2.9}_{-4.1}$	$24.2^{+1.4}_{-1.1}$	$0.07^{+0.12}_{-0.11}$	$53.4^{+3.2}_{-2.4}$	$0.72^{+0.07}_{-0.05}$	$2.7^{+0.4}_{-0.3}$	$3.7^{+0.4}_{-0.5}\times10^{56}$	580^{+160}_{-210}	$0.12^{+0.03}_{-0.04}$	87
GW170817	$1.46^{+0.12}_{-0.10}$	$1.27^{+0.09}_{-0.09}$	$1.186^{+0.001}_{-0.001}$	$0.00^{+0.02}_{-0.01}$	≤ 2.8	≤ 0.89	≥ 0.04	$\geq 0.1\times10^{56}$	40^{+10}_{-10}	$0.01^{+0.00}_{-0.00}$	16
GW170818	$35.5^{+7.5}_{-4.7}$	$26.8^{+4.3}_{-5.2}$	$26.7^{+2.1}_{-1.7}$	$-0.09^{+0.18}_{-0.21}$	$59.8^{+4.8}_{-3.8}$	$0.67^{+0.07}_{-0.08}$	$2.7^{+0.5}_{-0.5}$	$3.4^{+0.5}_{-0.7}\times10^{56}$	1020^{+430}_{-360}	$0.20^{+0.07}_{-0.07}$	39
GW170823	$39.6^{+10.0}_{-6.6}$	$29.4^{+6.3}_{-7.1}$	$29.3^{+4.2}_{-3.2}$	$0.08^{+0.20}_{-0.22}$	$65.6^{+9.4}_{-6.6}$	$0.71^{+0.08}_{-0.10}$	$3.3^{+0.9}_{-0.8}$	$3.6^{+0.6}_{-0.9}\times10^{56}$	1850^{+840}_{-840}	$0.34^{+0.13}_{-0.14}$	1651

LSC 2018, O1+O2 detections

Extracting the BH masses

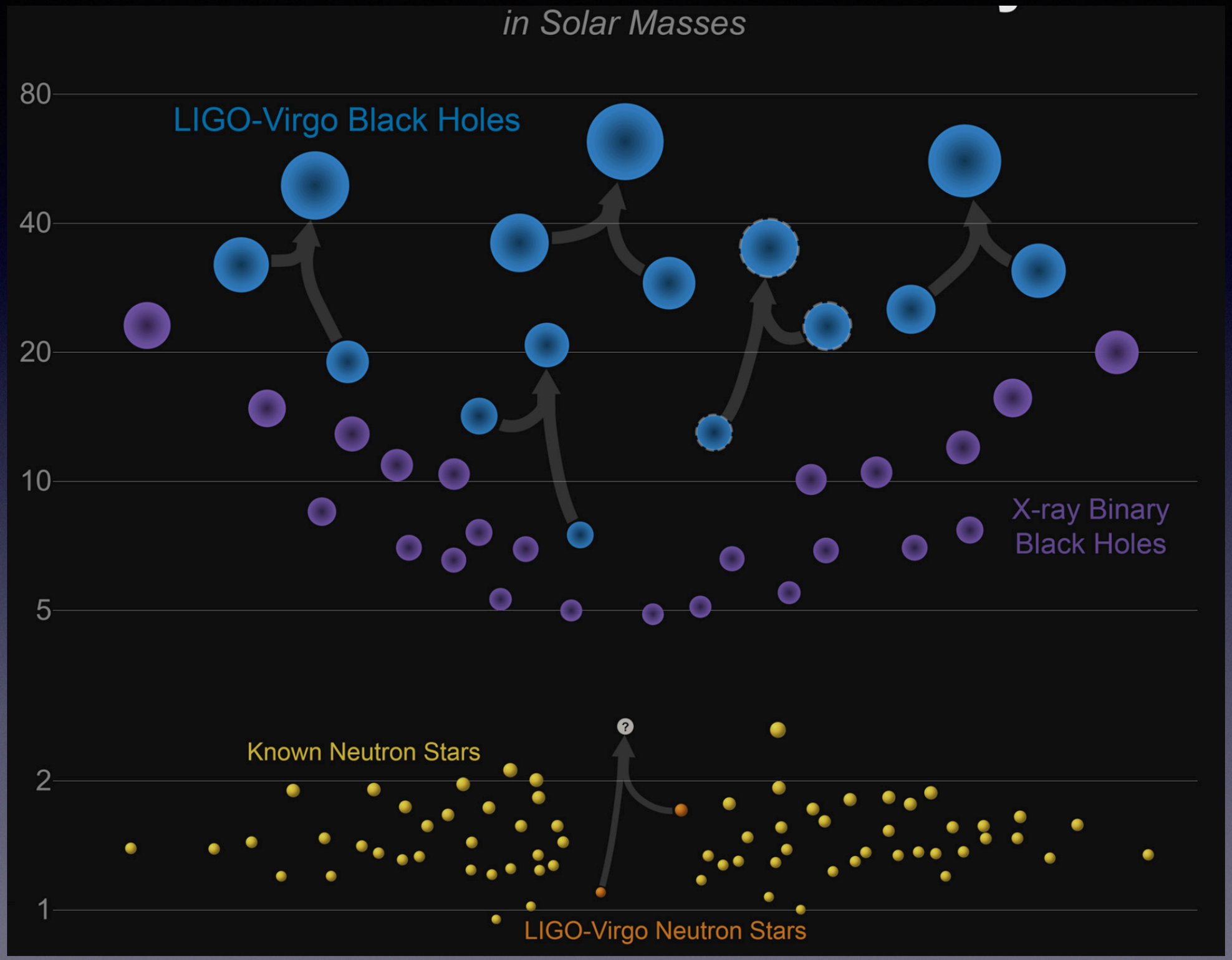

Figure: LSC collaboration 2018

The formation of stellar-mass BHs

- Stellar-mass BH form from massive stars
- Difficult problem: stellar evolution needed to understand mass loss from stellar winds, and explosion mechanism (core collapse SN, direct collapse to BH)
- Evolution depends on mass, metallicity, rotation

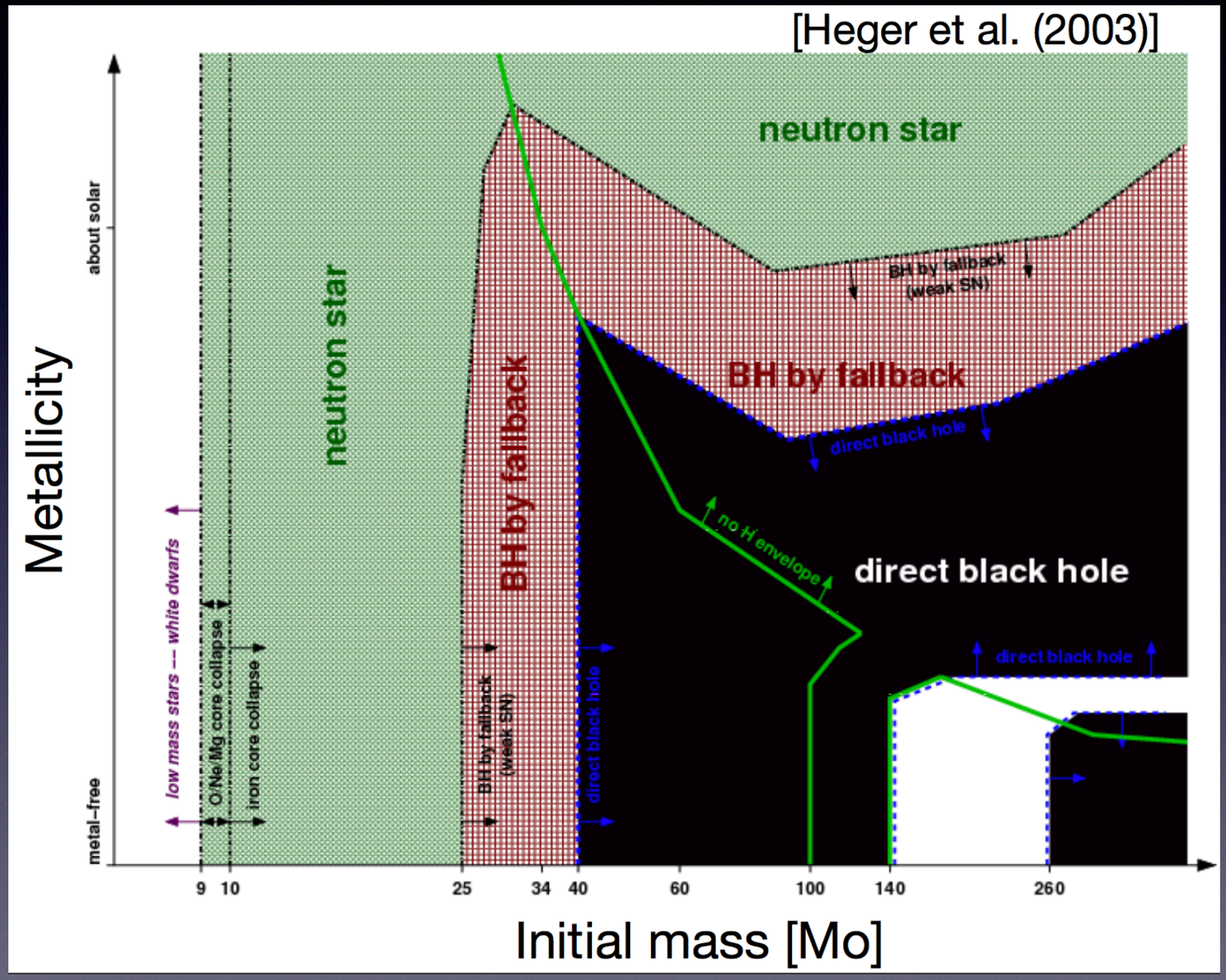

The role of metallicity and stellar winds

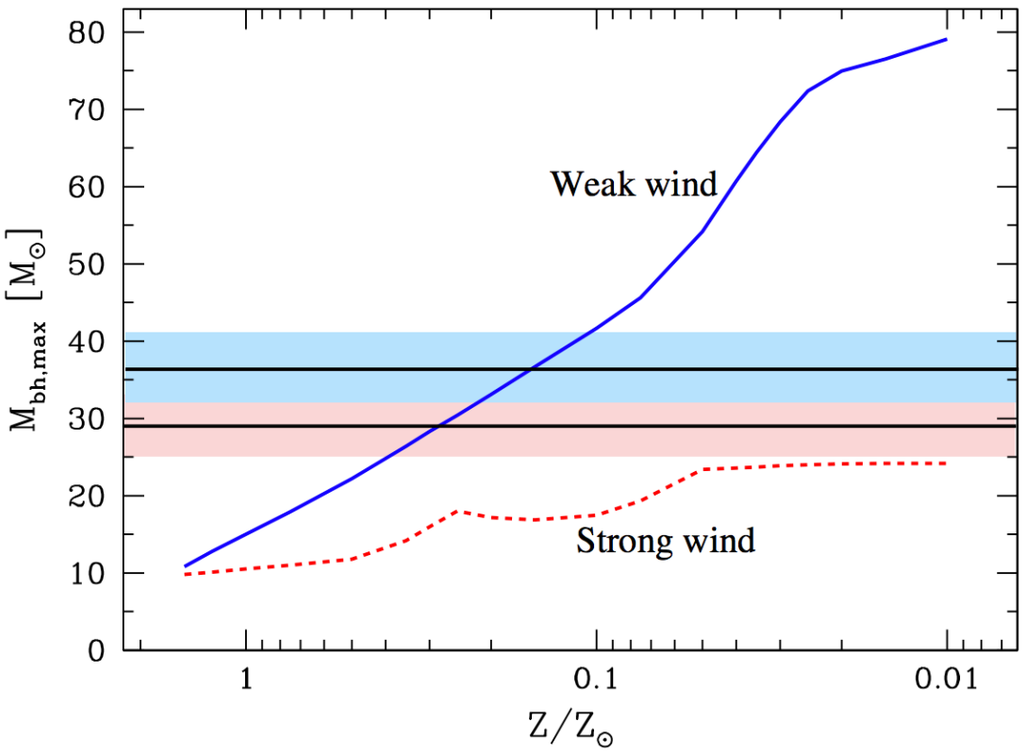

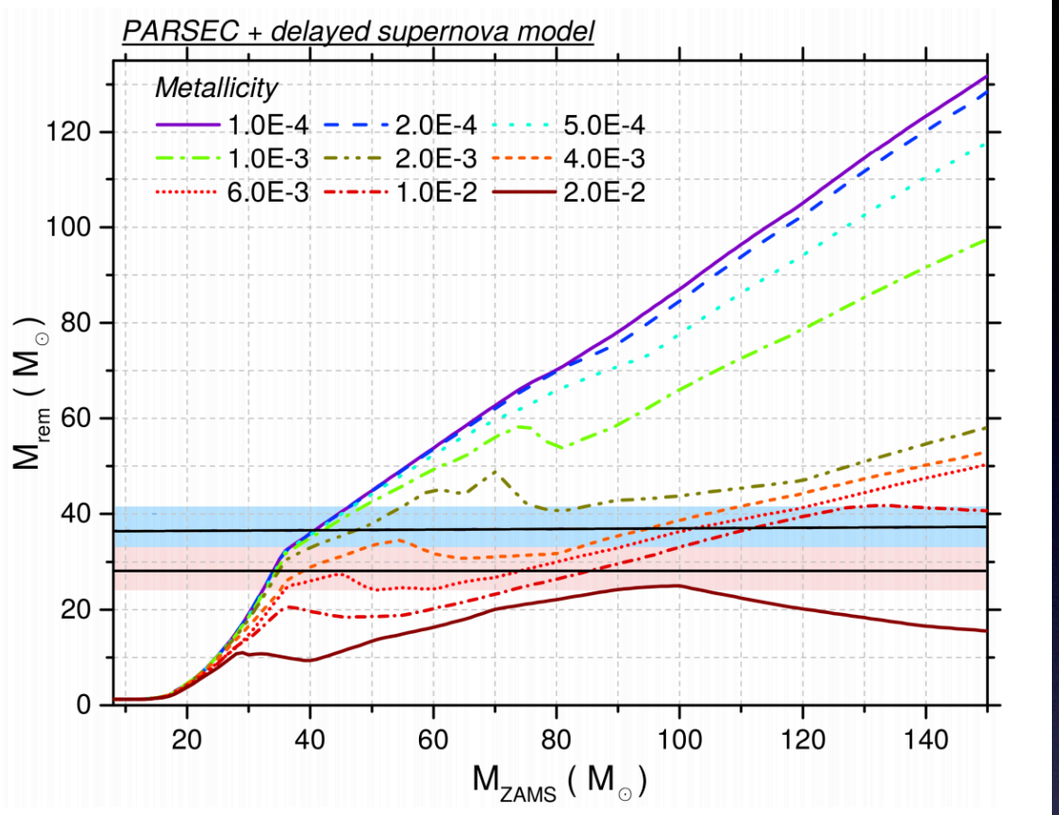

LSC 2015; Belczynski et al 2010; Spera et al 2015

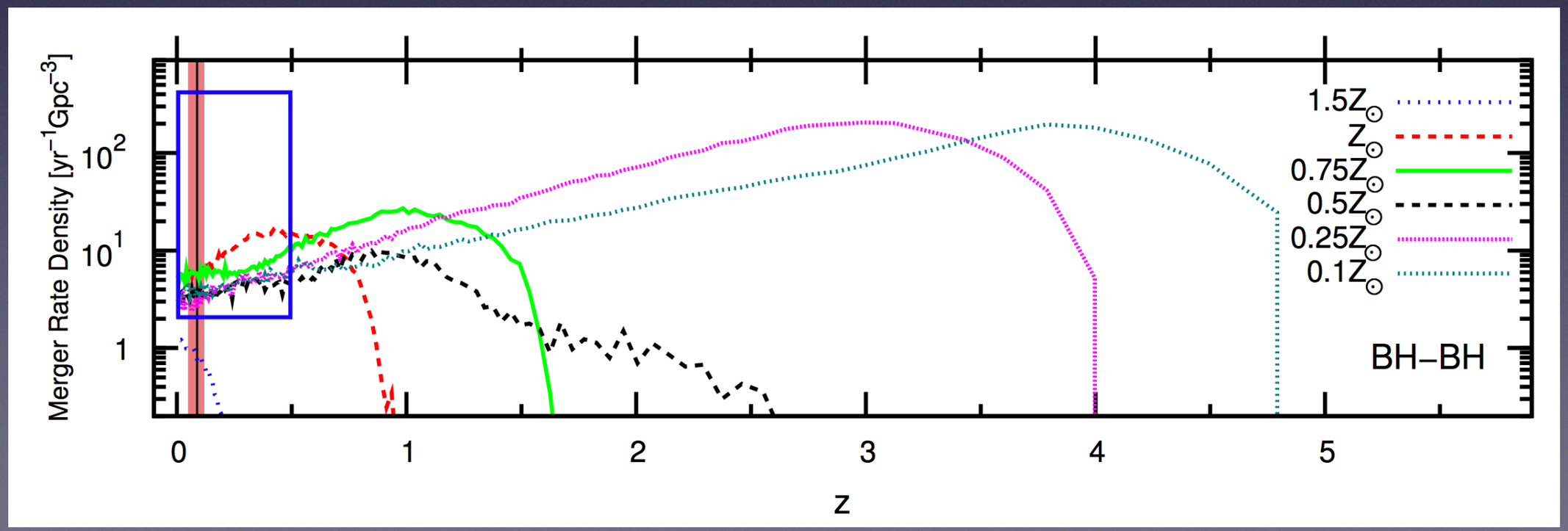

LSC 2015; Dominik et al 2013

The role of metallicity and stellar winds

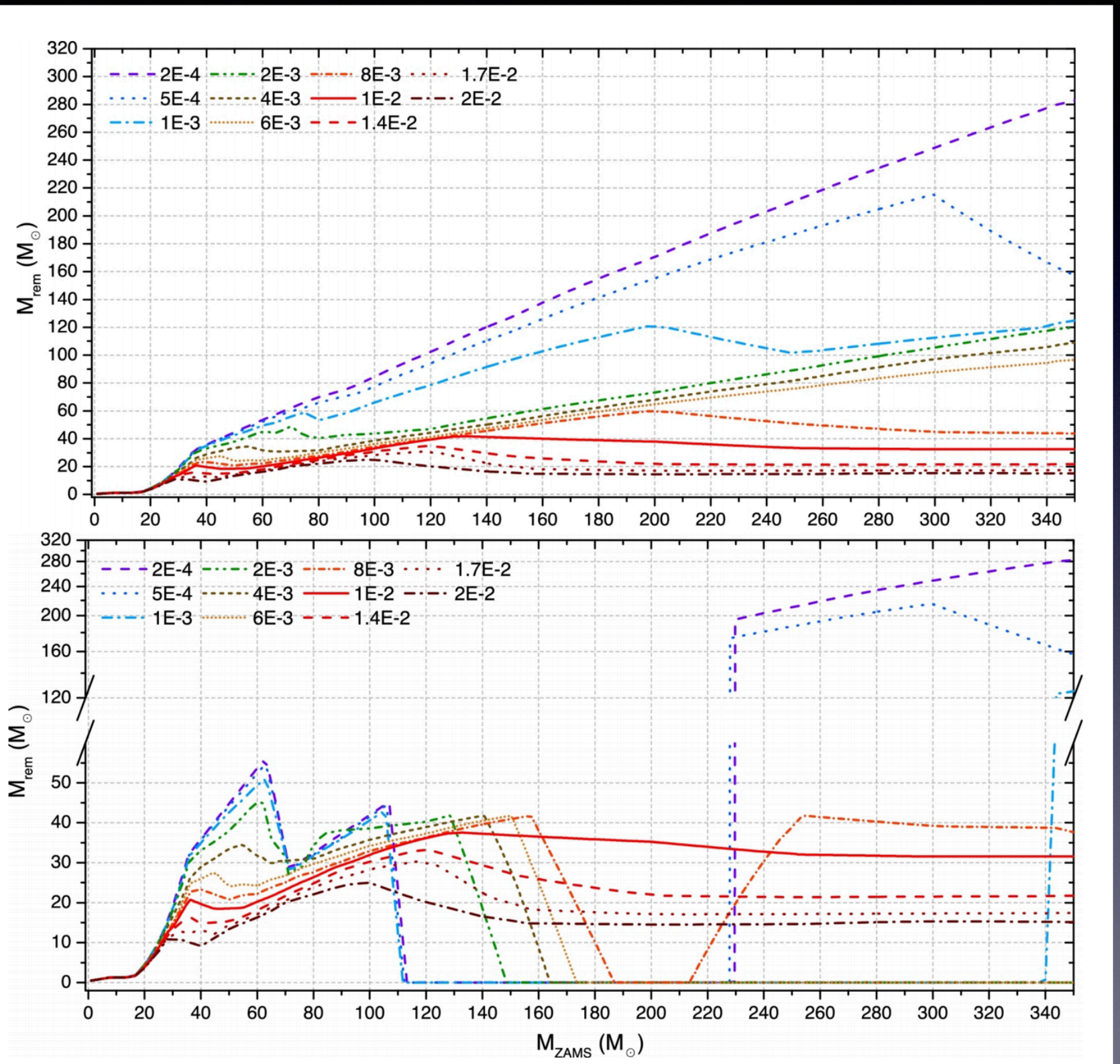

Mapelli 2018;
Spera & Mapelli 2017

Pair instability SN

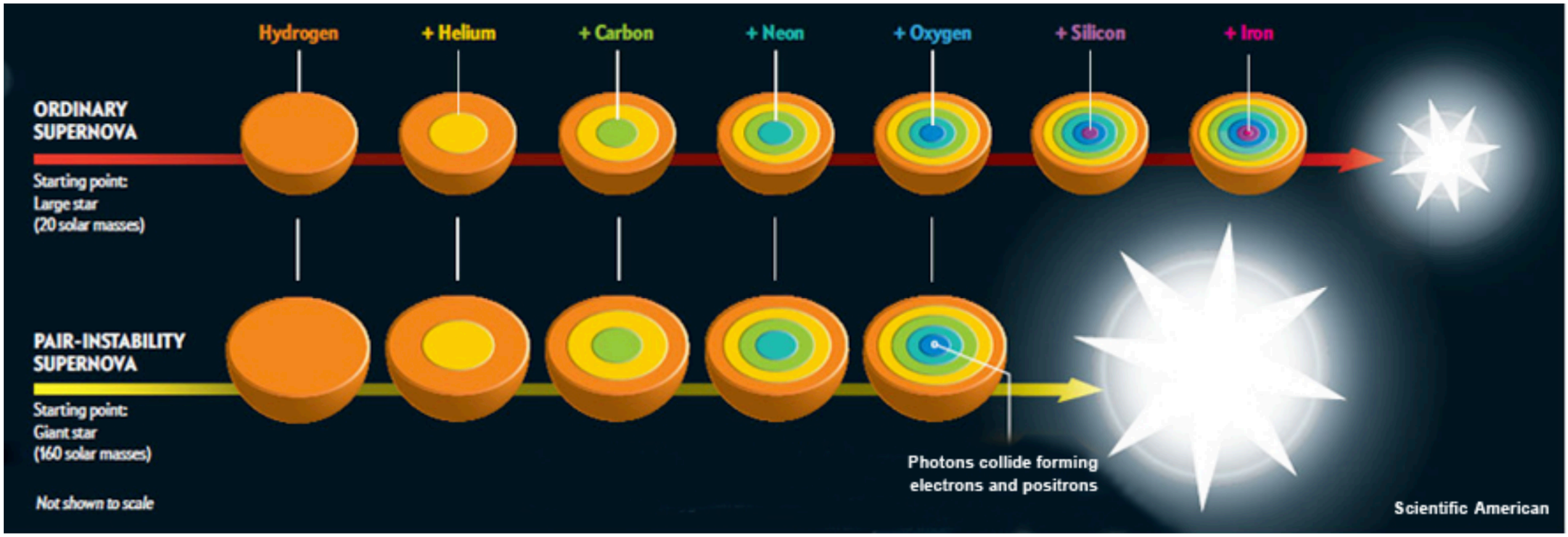

Mass at birth (solar masses)	Helium core mass (solar masses)	Compact remnant	Event
10–95	2–40	Neutron star, black hole	Ordinary supernova
95–130	40–60	Neutron star, black hole	Pulsational pair-instability supernova
130–260	60–137	Explosion, no remnant	Pair-instability supernova
>260	>137	Black hole	?

Woosley, Blinnikov, Heger (2007)

A cutoff at 40 Msun?

Mass at birth (solar masses)	Helium core mass (solar masses)	Compact remnant	Event
10–95	2–40	Neutron star, black hole	Ordinary supernova
95–130	40–60	Neutron star, black hole	Pulsational pair-instability supernova
130–260	60–137	Explosion, no remnant	Pair-instability supernova
>260	>137	Black hole	?

Woosley, Blinnikov, Heger (2007)

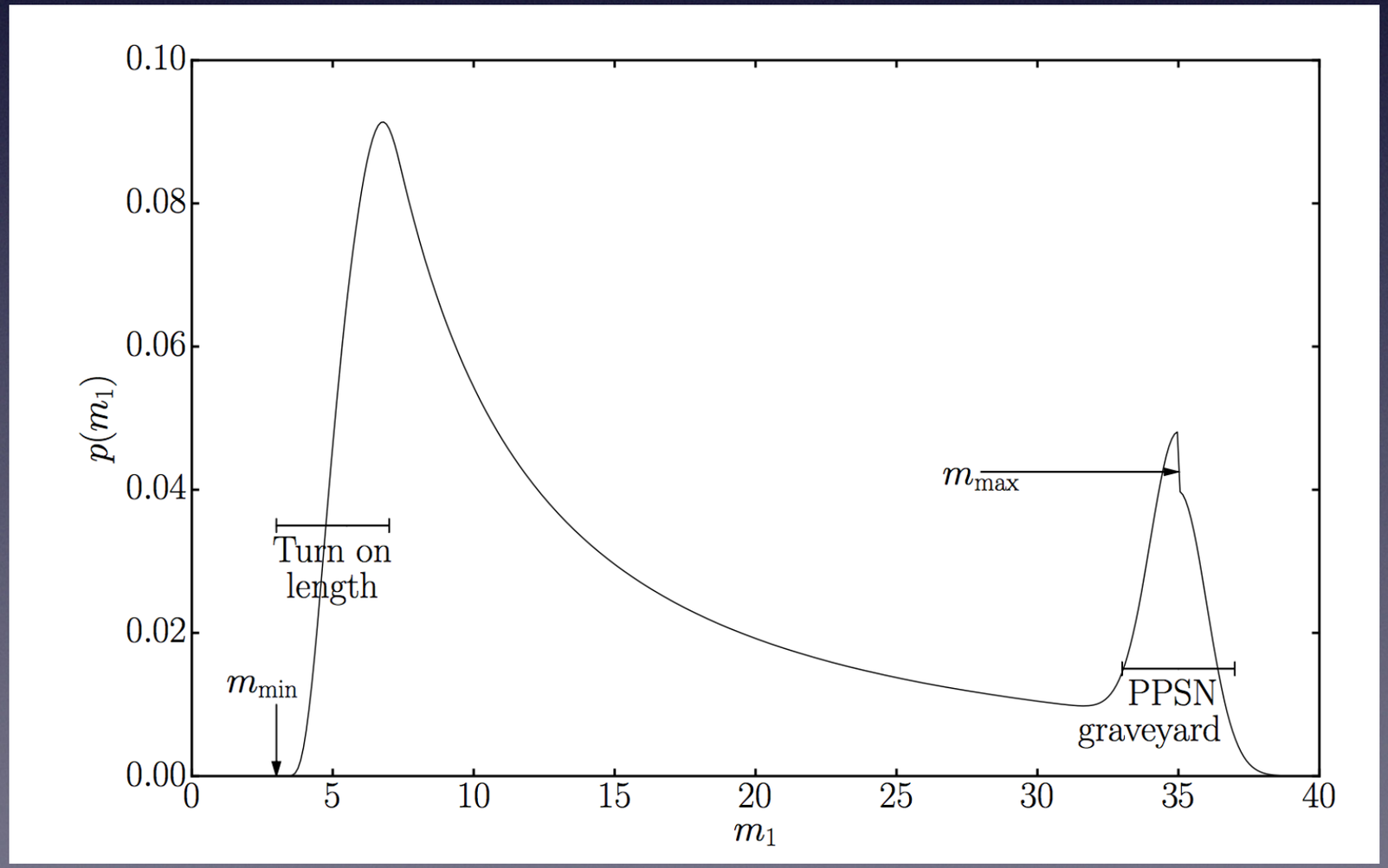

Talbot & Thrane 2018

Last week's updates!

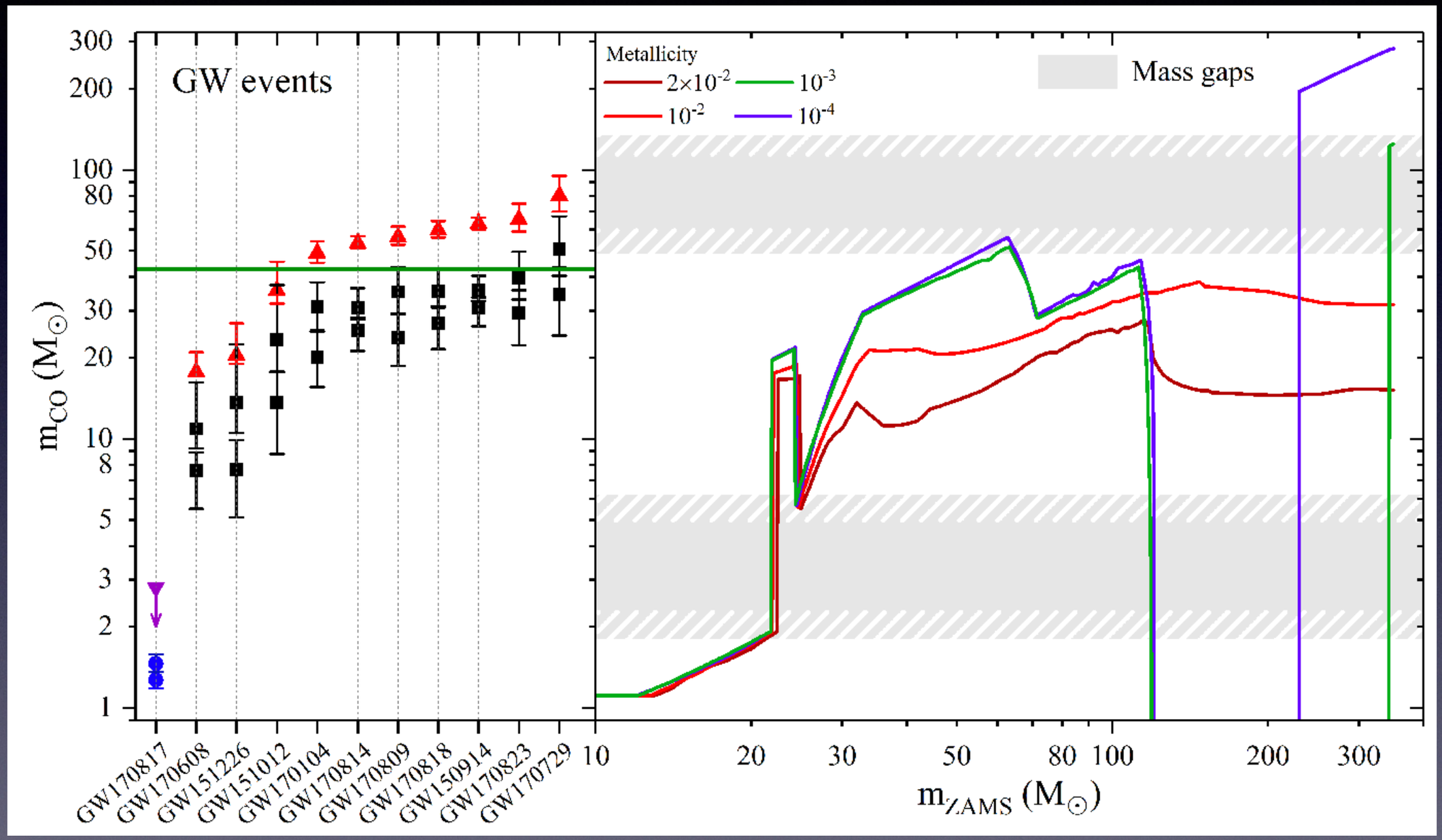

LSC 2018

How do stellar-mass BH *binaries* form?

- In the field (plausible because ~70% of massive stars have companion, c.f. Sana et al 2012)
- In dense environments (globular clusters/nuclear star clusters) via dynamical mechanisms
- Primordial BHs? But problems with CMB/absence of enough MW candidates in radio/X-rays if one wants to explain all of Dark Matter. Formation mechanism also unclear (clustering vs lack of clustering), conflicting predictions for spins

How do stellar-mass BH *binaries* form?

- In the field (plausible because ~70% of massive stars have companion, c.f. Sana et al 2012)
- In dense environments (globular clusters/nuclear star clusters) via dynamical mechanisms
- ~~Primordial BHs? But problems with CMB/absence of enough MW candidates in radio/X-rays if one wants to explain all of Dark Matter. Formation mechanism also unclear (clustering vs lack of clustering), conflicting predictions for spins~~

Field BH binaries

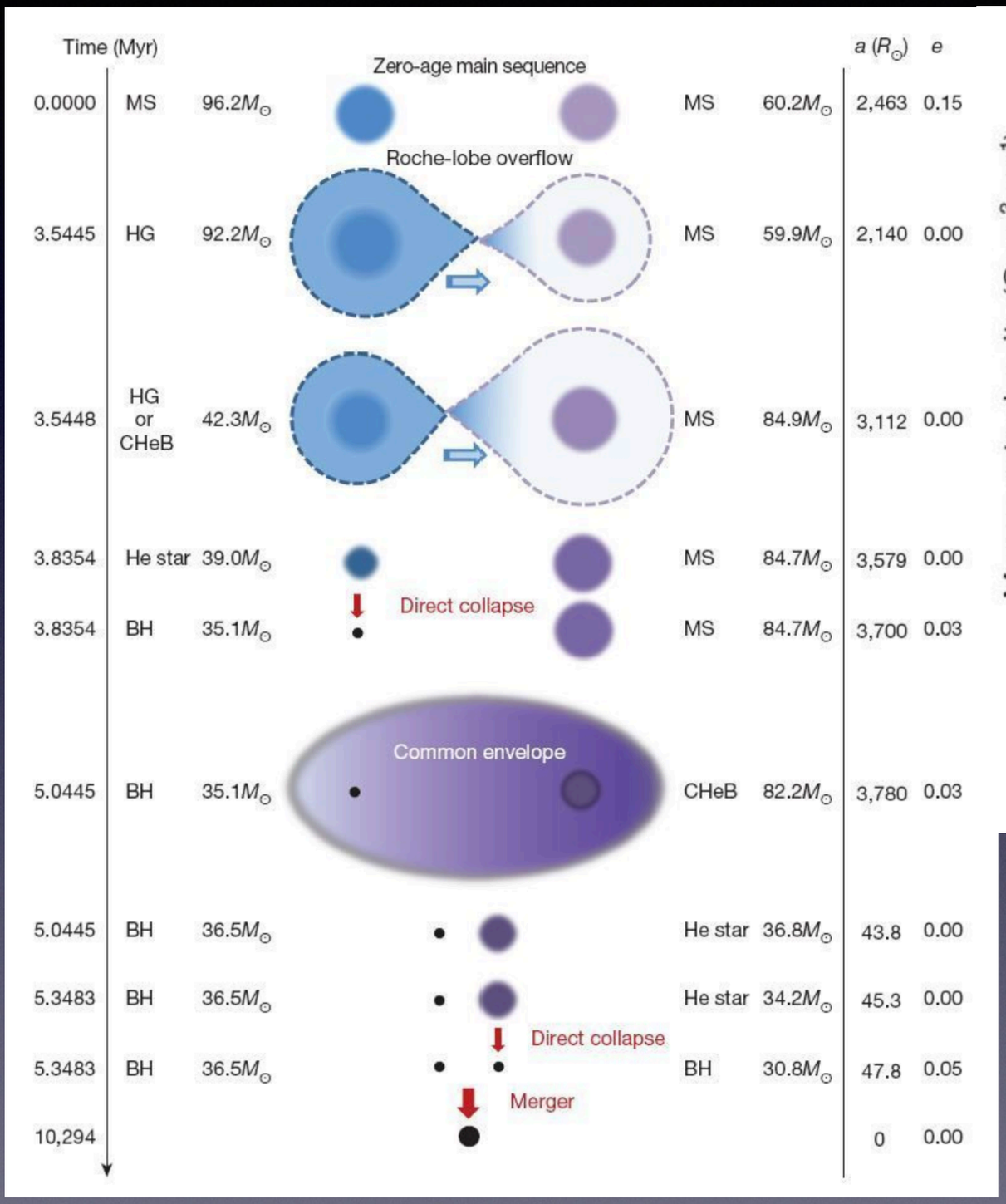

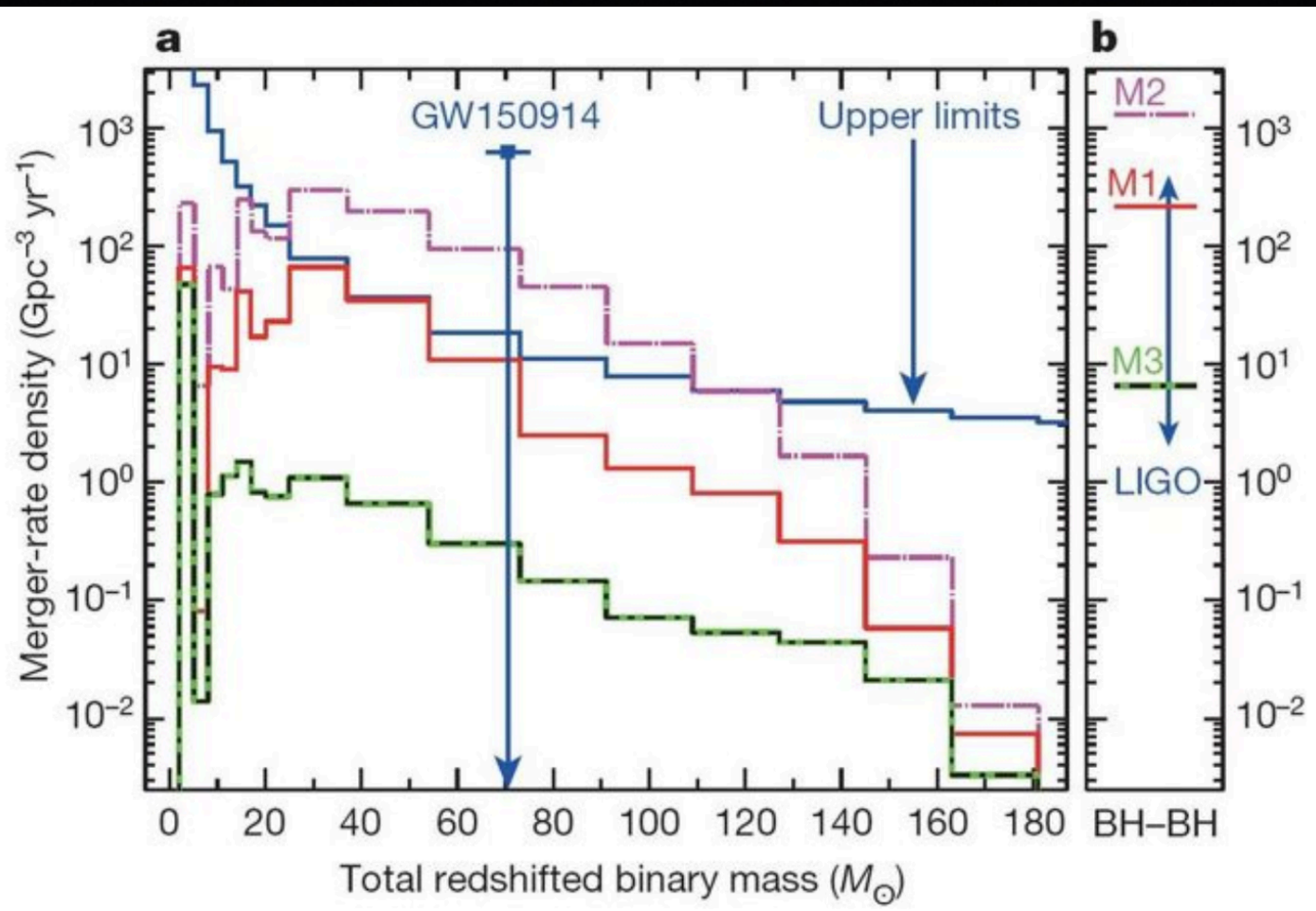

Merger rates for standard model (M1; red); optimistic common-envelope phase (M2; pink); and pessimistic large black-hole kicks (M3; green/black)

Belczynski et al 2016

Field BH binaries

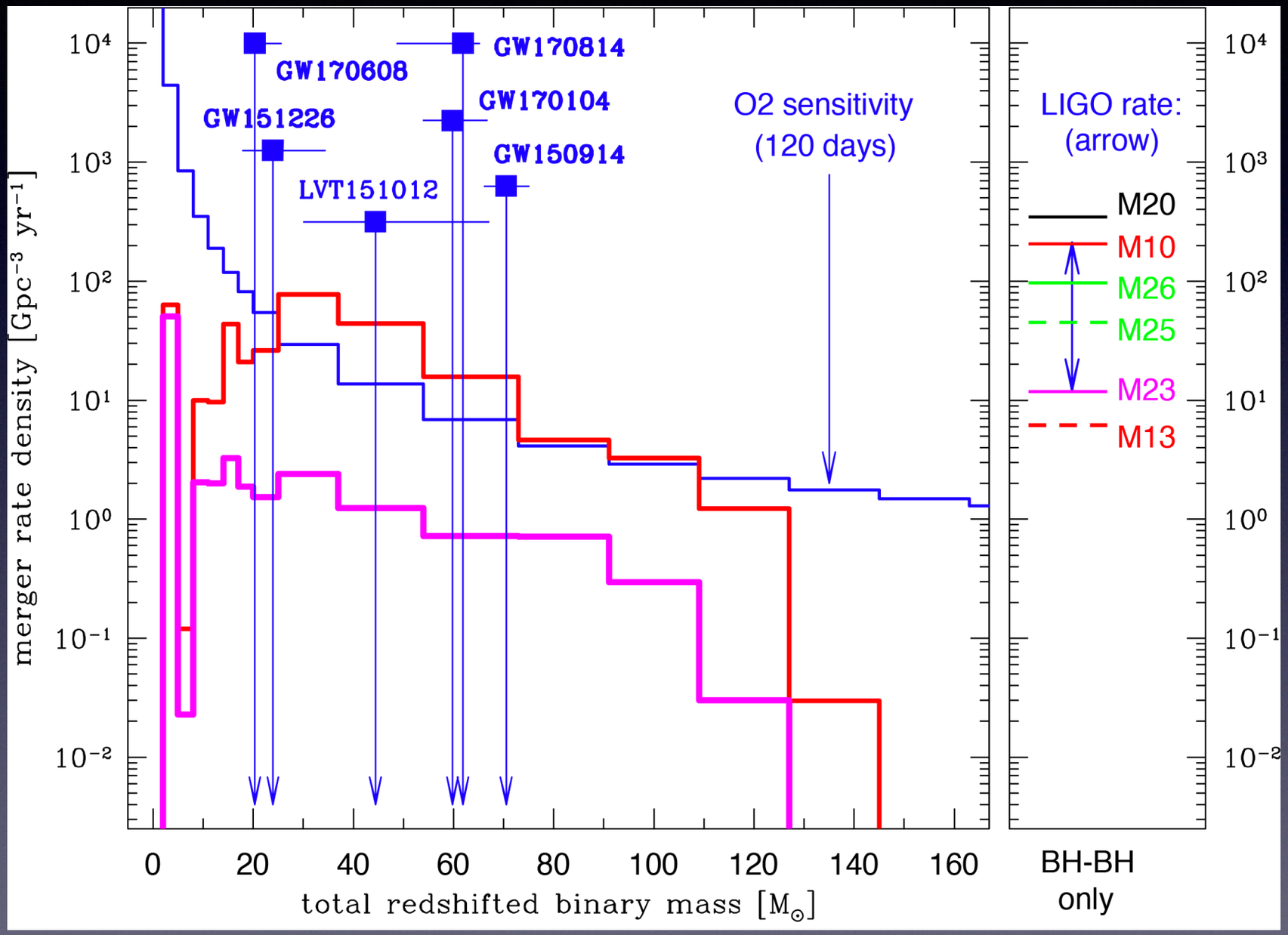

Decreasing natal kicks

From www.syntheticuniverse.org

Dynamical channel

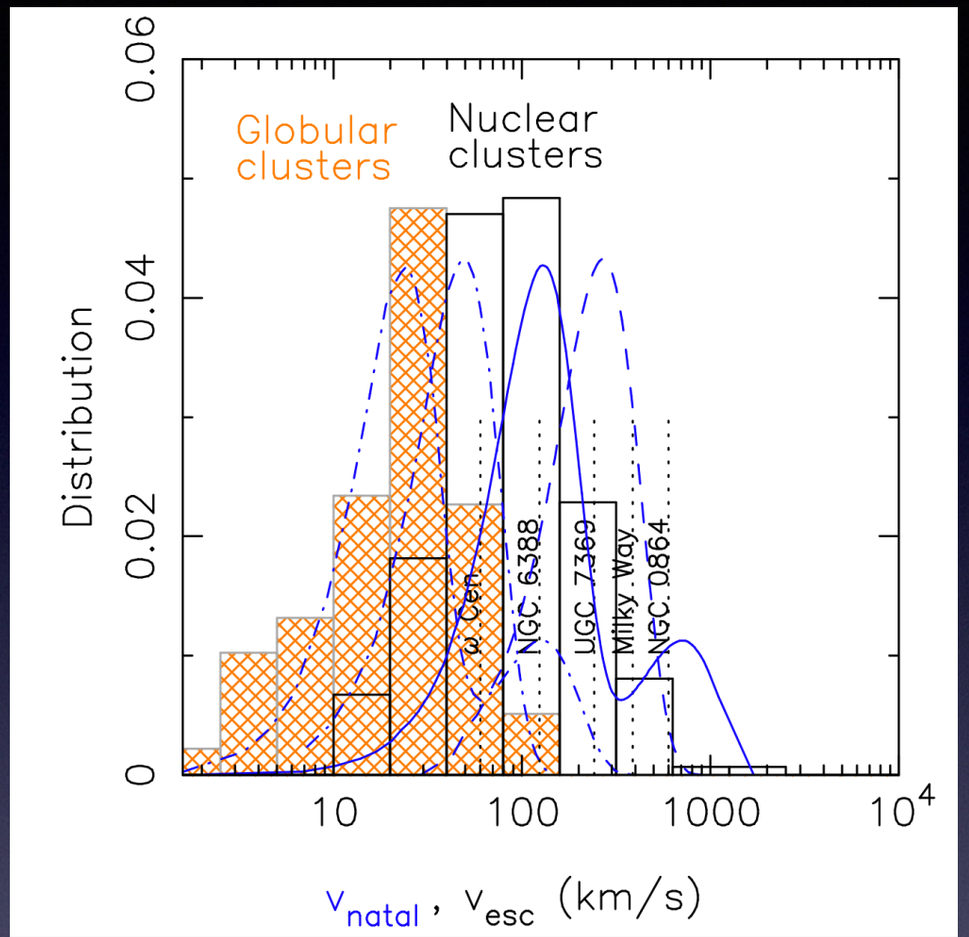

Antonini & Radio 2016

- Similar uncertainties (natal kicks)
- Possible in globular clusters and nuclear star clusters, or even in the field (field triples)
- May be as important as field channel

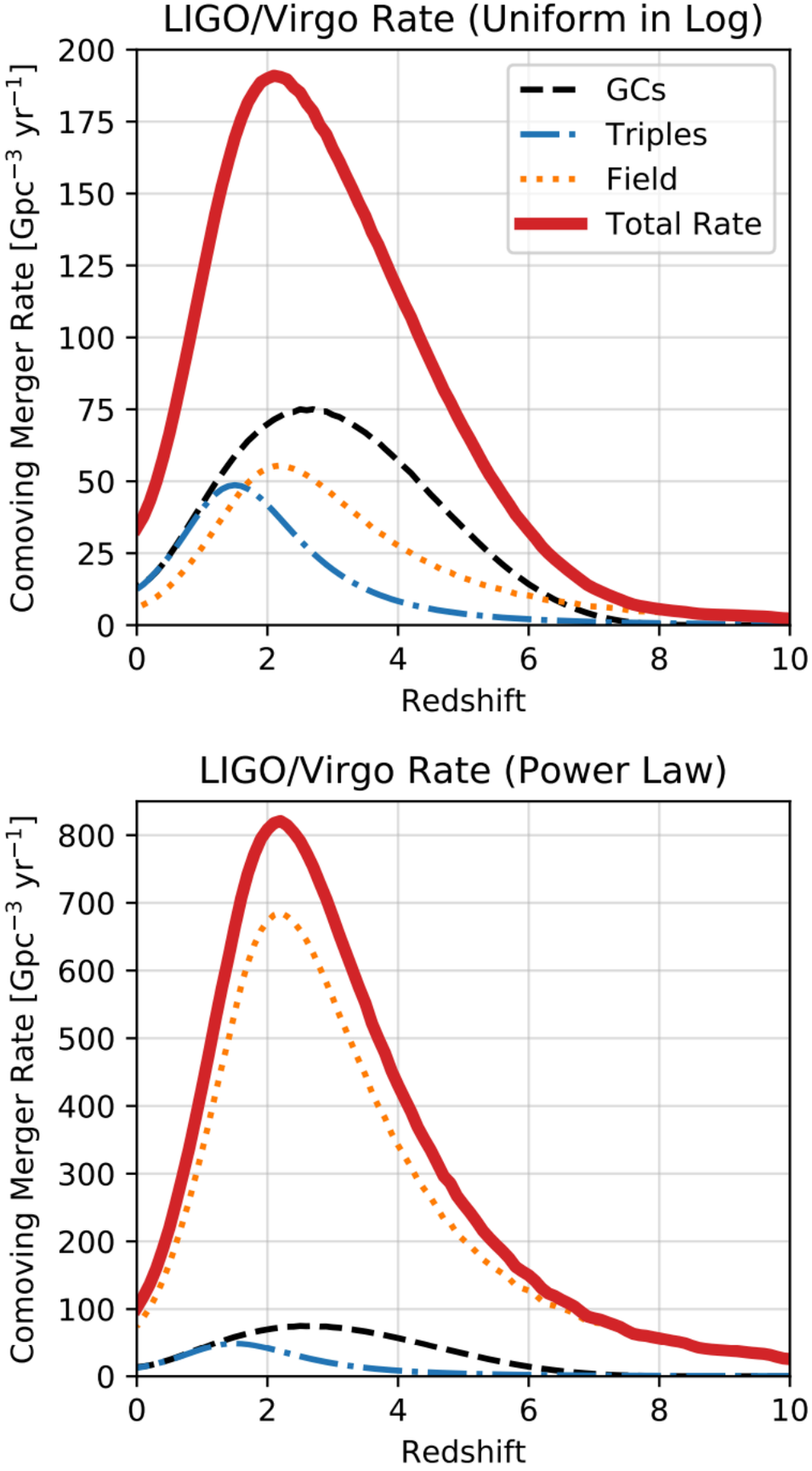

Rodriguez & Loeb 2018

The effect of BH spins: frame-dragging in binaries

- For large spins aligned with L, effective ISCO moves inward …

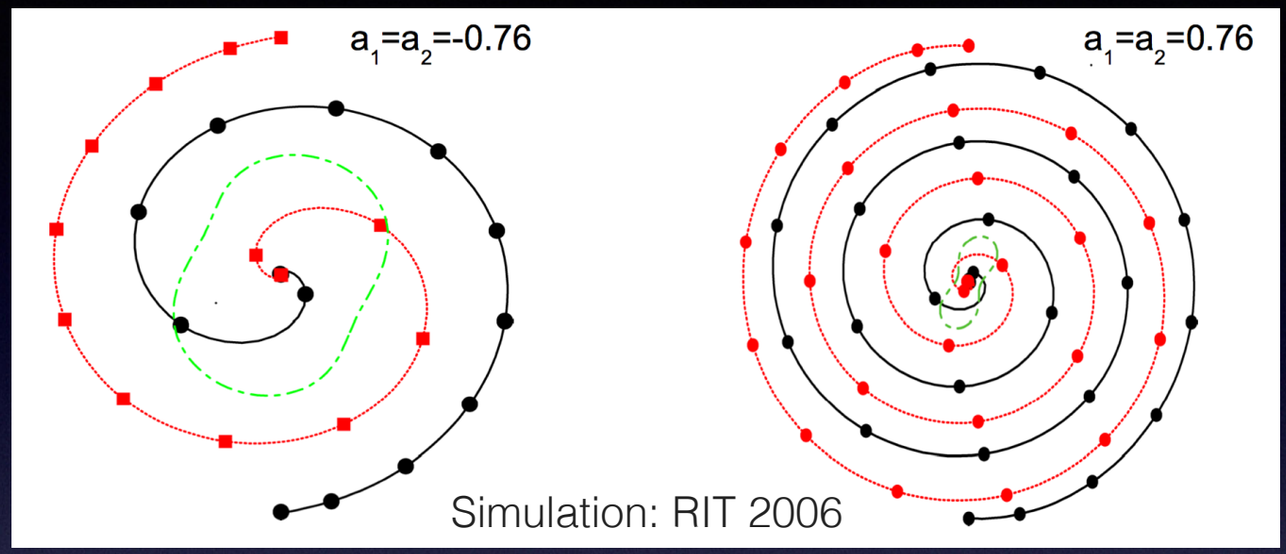

- ... and GW “efficiency” gets larger

Spins increase GW amplitudes

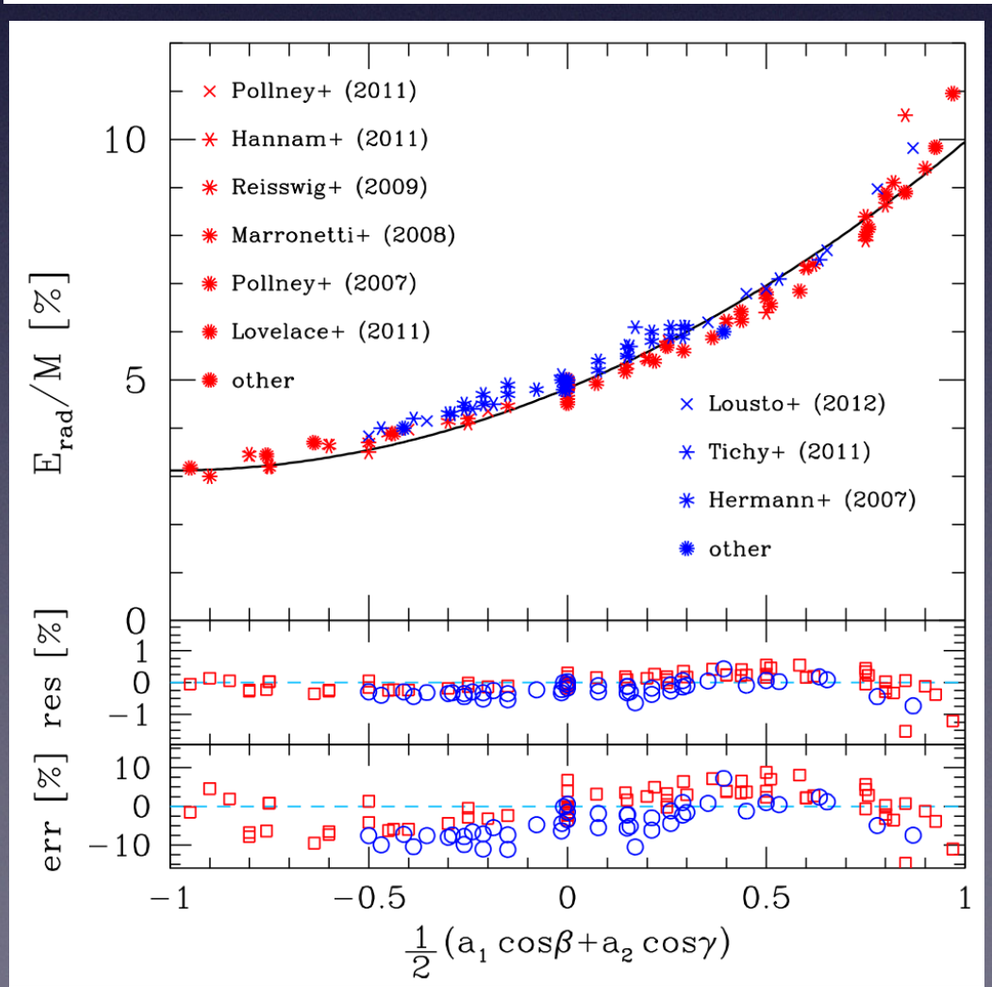

EB, Morozova & Rezzolla (2012)

BH spin precession

- Spin precesses around total angular momentum $J=L+S_1+S_2$
- Precession-induced modulations observable with GW detectors:

  - Increase SNR and improve measurements of binary parameters (e.g. luminosity distance and sky localization)

  - Allow measurements of angle between spins

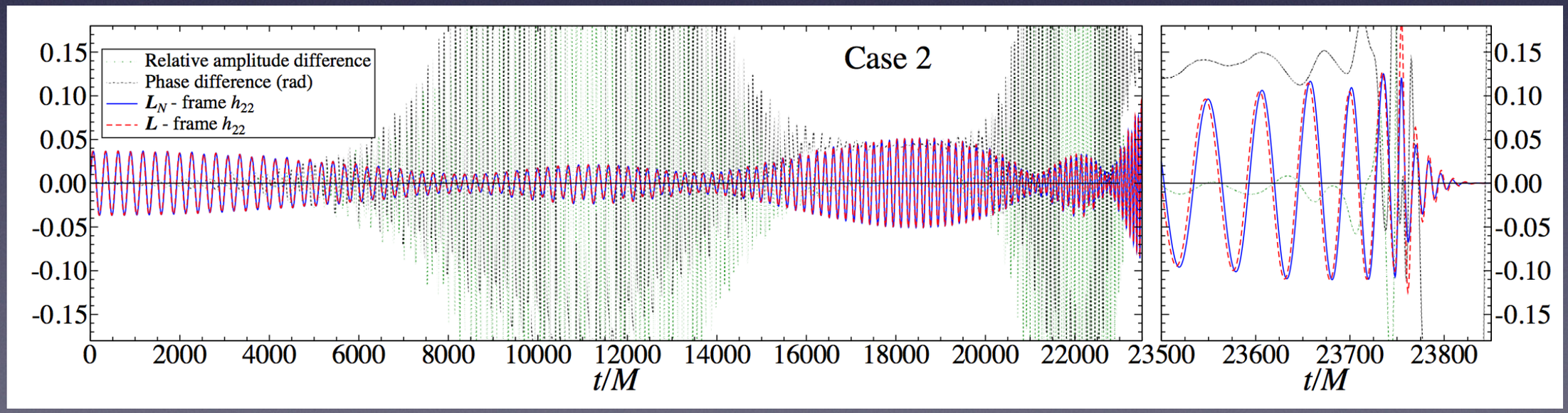

EOB waveforms for BH binary with mass ratio 1:6 and spins 0.6 and 0.8, from Pan et al (2013) [using spin-EOB model of EB & Buonanno 2010, 2011]

Measuring BH spins

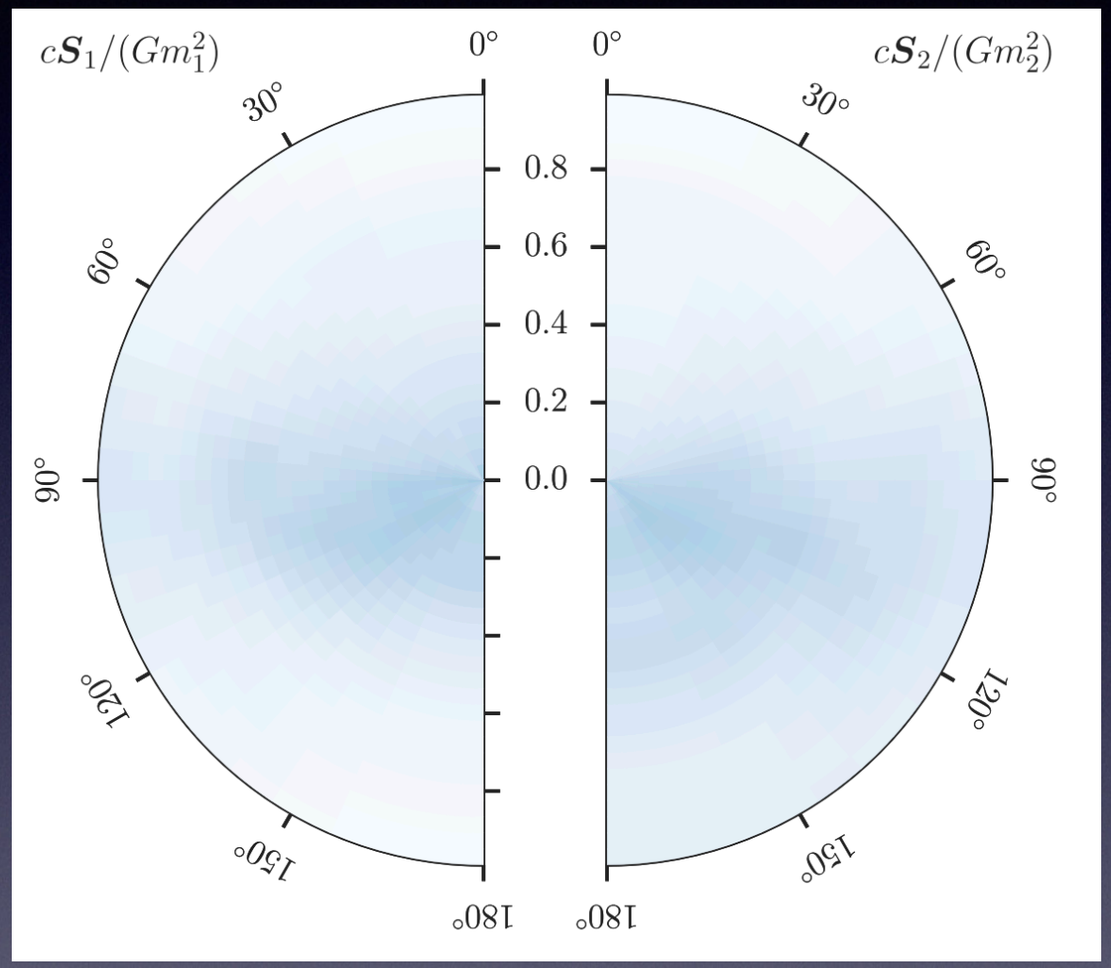

GW150914

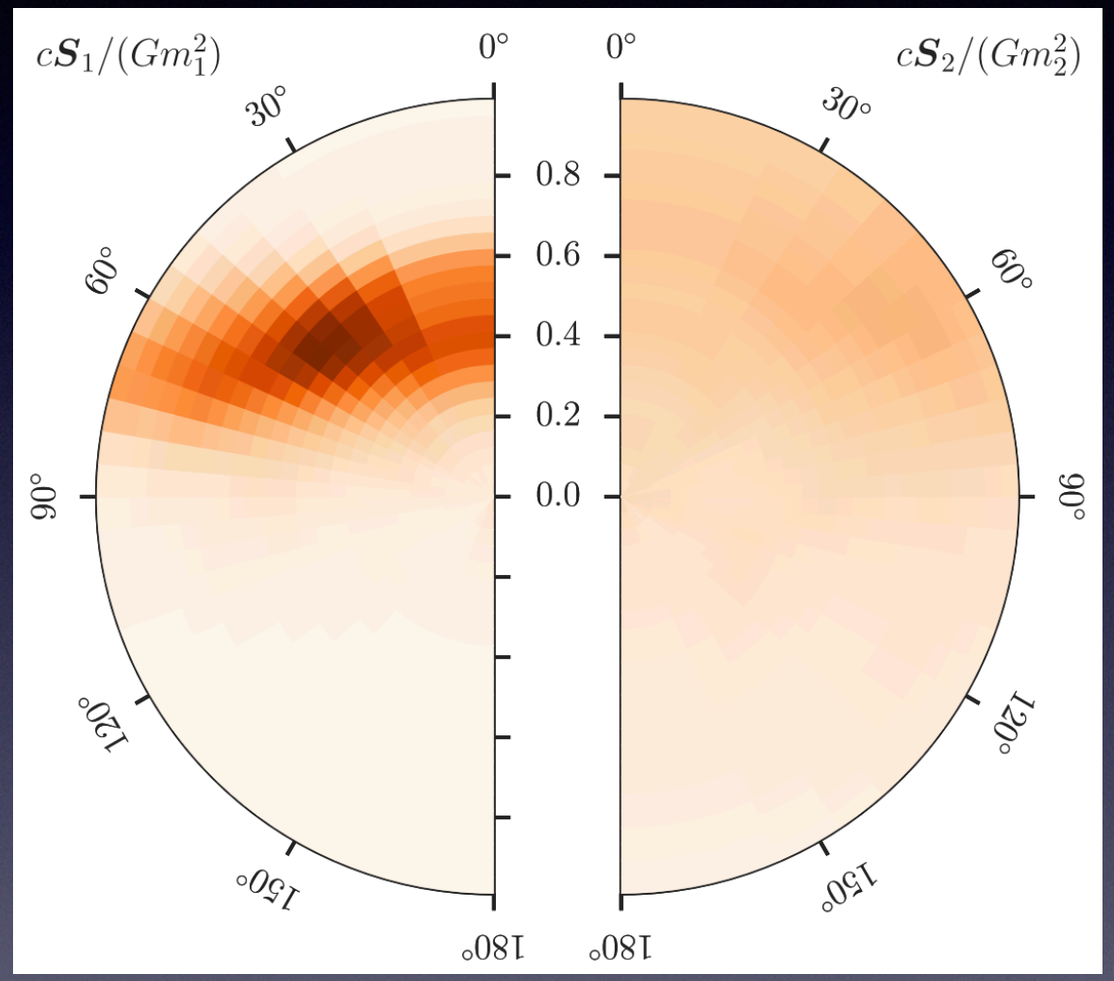

GW151226

Figures: LSC collaboration 2016

Measuring BH spins

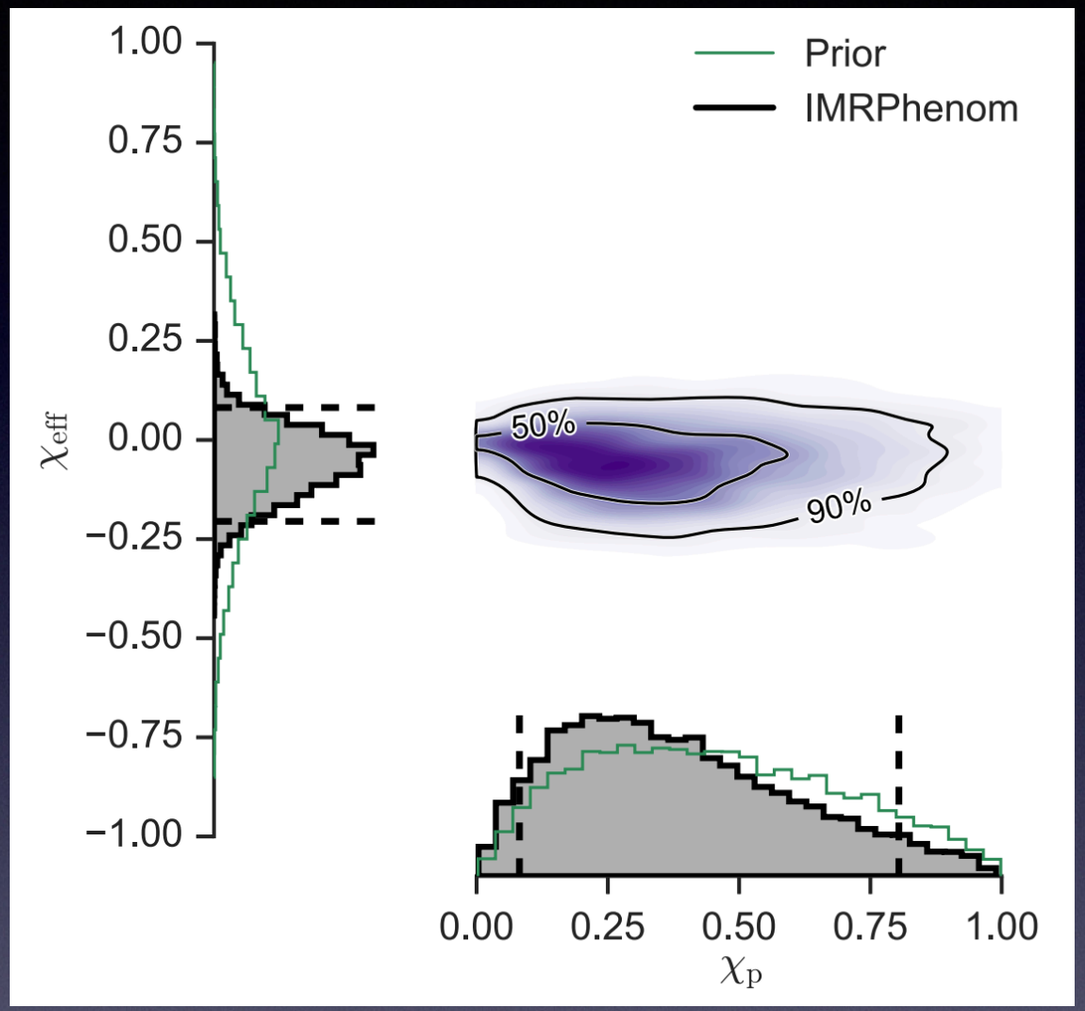

GW150914

$$\chi_{\rm eff} = \frac{c}{GM}\left(\frac{\boldsymbol{S}_1}{m_1} + \frac{\boldsymbol{S}_2}{m_2}\right) \cdot \frac{\boldsymbol{L}}{|\mathbf{L}|}$$

Figures: LSC collaboration 2016

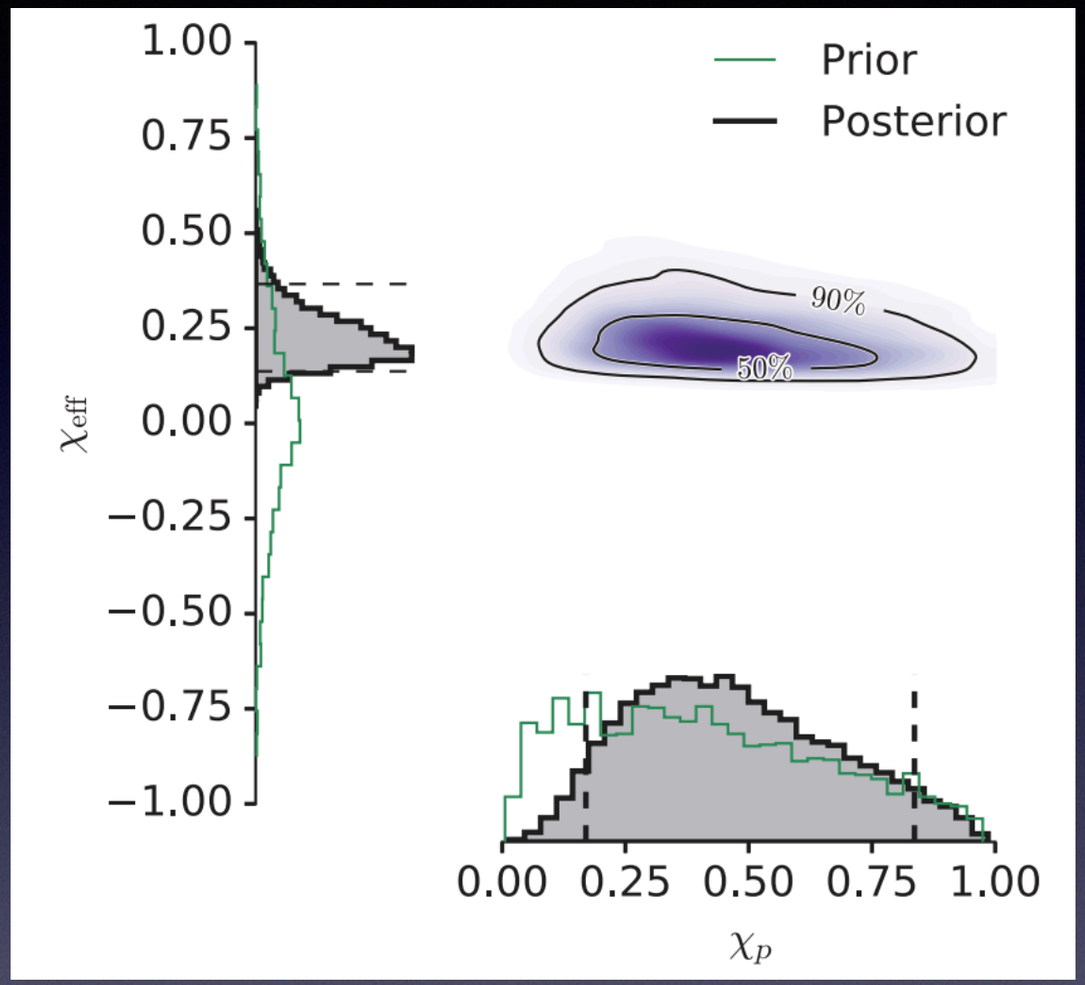

GW151226

Spins are either small or precessing

Comparison to models

Misaligned spins possible in field channel if large kicks, natural in dynamical channel

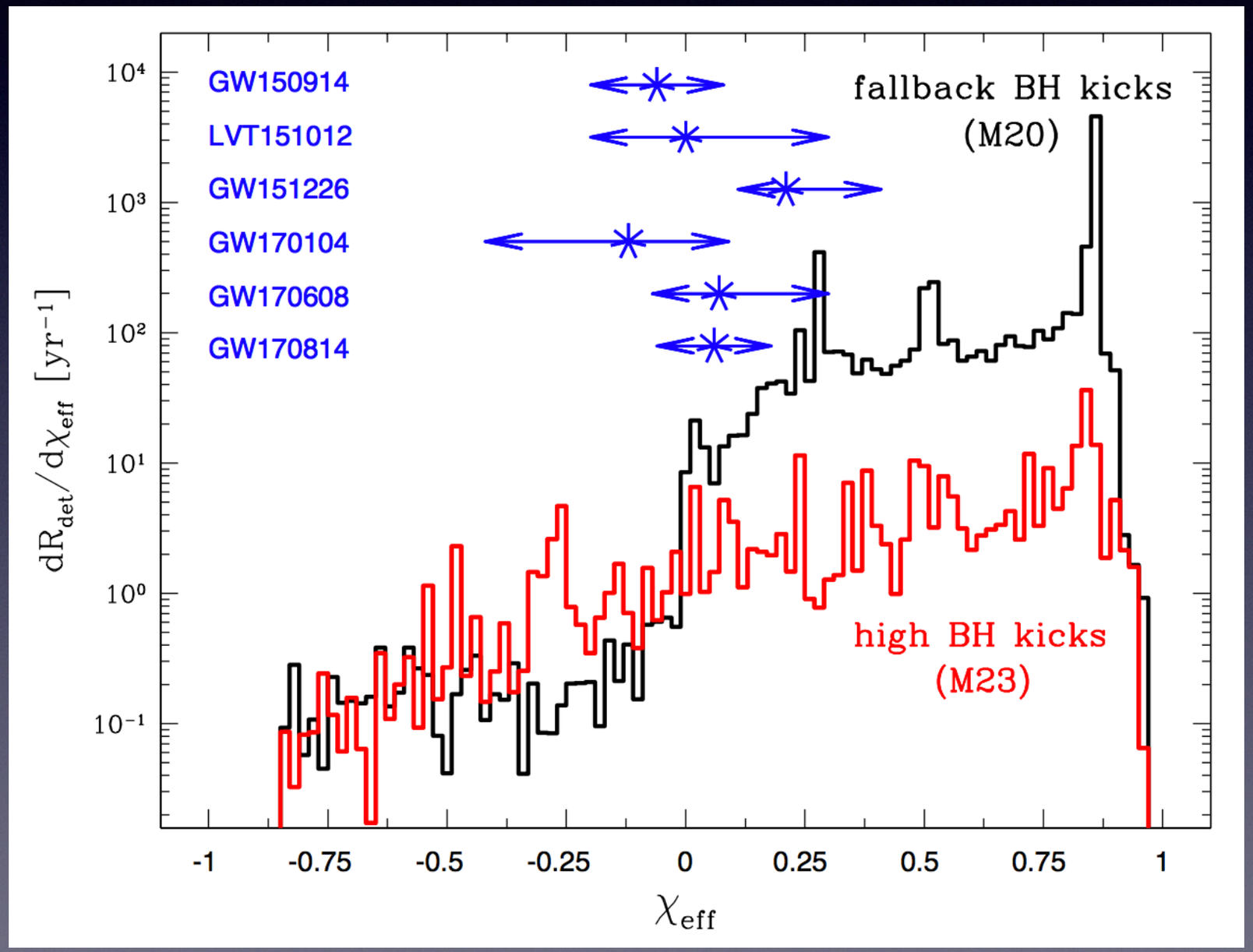

Figure from Belczynski et al 2017

Last week's updates

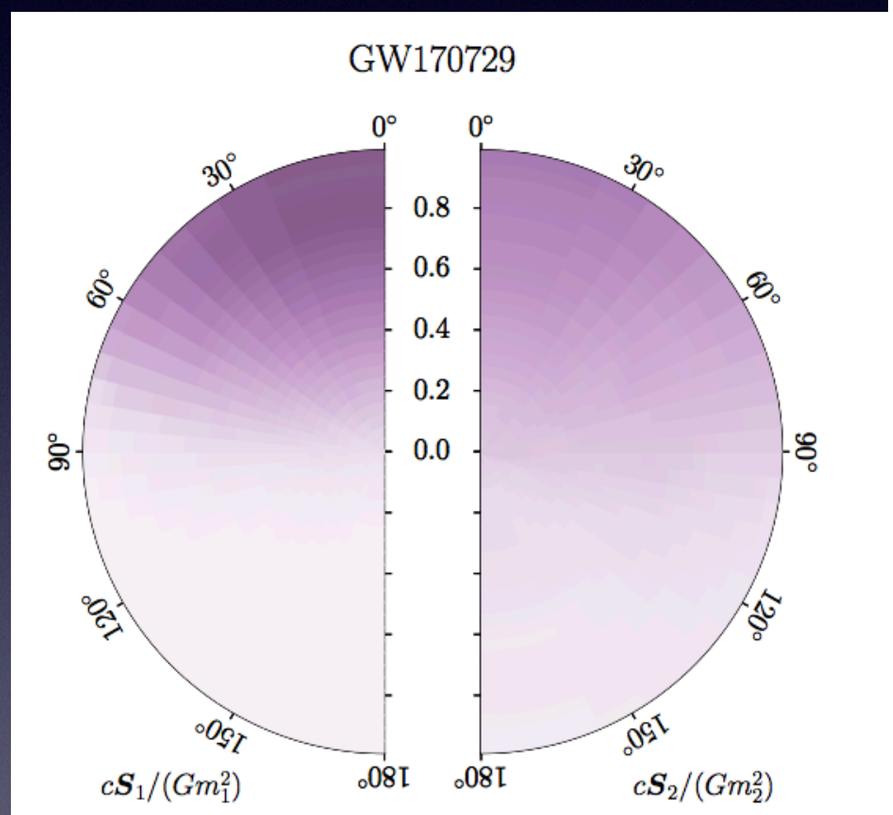

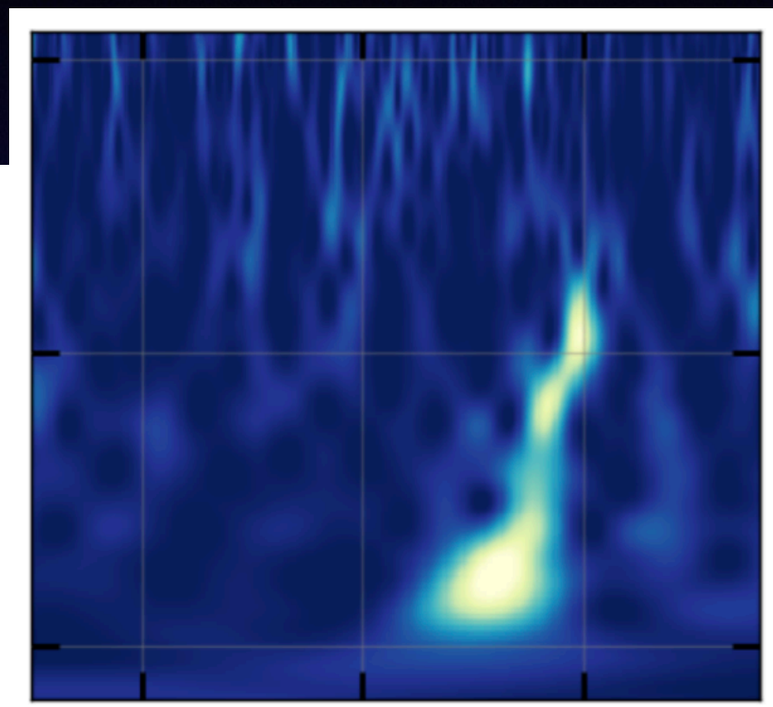

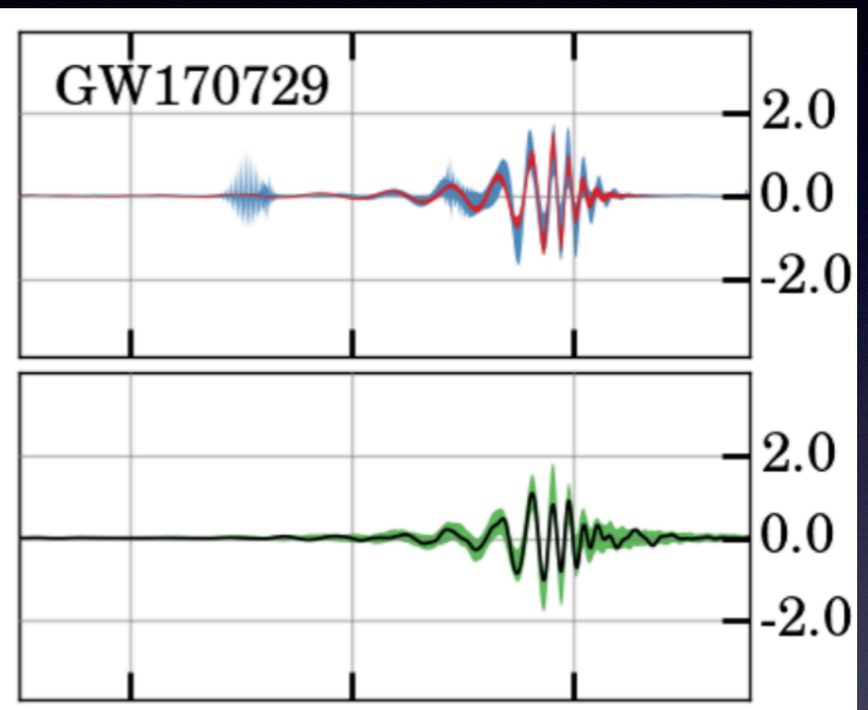

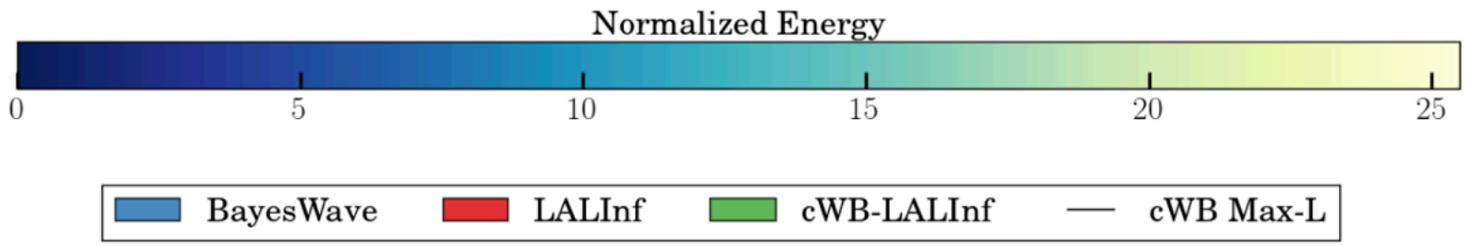

LSC 2018

Parametrized inspiral tests of GR

$$h_{ppE}(f) = h_{GR}(f)(1 + \alpha u^a)e^{i\beta u^b}$$

$$u = (\pi \mathcal{M} f)^{1/3}$$

waveform regime	parameter	$f-$dependence
early-inspiral regime	$\delta\hat{\varphi}_0$	$f^{-5/3}$
	$\delta\hat{\varphi}_1$	$f^{-4/3}$
	$\delta\hat{\varphi}_2$	f^{-1}
	$\delta\hat{\varphi}_3$	$f^{-2/3}$
	$\delta\hat{\varphi}_4$	$f^{-1/3}$
	$\delta\hat{\varphi}_{5l}$	$\log(f)$
	$\delta\hat{\varphi}_6$	$f^{1/3}$
	$\delta\hat{\varphi}_{6l}$	$f^{1/3}\log(f)$
	$\delta\hat{\varphi}_7$	$f^{2/3}$

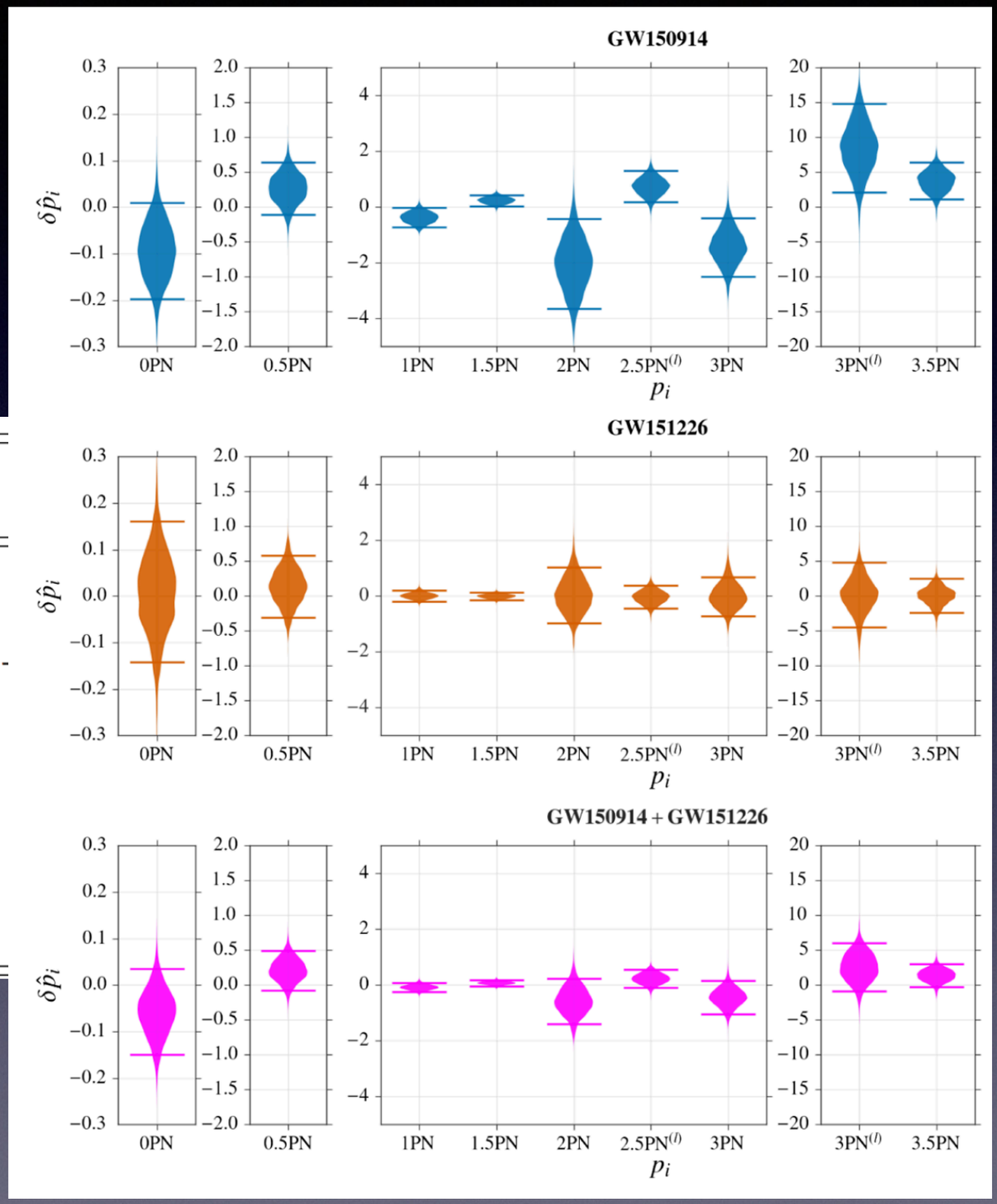

Caveat: ppE parameters may depend on sources (should be viewed as BH charges), so stacking may not be physically meaningful!

GWs from binary BHs

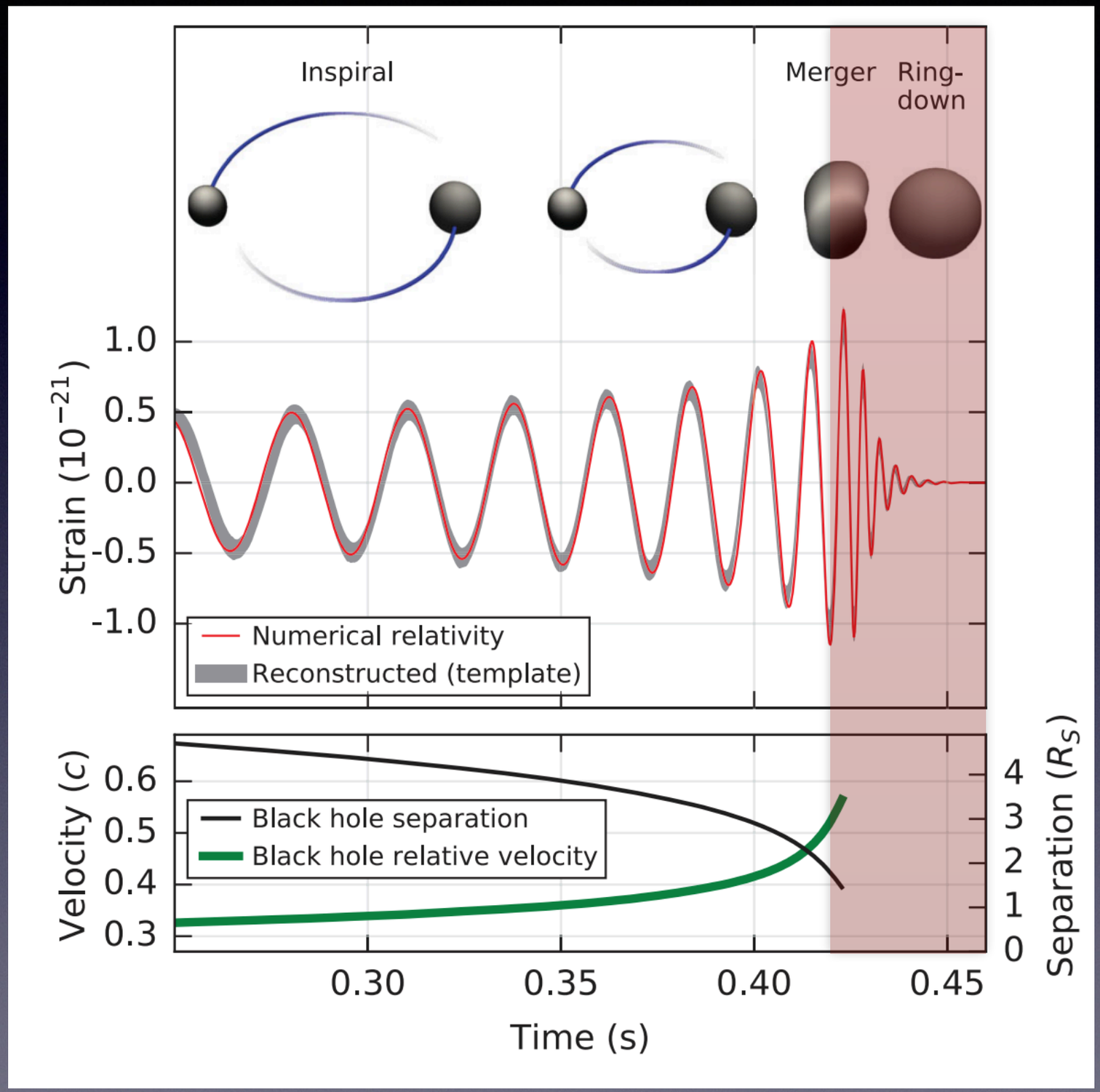

LSC collaboration 2015

Perturbations of non-spinning BHs

- Consider scalar field toy model first $g^{\mu\nu}\nabla_\mu\nabla_\nu\varphi = 0$
- On Schwarzschild, decompose in spherical harmonics

$$\varphi = \sum_{\ell,m} \frac{R_{\ell m}(r)}{r} Y_{\ell m}(\theta,\phi) e^{-i\omega t}$$

- Because of symmetry, equations “separate”:

$$\frac{\mathrm{d}^2 R}{\mathrm{d}r_*^2} + (\omega^2 - V)R = 0$$

$$r_* \equiv r + 2M \ln\left(\frac{r}{2M} - 1\right)$$

Tortoise coordinates ranging +/- ∞

$$V(r) \equiv \left(1 - \frac{2M}{r}\right)\left[\frac{l\,(l+1)}{r^2} + p\right]$$

$$p = 2M/r^3$$

Perturbations of non-spinning BHs

- Ingoing/Outgoing boundary conditions at event horizon/infinity
- Akin to solving Schrodinger equation in 1D in quantum mechanics 101
- Counting of degrees of freedom + continuity = discrete complex quasinormal mode frequencies
- Imaginary part of frequency shows linear stability
- Peak at ~ 3M as *l* diverges (because geometric optics limit of Klein-Gordon equation is geodesics equation)

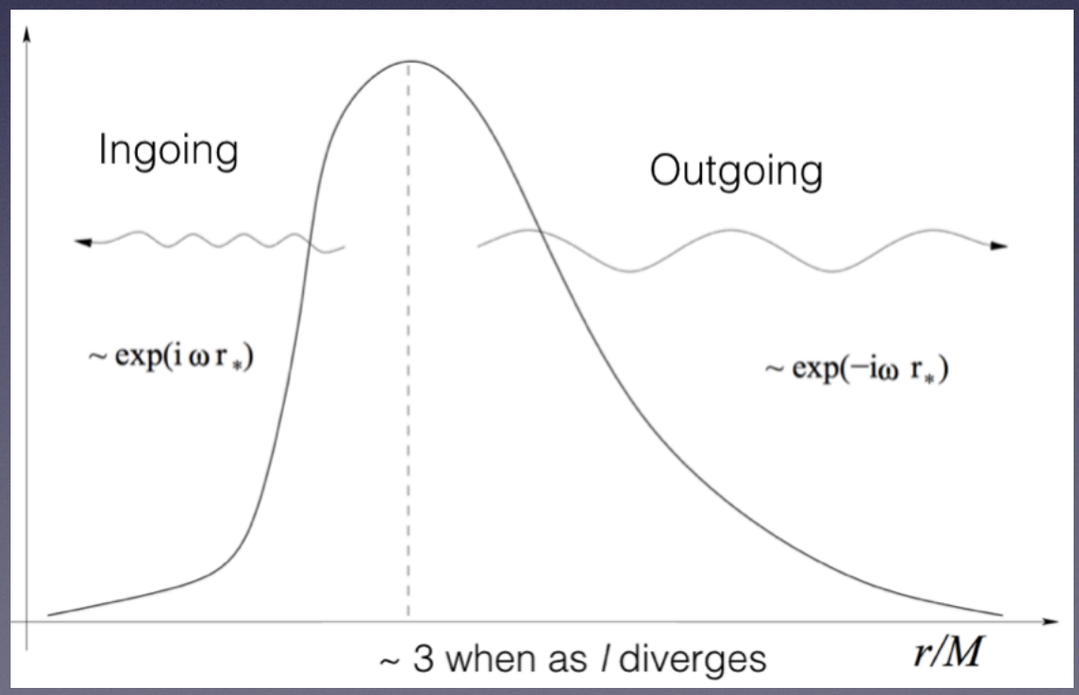

Perturbations of non-spinning BHs

- Separability on Schwarzschild extend to vector and tensor perturbations
- Expand in vector and tensor harmonics (of even/odd parity, c.f. E/B modes of CMB)

$$\psi_{L^M,\mu} = \text{const} \frac{\partial}{\partial x^\mu} Y_{L^M}(x_2 x_3), \quad \text{parity } (-)^L;$$

$$\phi_{L^M,\mu} = \text{const}\, \epsilon_\mu{}^\nu \frac{\partial}{\partial x_\nu} Y_{L^M}(x_2 x_3), \quad \text{parity } (-)^{L+1}.$$

Basis for vectors on 2-sphere

$$\psi_{L^M\mu\nu} = \text{const}\, Y_{L^M;\mu\nu} (\text{covariant derivatives}), \quad \text{parity } (-)^L;$$

$$\phi_{L^M\mu\nu} = \text{const}\, \gamma_{\mu\nu} Y_{L^M}, \quad \text{parity } (-)^L;$$

$$\chi_{L^M\mu\nu} = \tfrac{1}{2}\, \text{const} [\epsilon_\mu{}^\lambda \psi_{L^M\lambda\nu} + \epsilon_\nu{}^\lambda \psi_{L^M\lambda\mu}], \quad \text{parity } (-)^{L+1}.$$

Basis for tensors on 2-sphere

Perturbations of non-spinning BHs

$$h_{\mu\nu}=\begin{vmatrix} 0 & 0 & -h_0(T,r)(\partial/\sin\theta\partial\varphi)Y_L{}^M & h_0(T,r)(\sin\theta\partial/\partial\theta)Y_L{}^M \\ 0 & 0 & -h_1(T,r)(\partial/\sin\theta\partial\varphi)Y_L{}^M & h_1(T,r)(\sin\theta\partial/\partial\theta)Y_L{}^M \\ \mathrm{Sym} & \mathrm{Sym} & h_2(T,r)(\partial^2/\sin\theta\partial\theta\partial\varphi-\cos\theta\partial/\sin^2\theta\partial\varphi)Y_L{}^M & \mathrm{Sym} \\ \mathrm{Sym} & \mathrm{Sym} & \tfrac{1}{2}h_2(T,r)(\partial^2/\sin\theta\partial\varphi\partial\varphi+\cos\theta\partial/\partial\theta-\sin\theta\partial^2/\partial\theta\partial\theta)Y_L{}^M & -h_2(T,r)(\sin\theta\partial^2/\partial\theta\partial\varphi-\cos\theta\partial/\partial\varphi)Y_L{}^M \end{vmatrix}$$

Odd-parity metric perturbations (Regge-Wheeler 1957)

$$h_{\mu\nu}=\begin{vmatrix} (1-2m^*/r)H_0(T,r)Y_L{}^M & H_1(T,r)Y_L{}^M & h_0(T,r)(\partial/\partial\theta)Y_L{}^M & h_0(T,r)(\partial/\partial\varphi)Y_L{}^M \\ H_1(T,r)Y_L{}^M & (1-2m^*/r)^{-1}H_2(T,r)Y_L{}^M & h_1(T,r)(\partial/\partial\theta)Y_L{}^M & h_1(T,r)(\partial/\partial\varphi)Y_L{}^M \\ \mathrm{Sym} & \mathrm{Sym} & r^2[K(T,r) & \mathrm{Sym} \\ & & \quad +G(T,r)(\partial^2/\partial\theta^2)]Y_L{}^M & \\ \mathrm{Sym} & \mathrm{Sym} & r^2G(T,r)(\partial^2/\partial\theta\partial\varphi & r^2[K(T,r)\sin^2\theta \\ & & \quad -\cos\theta\partial/\sin\theta\partial\varphi)Y_L{}^M & \quad +G(T,r)(\partial^2/\partial\varphi\partial\varphi \\ & & & \quad +\sin\theta\cos\theta\partial/\partial\theta)]Y_L{}^M \end{vmatrix}.$$

Even-parity metric perturbations (Regge-Wheeler 1957, Zerilli 1970)

Perturbations of non-spinning BHs

$$h_{\mu\nu}=\begin{vmatrix} 0 & 0 & -h_0(T,r)(\partial/\sin\theta\partial\varphi)Y_L{}^M & h_0(T,r)(\sin\theta\partial/\partial\theta)Y_L{}^M \\ 0 & 0 & -h_1(T,r)(\partial/\sin\theta\partial\varphi)Y_L{}^M & h_1(T,r)(\sin\theta\partial/\partial\theta)Y_L{}^M \\ \mathrm{Sym} & \mathrm{Sym} & h_2(T,r)(\partial^2/\sin\theta\partial\theta\partial\varphi-\cos\theta\partial/\sin^2\theta\partial\varphi)Y_L{}^M & \mathrm{Sym} \\ \mathrm{Sym} & \mathrm{Sym} & \tfrac{1}{2}h_2(T,r)(\partial^2/\sin\theta\partial\varphi\partial\varphi+\cos\theta\partial/\partial\theta-\sin\theta\partial^2/\partial\theta\partial\theta)Y_L{}^M & h_2(T,r)(\sin\theta\partial^2/\partial\theta\partial\varphi-\cos\theta\partial/\partial\varphi)Y_L{}^M \end{vmatrix}$$

Odd-parity metric perturbations (Regge-Wheeler 1957):
2 free radial functions

$$h_{\mu\nu}=\begin{vmatrix} (1-2m^*/r)H_0(T,r)Y_L{}^M & H_1(T,r)Y_L{}^M & h_0(T,r)(\partial/\partial\theta)Y_L{}^M & h_0(T,r)(\partial/\partial\varphi)Y_L{}^M \\ H_1(T,r)Y_L{}^M & (1-2m^*/r)^{-1}H_2(T,r)Y_L{}^M & h_1(T,r)(\partial/\partial\theta)Y_L{}^M & h_1(T,r)(\partial/\partial\varphi)Y_L{}^M \\ \mathrm{Sym} & \mathrm{Sym} & r^2[K(T,r) & \mathrm{Sym} \\ & & \quad +G(T,r)(\partial^2/\partial\theta^2)]Y_L{}^M & \\ \mathrm{Sym} & \mathrm{Sym} & r^2G(T,r)(\partial^2/\partial\theta\partial\varphi & r^2[K(T,r)\sin^2\theta \\ & & \quad -\cos\theta\partial/\sin\theta\partial\varphi)Y_L{}^M & \quad +G(T,r)(\partial^2/\partial\varphi\partial\varphi \\ & & & \quad +\sin\theta\cos\theta\partial/\partial\theta)]Y_L{}^M \end{vmatrix}.$$

Even-parity metric perturbations (Regge-Wheeler 1957, Zerilli 1970):
4 free radial functions, but 2 algebraic relations from Einstein eps

Perturbations of non-spinning BHs

Construct complex variables out of each pair of free radial functions

$$\frac{d^2\Psi_s}{dr_*^2} + \left(\omega^2 - V_s\right)\Psi_s = 0\,.$$

$$V^{-}_{s=2} = f(r)\left[\frac{l(l+1)}{r^2} - \frac{6M}{r^3}\right]$$

Odd-parity

$$V^{+}_{s=2} = \frac{2f(r)}{r^3}\frac{9M^3 + 3\lambda^2 M r^2 + \lambda^2(1+\lambda)r^3 + 9M^2\lambda r}{(3M+\lambda r)^2}$$

Even-parity

$$\lambda \equiv (l-1)(l+2)/2 \qquad f(r) = 1 - 2M/r$$

Effective potentials peak at r=3M in the large l limit
(i.e. in the geodesics limit)

Perturbations of spinning BHs

- Separability of equations not at all obvious in Kerr, but possible due to “hidden symmetry” (c.f. Carter’s constant)

- Use Newman-Penrose scalars (projections of Weyl curvature on null tetrad) to get Teukolsky equation

$$\Psi_0 = -C_{1313} = -C_{\mu\nu\lambda\sigma} l^\mu m^\nu l^\lambda m^\sigma ,$$
$$\Psi_4 = -C_{2424} = -C_{\mu\nu\lambda\sigma} n^\mu m^{*\nu} n^\lambda m^{*\sigma}$$

$$\psi(t\,,r\,,\theta\,,\phi) = \frac{1}{2\pi}\int e^{-i\omega t}\sum_{l=|s|}^{\infty}\sum_{m=-l}^{l} e^{im\phi}\,{}_sS_{lm}(\theta)R_{lm}(r)d\omega$$

$$\left[\frac{\partial}{\partial u}(1-u^2)\frac{\partial}{\partial u}\right]{}_sS_{lm}$$ Spin-weighted spheroidal harmonics

$$+\left[a^2\omega^2u^2 - 2a\omega su + s + {}_sA_{lm} - \frac{(m+su)^2}{1-u^2}\right]{}_sS_{lm} = 0$$

$$\Delta\partial_r^2 R_{lm} + (s+1)(2r-2M)\partial_r R_{lm} + V R_{lm} = 0\,.$$

s	$(+2,-2)$
ψ	$(\Psi_0, \rho^{-4}\Psi_4)$

$$V = 2is\omega r - a^2\omega^2 - {}_sA_{lm} + \frac{1}{\Delta}\left[(r^2+a^2)^2\omega^2 - 4Mam\omega r + a^2m^2 \;+ is\left(am(2r-2M) - 2M\omega(r^2-a^2)\right)\right]$$

$u \equiv \cos\theta,\ \Delta = (r-r_-)(r-r_+)$

${}_sA_{lm}(a=0) = l(l+1) - s(s+1)$ Separation constant

Perturbations of spinning BHs

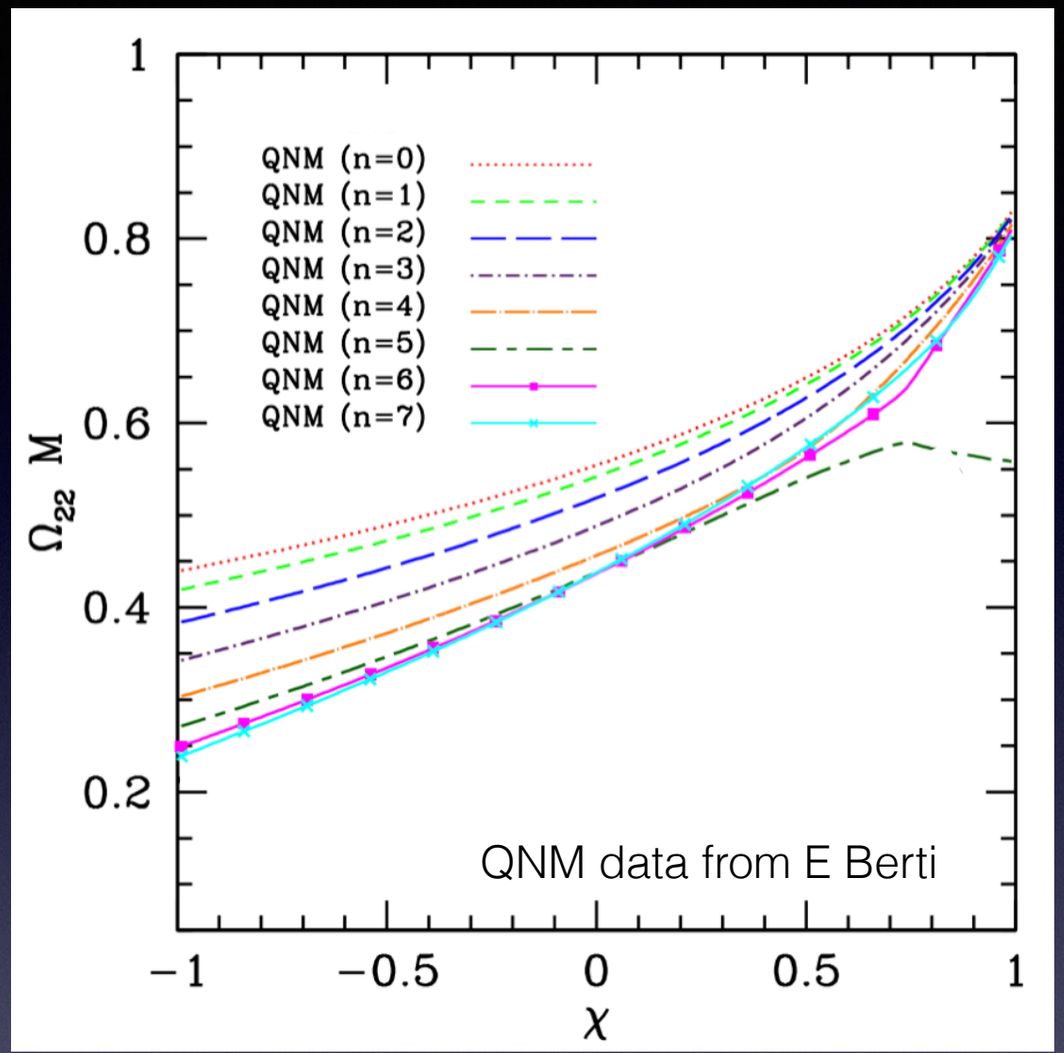

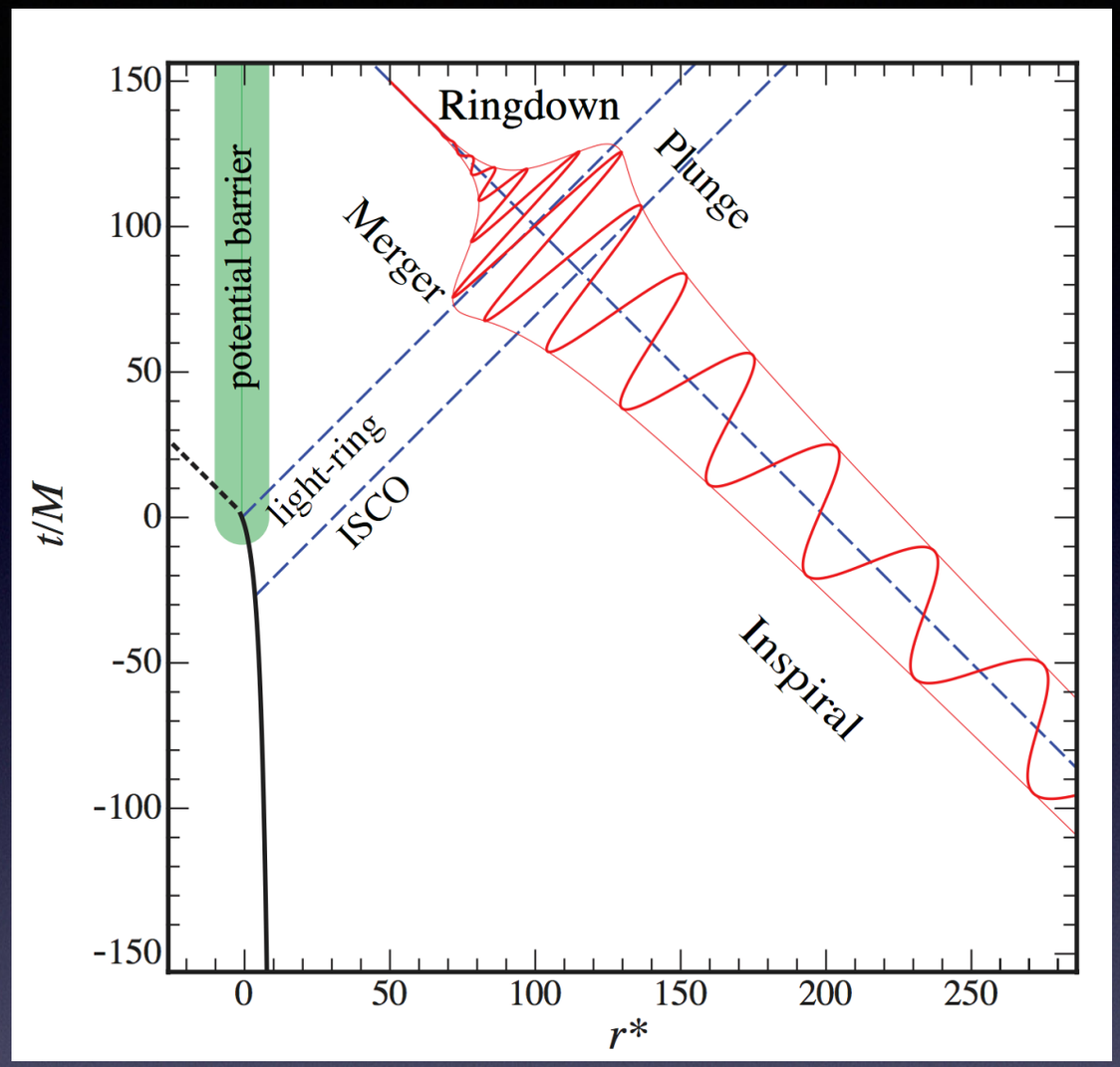

- Connection to circular photon orbit frequency ω and Lyapunov coefficient λ (i.e. curvature of geodesics effective potential) in geometric optics limit!

$$\omega_{ln}^{m=l} \approx l\omega_{+} - i\lambda_{+}(n+1/2)$$

- Amplitude of modes depends on merger physics/initial conditions; set by “continuity” near circular photon orbit in phenomenological waveform models (e.g. EOB)

EOB vs numerical relativity

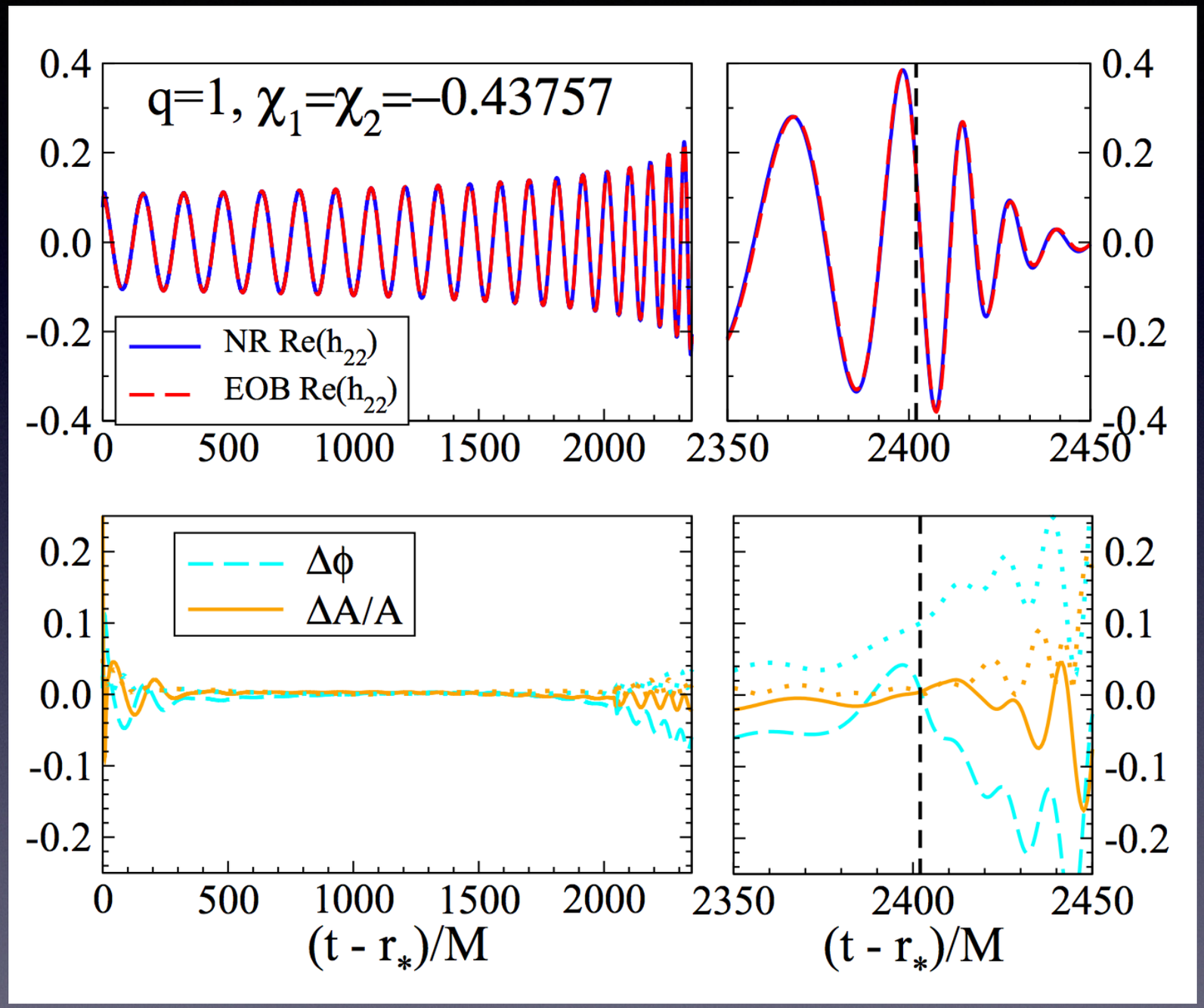

Example from Taracchini et al 2012, c.f. also phenomenological waveforms

Ringdown tests of the no-hair theorem

$$\omega_{\ell m} = \omega^{GR}_{\ell m}(M, J)(1 + \delta\omega_{\ell m}) \qquad \tau_{\ell m} = \tau^{GR}_{\ell m}(M, J)(1 + \delta\tau_{\ell m})$$

- Difficult with advanced detectors because little SNR in ringdown

- Can perform consistency tests between merger/ringdown

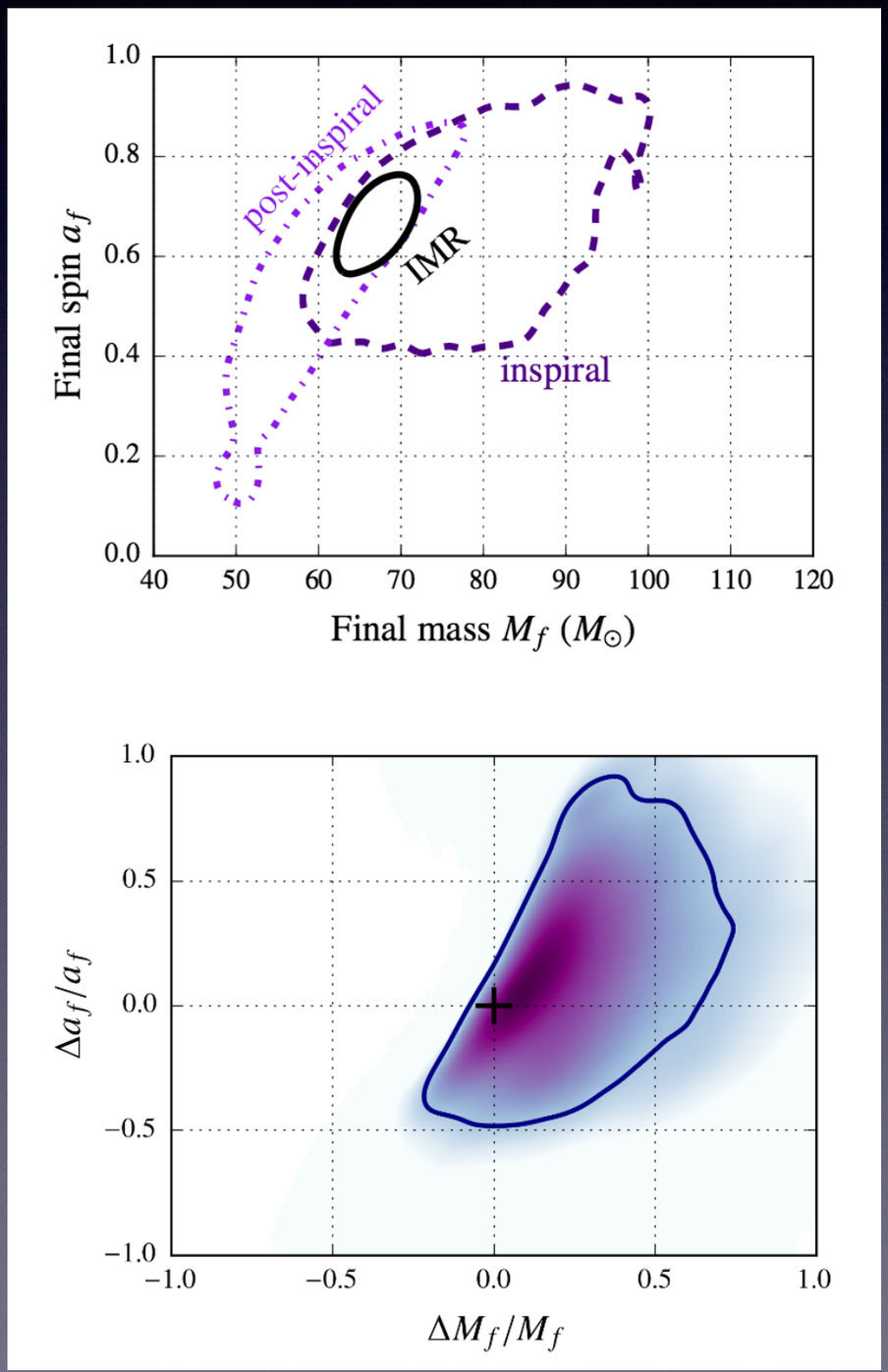

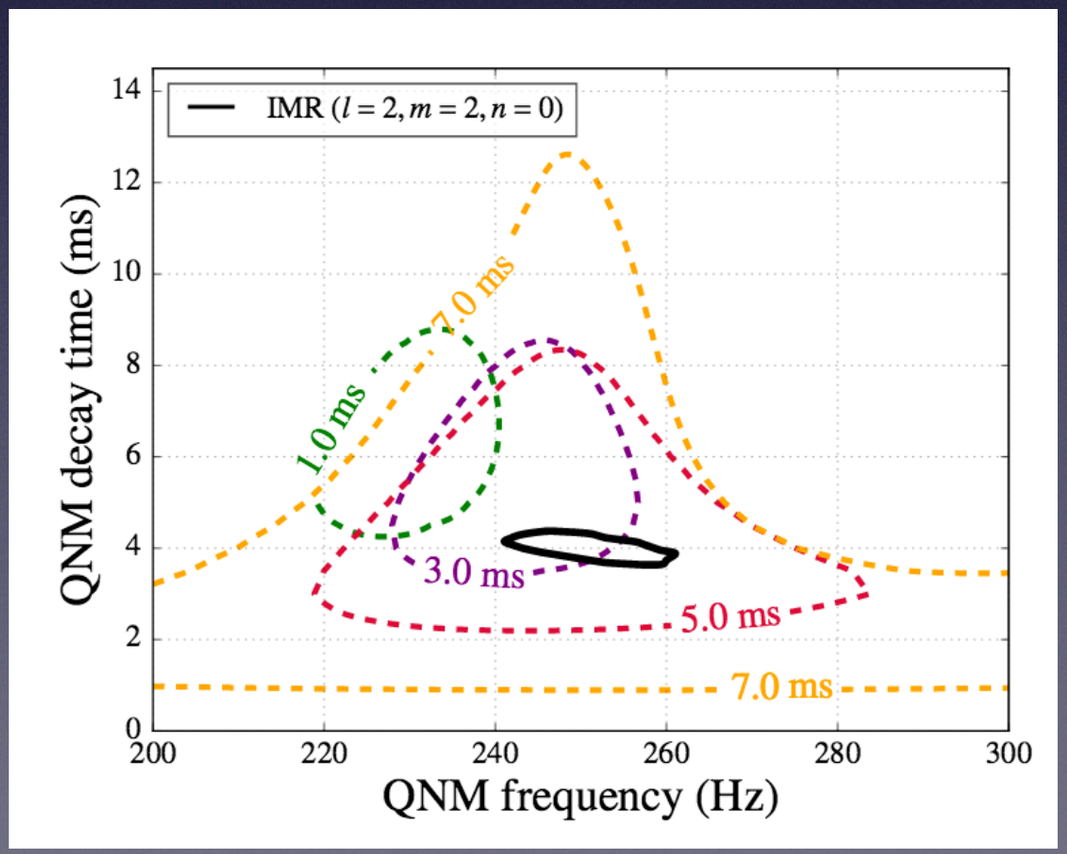

From the LSC paper on tests of GR

The first direct observation of GWs and … BHs!

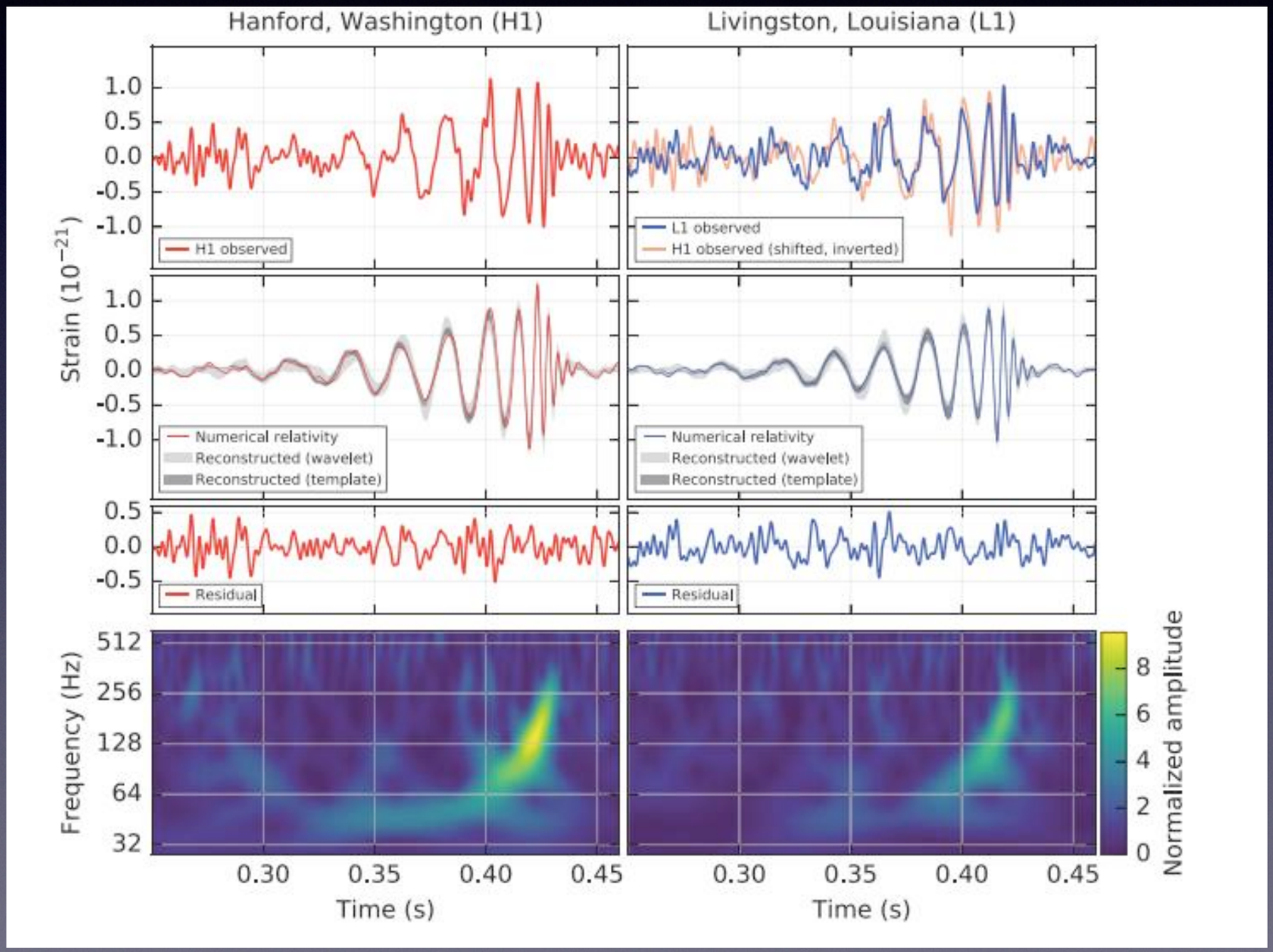

LSC collaboration 2015

Not the biggest BHs in the Universe!

A monster of 4.5 million solar masses in the centre of our Galaxy!

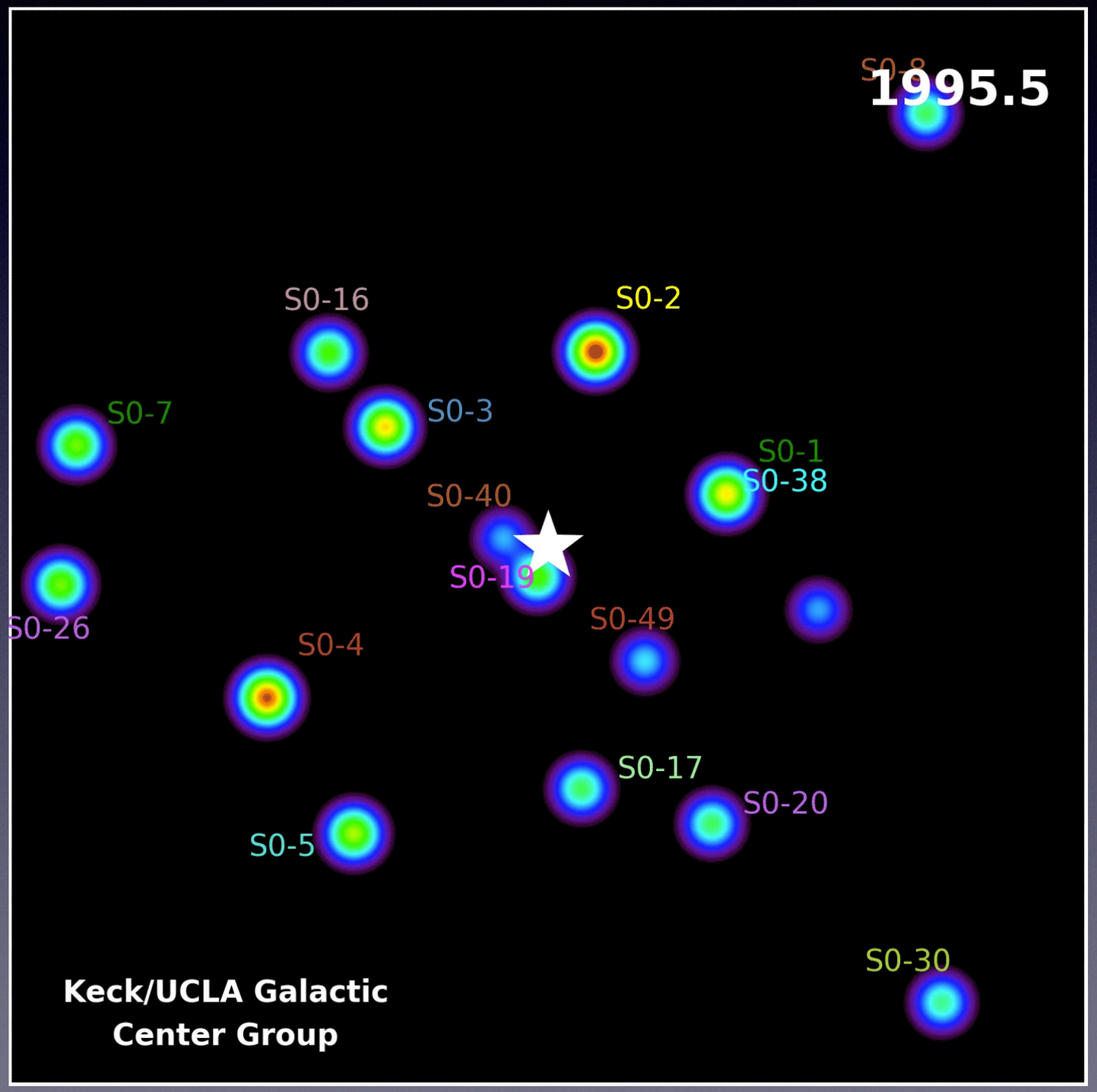

Galaxies merge…

… so massive BHs must merge too!

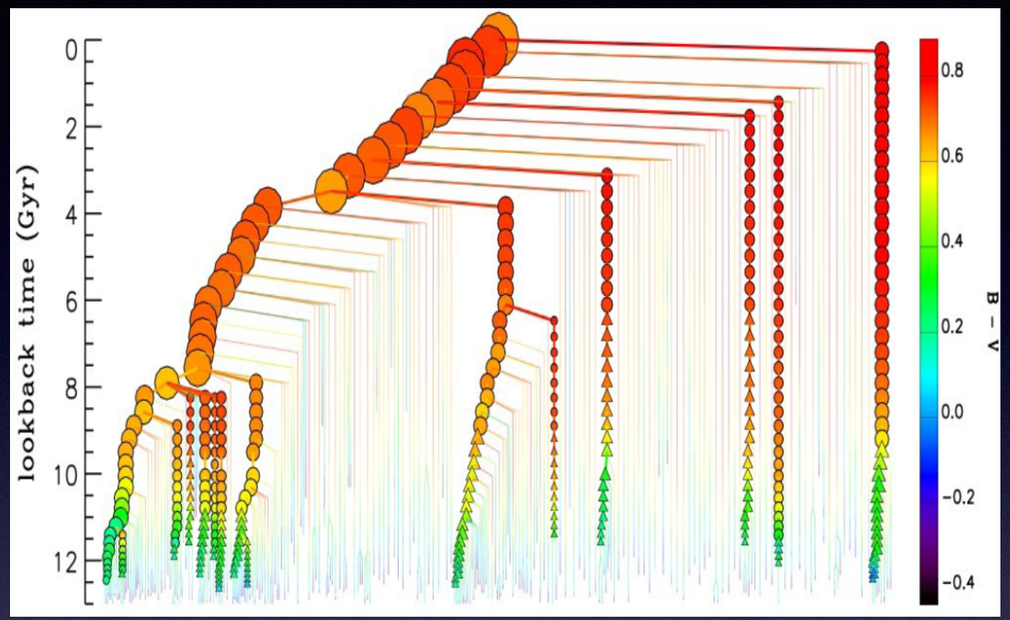

Figure from De Lucia & Blaizot 2007

+

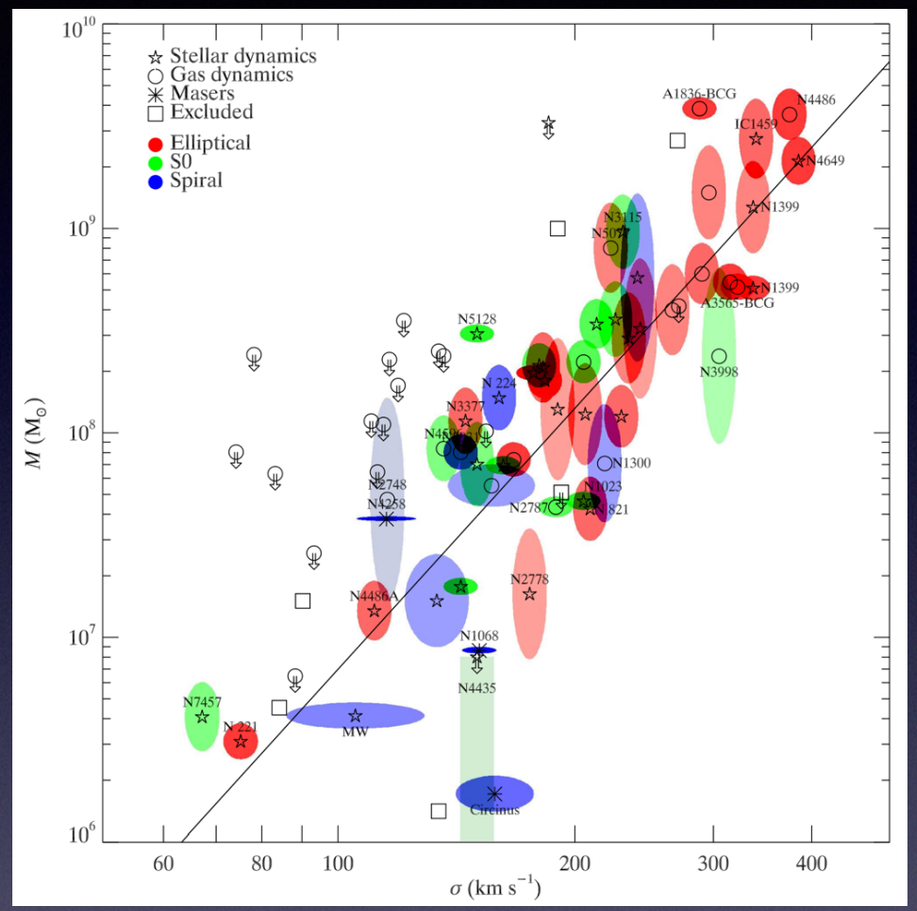

Ferrarese & Merritt 2000
Gebhardt et al. 2000,
Gültekin et al (2009)

=

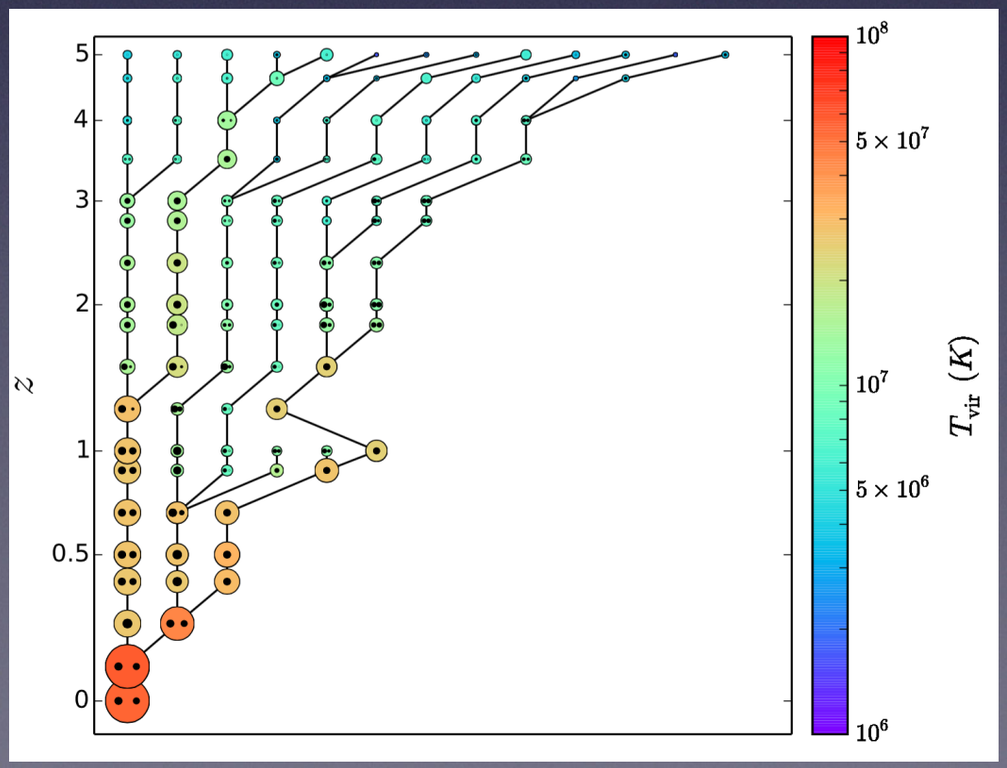

EB 2012
Figure credits: Lucy Ward

What links large and small scale?

- Small to large: BH jets or disk winds transfer kinetic energy to the galaxy and keep it “hot”, quenching star formation (”AGN feedback”). Needed to reconcile ΛCDM bottom-up structure formation with observed “downsizing” of cosmic galaxies

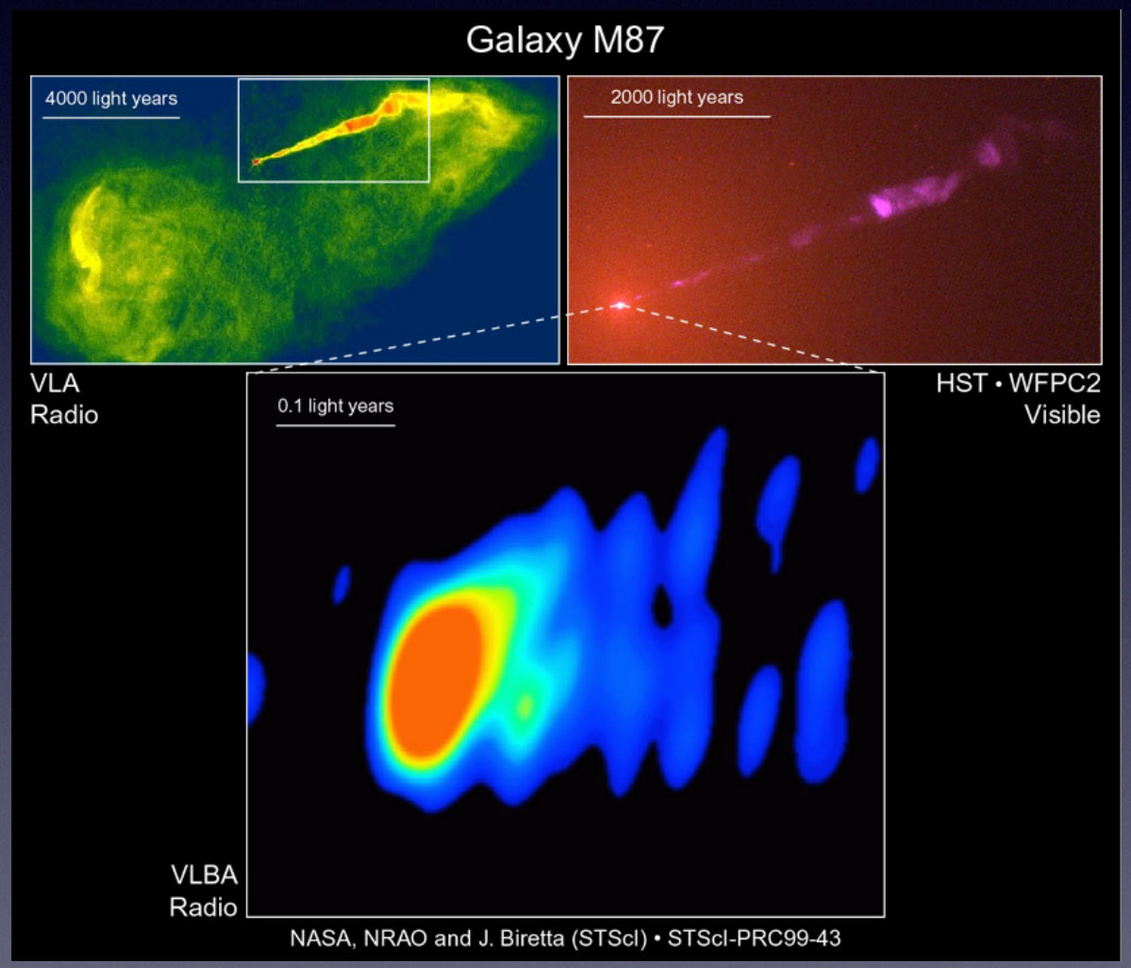

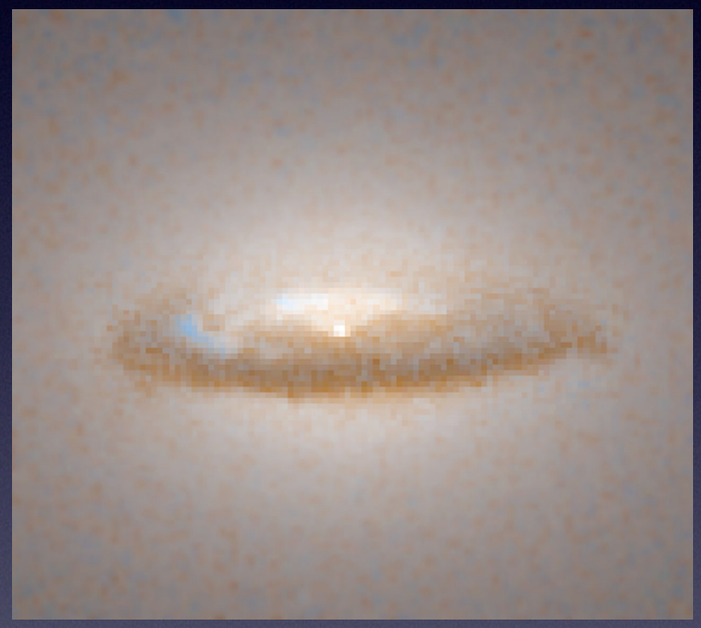

Disk of dust and gas around the massive BH in NGC 7052

- Large to small: galaxies provide fuel to BHs to grow (”accretion”)

Fossil evidence for massive BH mergers

- Nuclear Star Clusters: masses up to ~10^7 M_{sun}, r ~ pc
- BH binaries eject stars by slingshot effect and through remnant's recoil ("erosion")
- Erosion by BH binaries crucial to reproduce NSC scaling relations

$$M_{\rm ej} \approx 0.7 q^{0.2} M_{\rm bin} + 0.5 M_{\rm bin} \ln\left(\frac{a_{\rm h}}{a_{\rm gr}}\right) + 5 M_{\rm bin} \left(V_{\rm kick}/V_{\rm esc}\right)^{1.75} ,$$

Antonini, EB and Silk 2015a,b

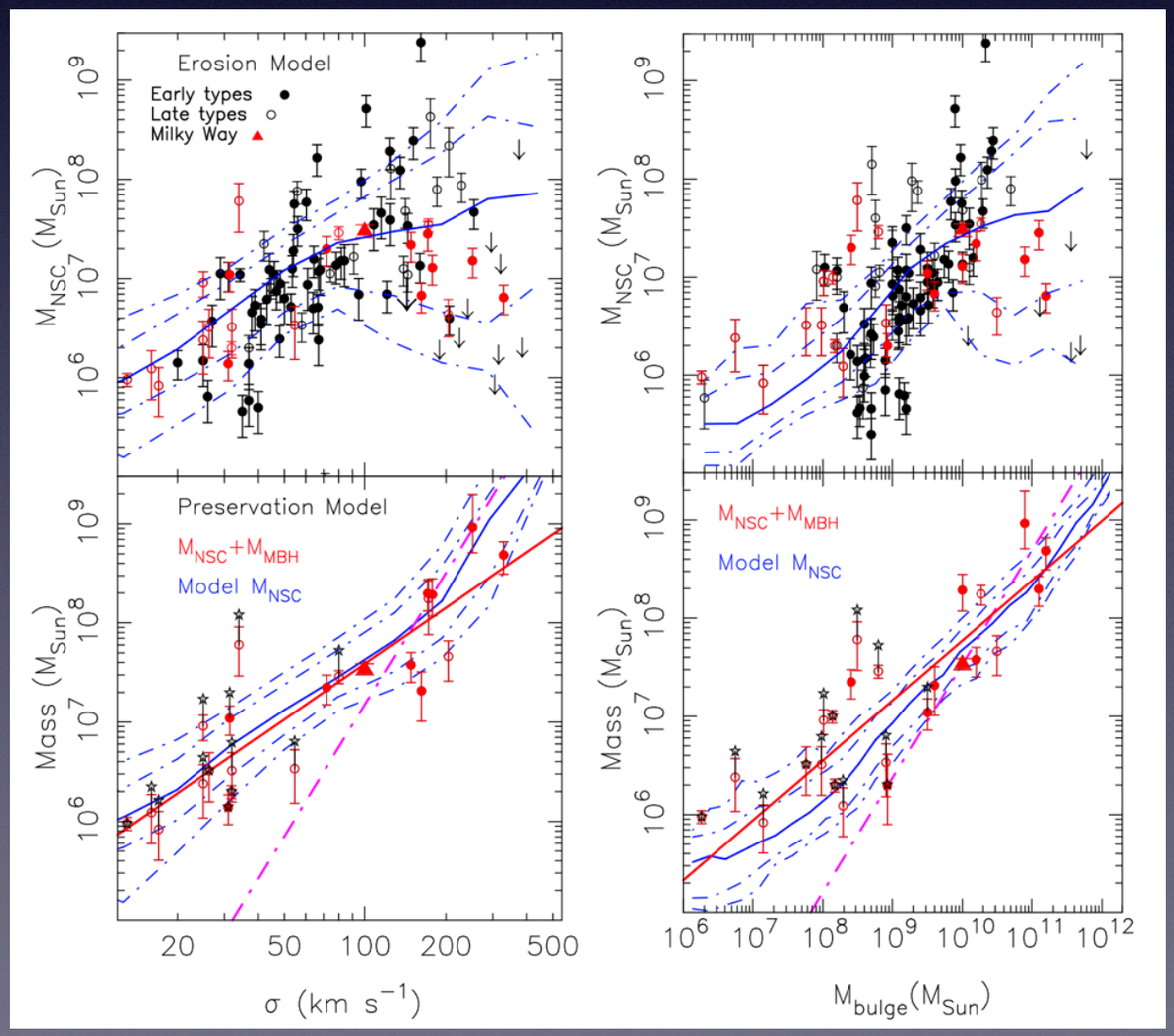

GWs from massive BHs

$$f_{\rm GW} = \frac{6\times 10^4}{\tilde{m}\tilde{R}^{3/2}}{\rm Hz} \qquad \tilde{R} = R/(Gm/c^2) \qquad \tilde{m} = m/M_\odot$$

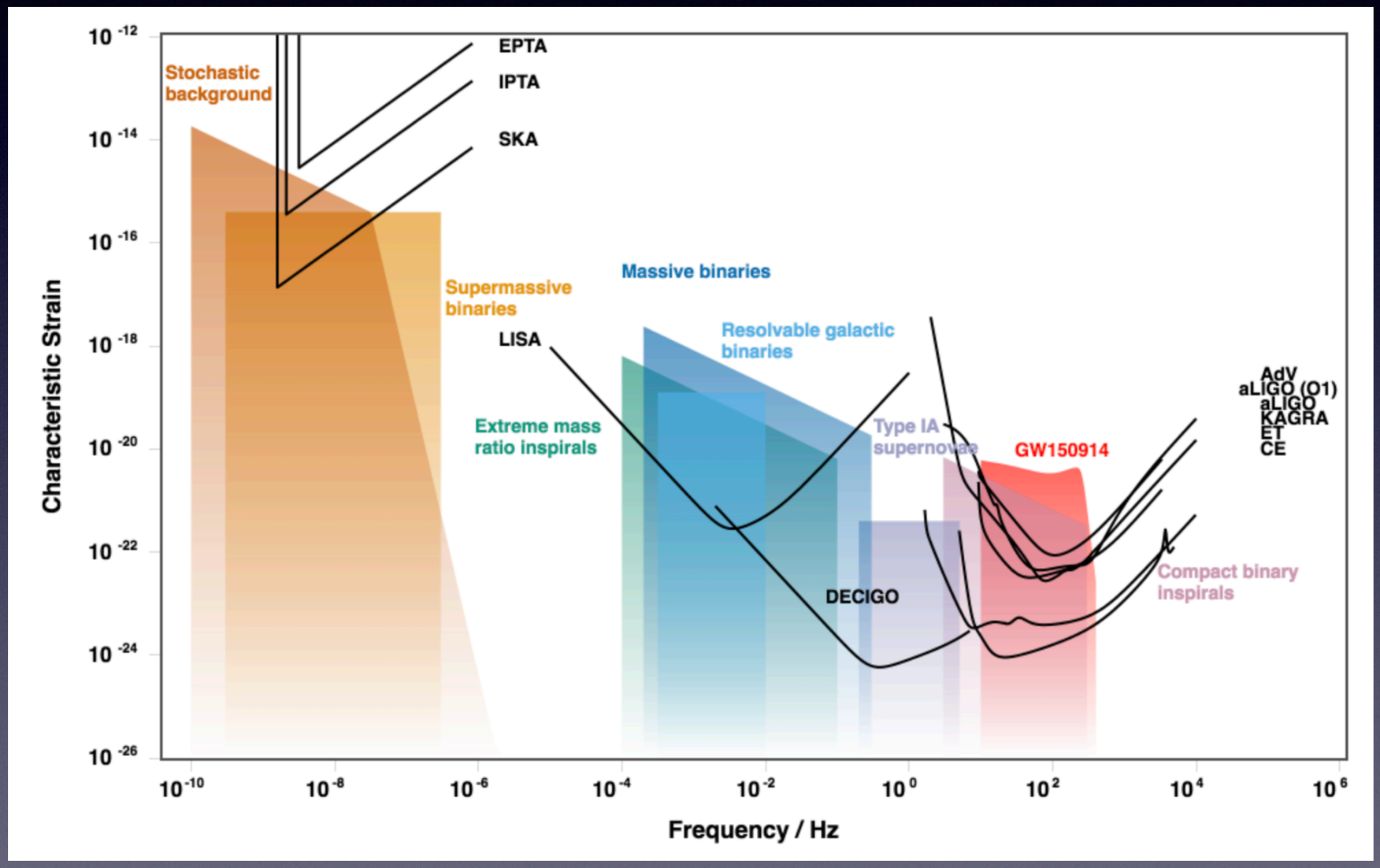

Figure generated by http://gwplotter.com

Problem: terrestrial detectors blind at f ≲ 1-10 Hz (seismic noise)

The space race!

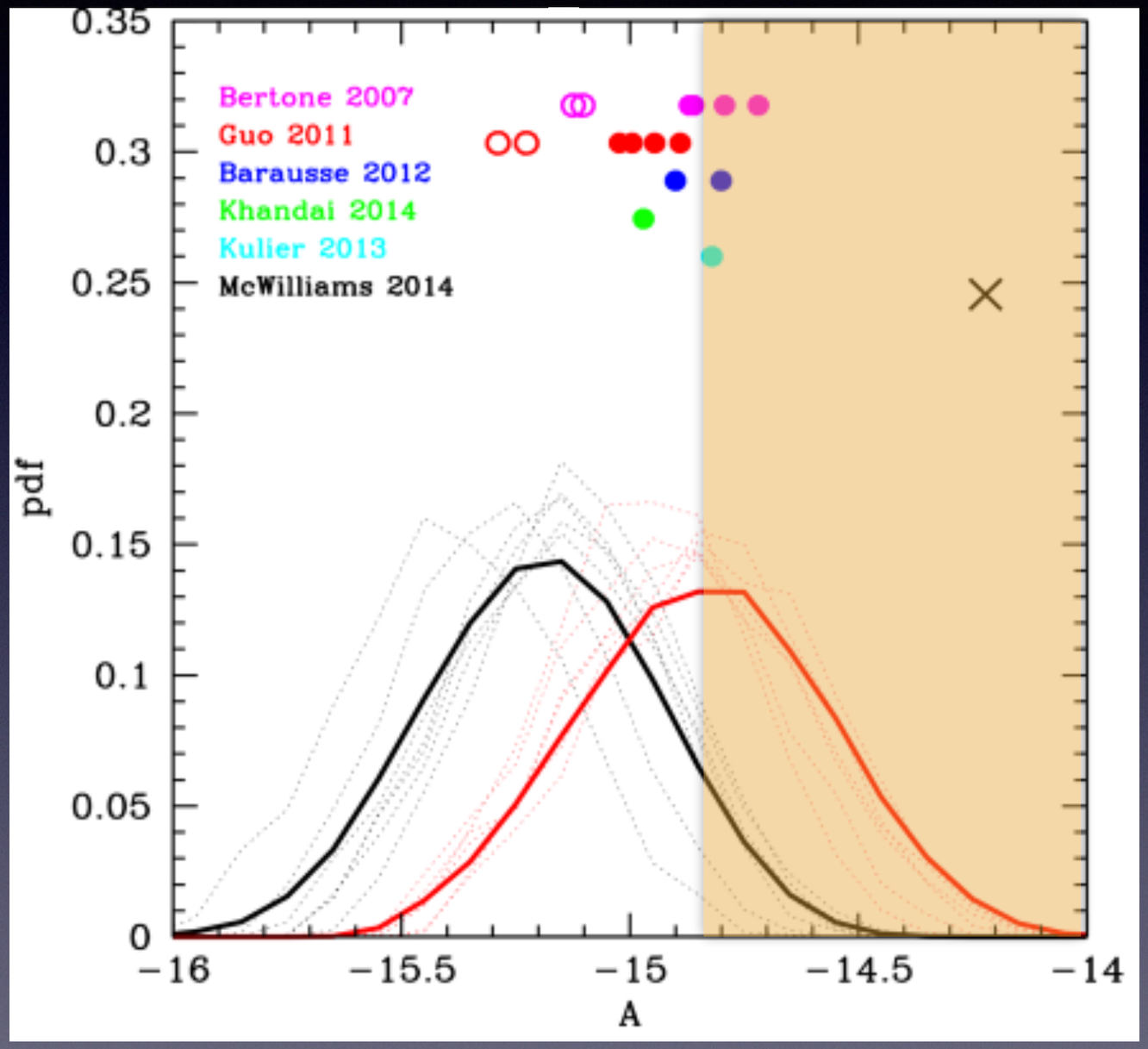

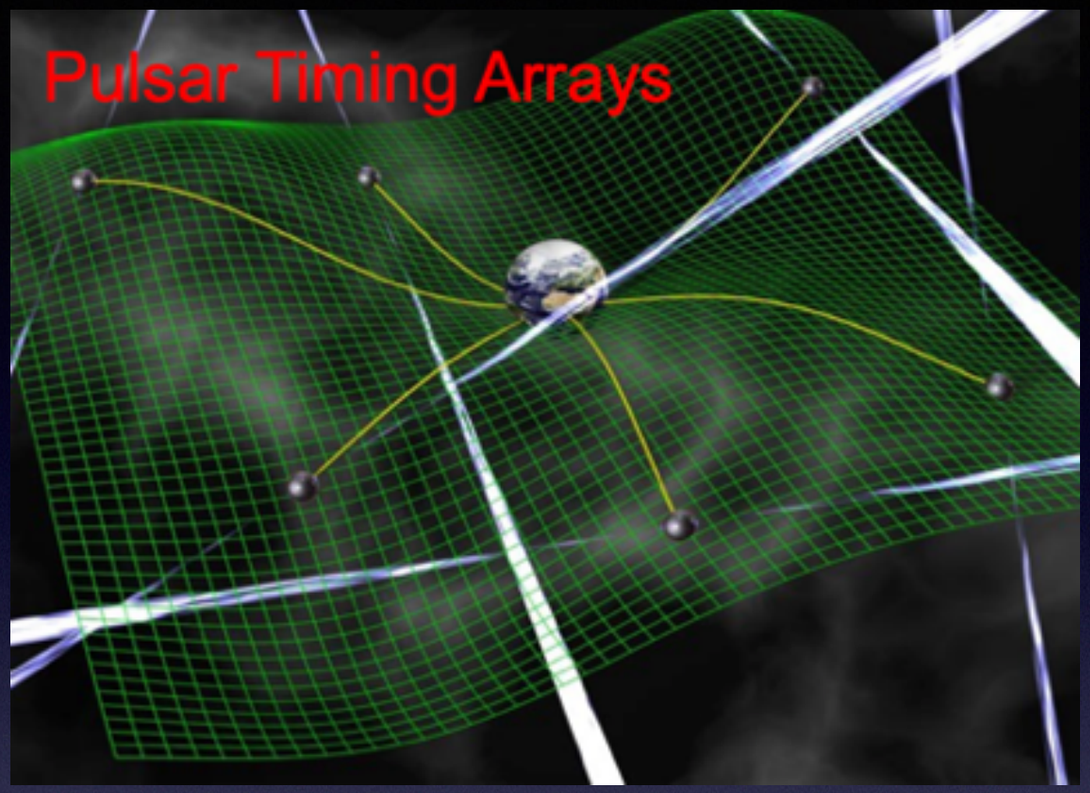

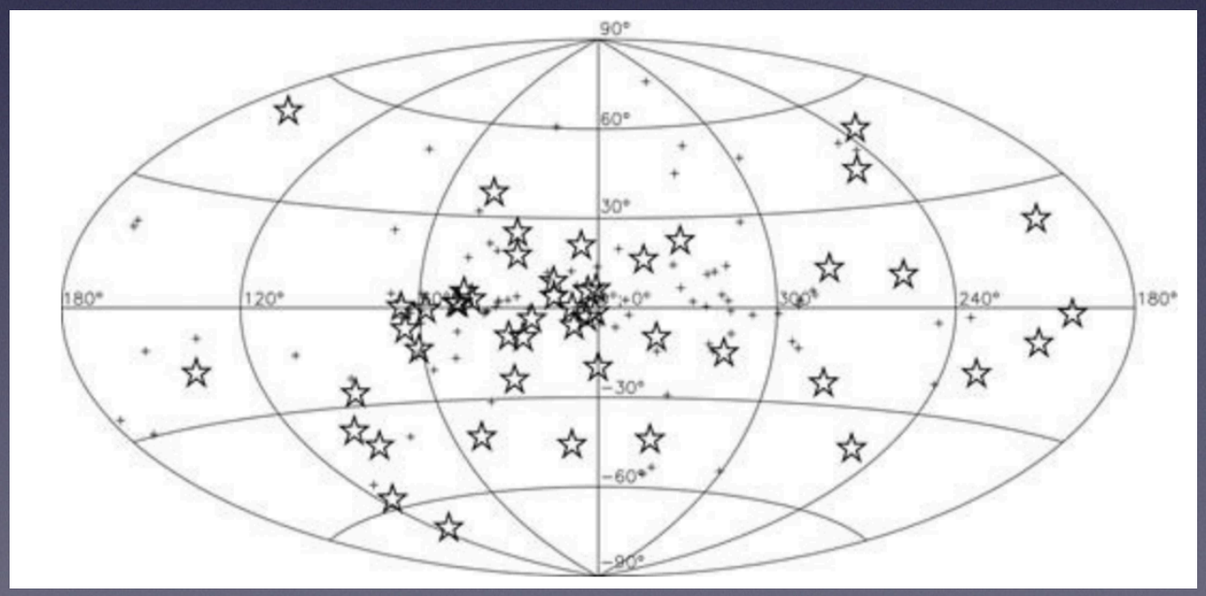

Background characteristic strain at f=1/yr is $A<1.45 \times 10^{-15}$ (Nanograv 2018)

Laser Interferometer Space Antenna (LISA)

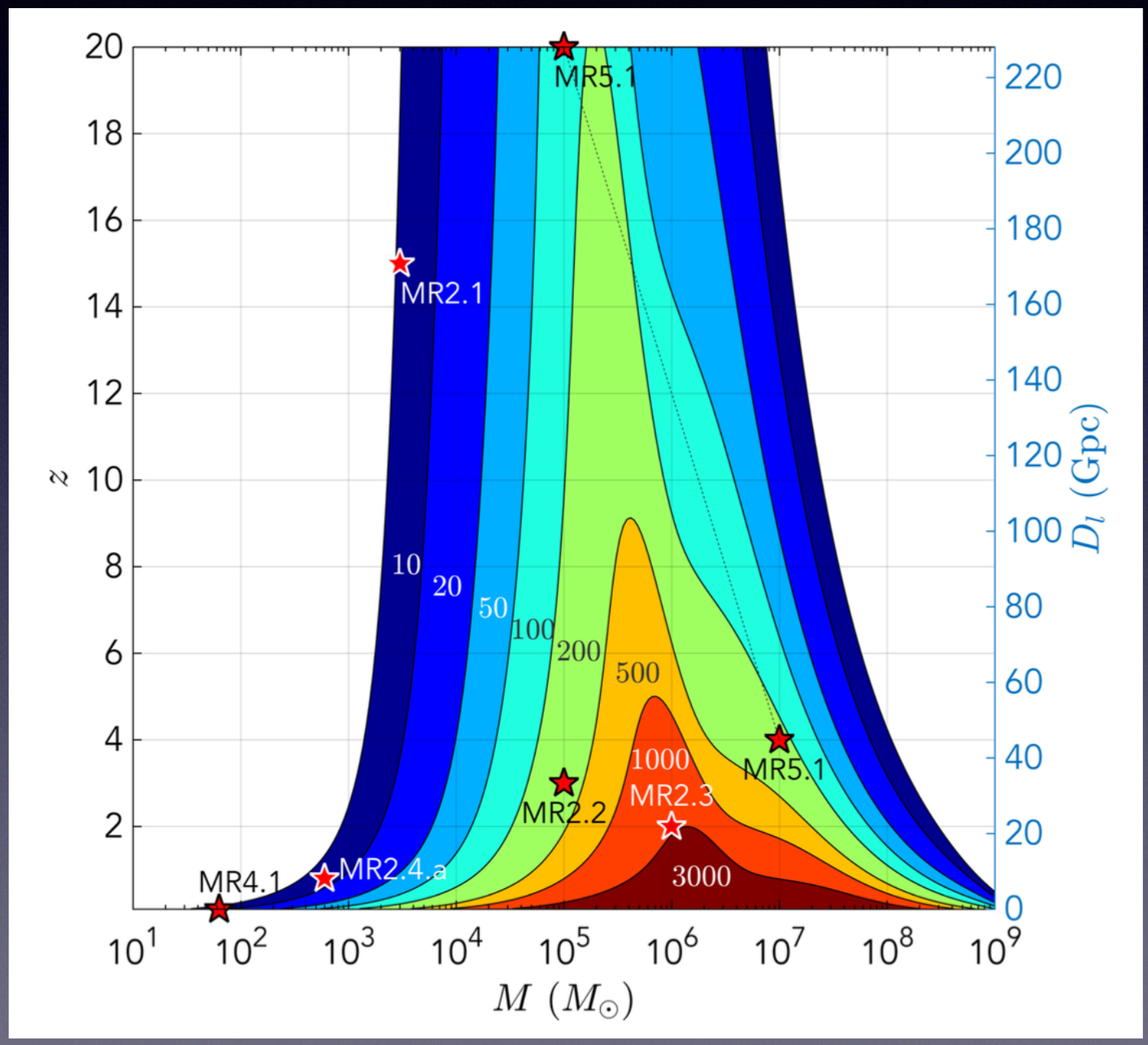

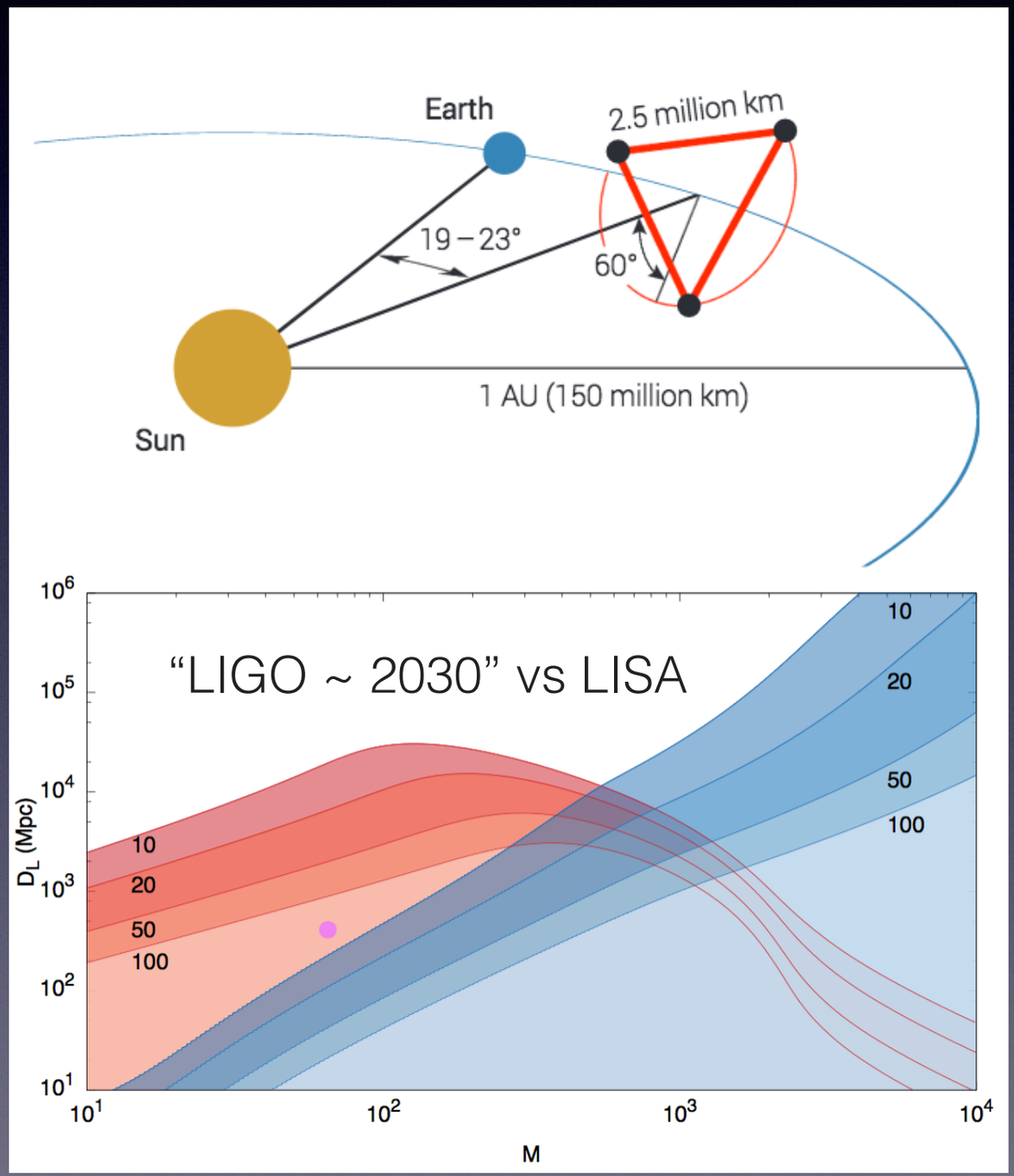

LISA status and timeline

- LISA Pathfinder mission a success (surprisingly stable)
- LISA is now a mission (June 2017)
- Phase 0 ended; currently (2018-19) in Phase A, then ~ 10 yrs of industrial production, with launch ~ 2030-34
- Phase 0/A: finalization of mission design (options analyzed by ESA's Gravitational Wave Advisory Team in collaboration with industry & LISA Consortium) + consortium re-organization

Detector designs considered in ESA studies

- Armlength L= 1, 2, 5 Gm (A1, A2, A5)
- Low-frequency (acceleration) noise at the LISA requirement level of LISA Pathfinder (N2) or 10 times worse (N1): we know it's N2!
- 4 or 6 links (L4, L6), 2 or 5 year mission (M2, M5)
- Laser power of 0.7 W for A1 and 2 W for A2 and A5; telescope mirror size of 25 cm for A1, 28 cm for A2, 40 cm for A5.
  2W laser and 40 cm telescope improve high-frequency performance

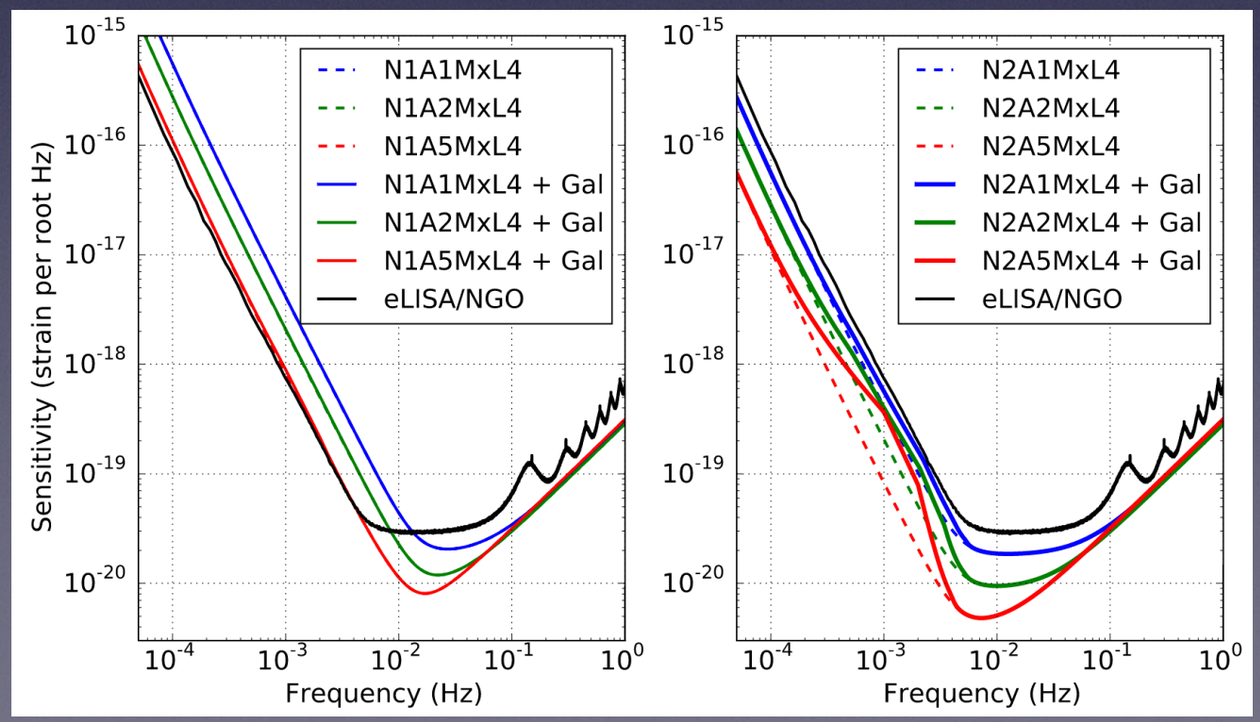

From
Klein EB et al 2015

Galaxy/BH co-evolution

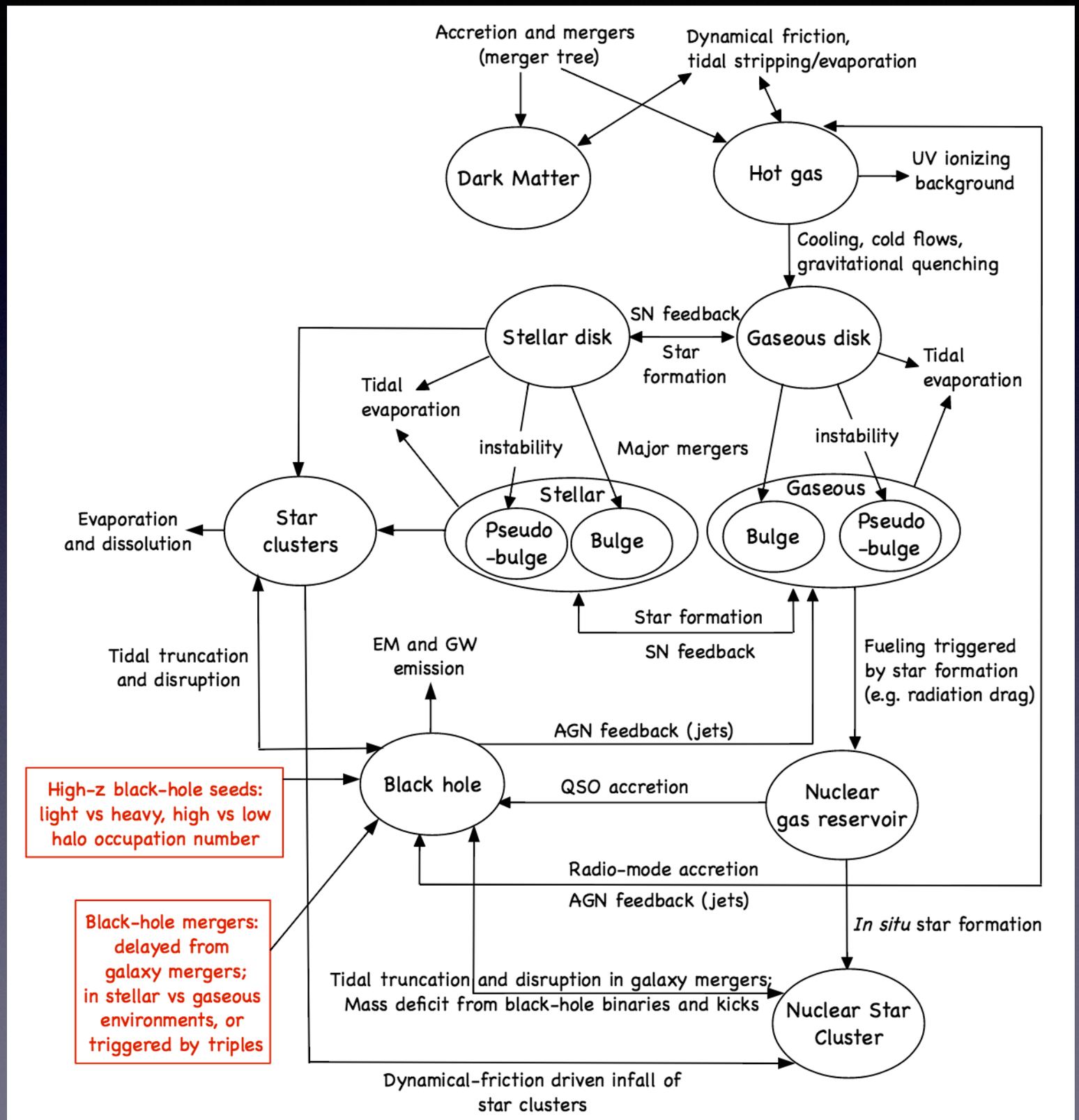

EB 2012

The “final pc problem”

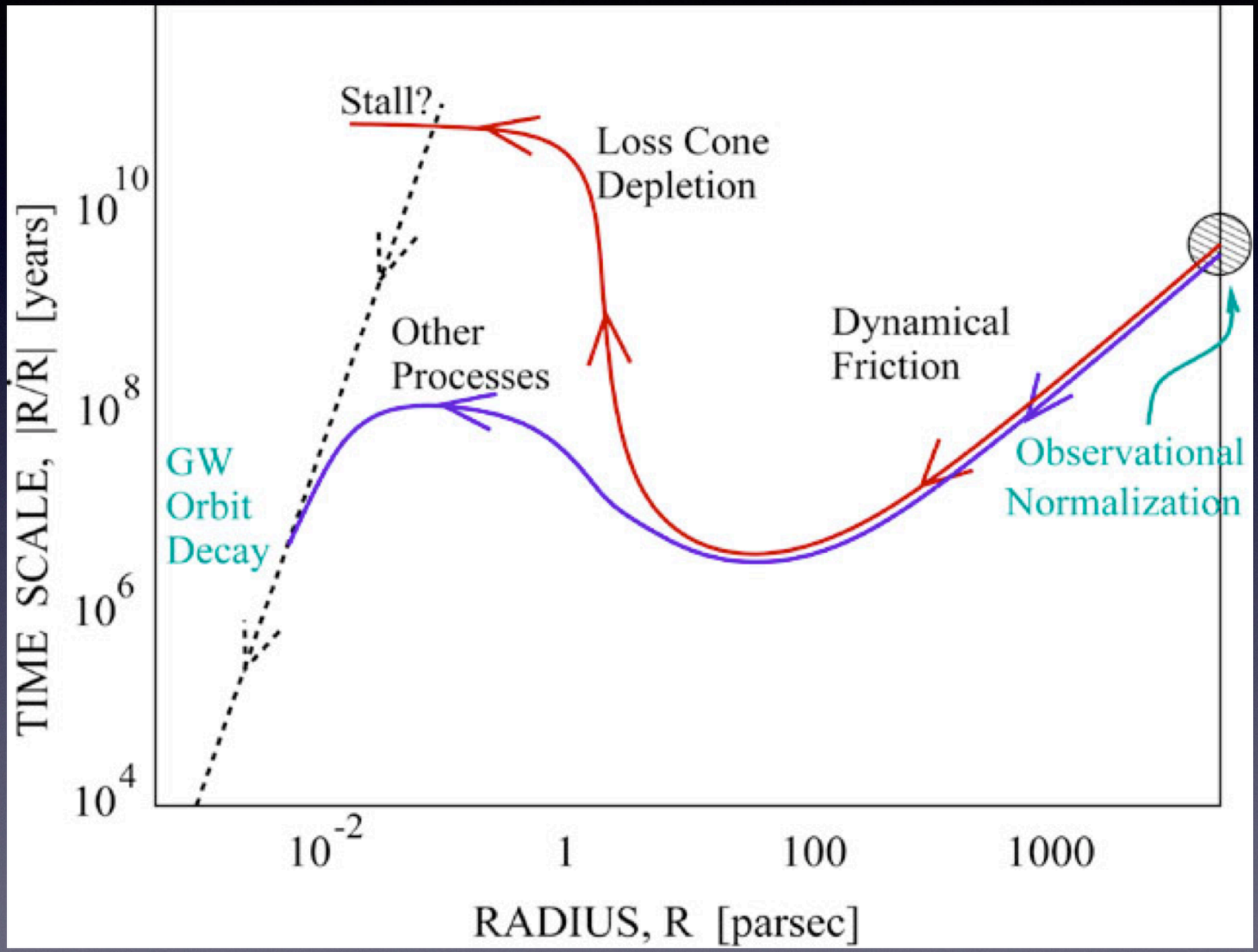

Begelman, Blandford & Rees 1980

Massive BH model's uncertainties

- Seed model: light seeds from PopIII stars (~100 M_{sun}) vs heavy seeds from instabilities of protogalactic disks (~10^5 M_{sun})

- No delays between galaxy and BH mergers, or delays depending on environment/presence of gas:
  - 3-body interactions with stars on timescales of 1-10 Gyr
  - Gas-driven planetary-like migration on timescales ≳ 10 Myr
  - Triple massive BH systems on timescales of 0.1-1 Gyr

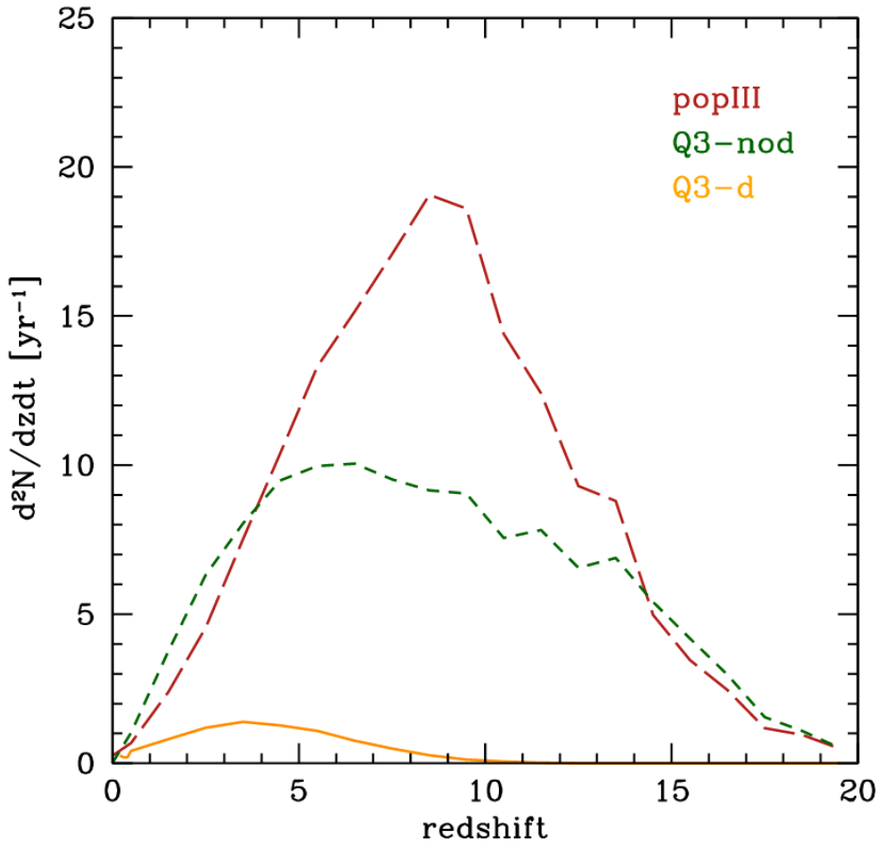

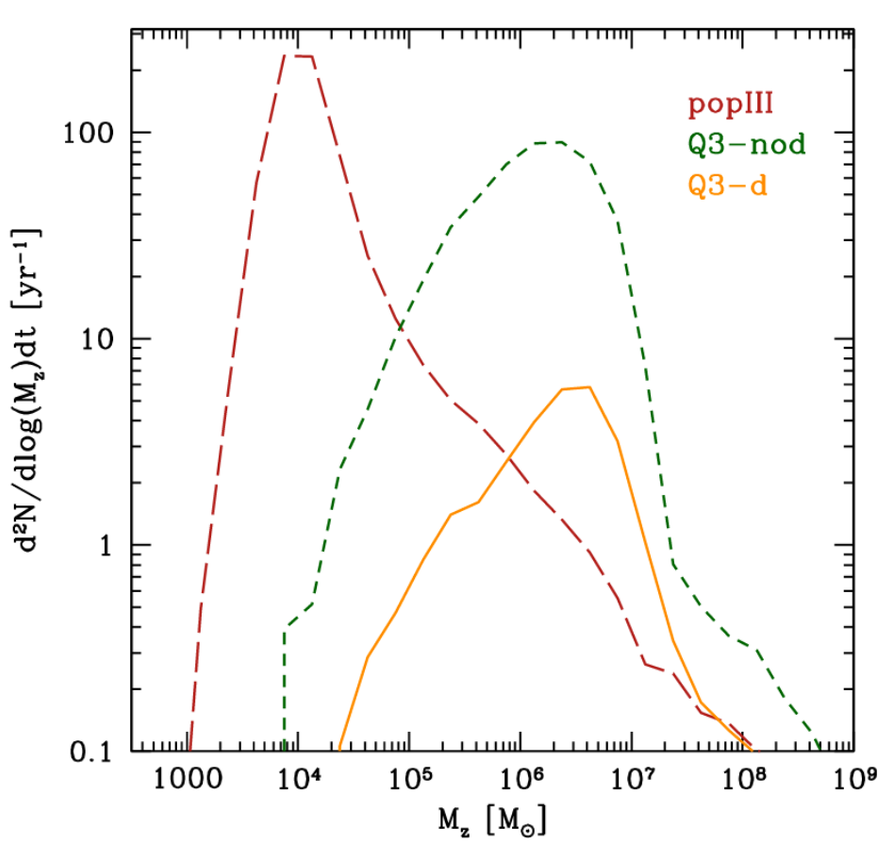

PopIII=light seeds, delays (but similar results with no delays)

Q3-d= heavy seeds, delays
Q3-nod= heavy seeds, no delays

From Klein EB et al 2015

Detection rates

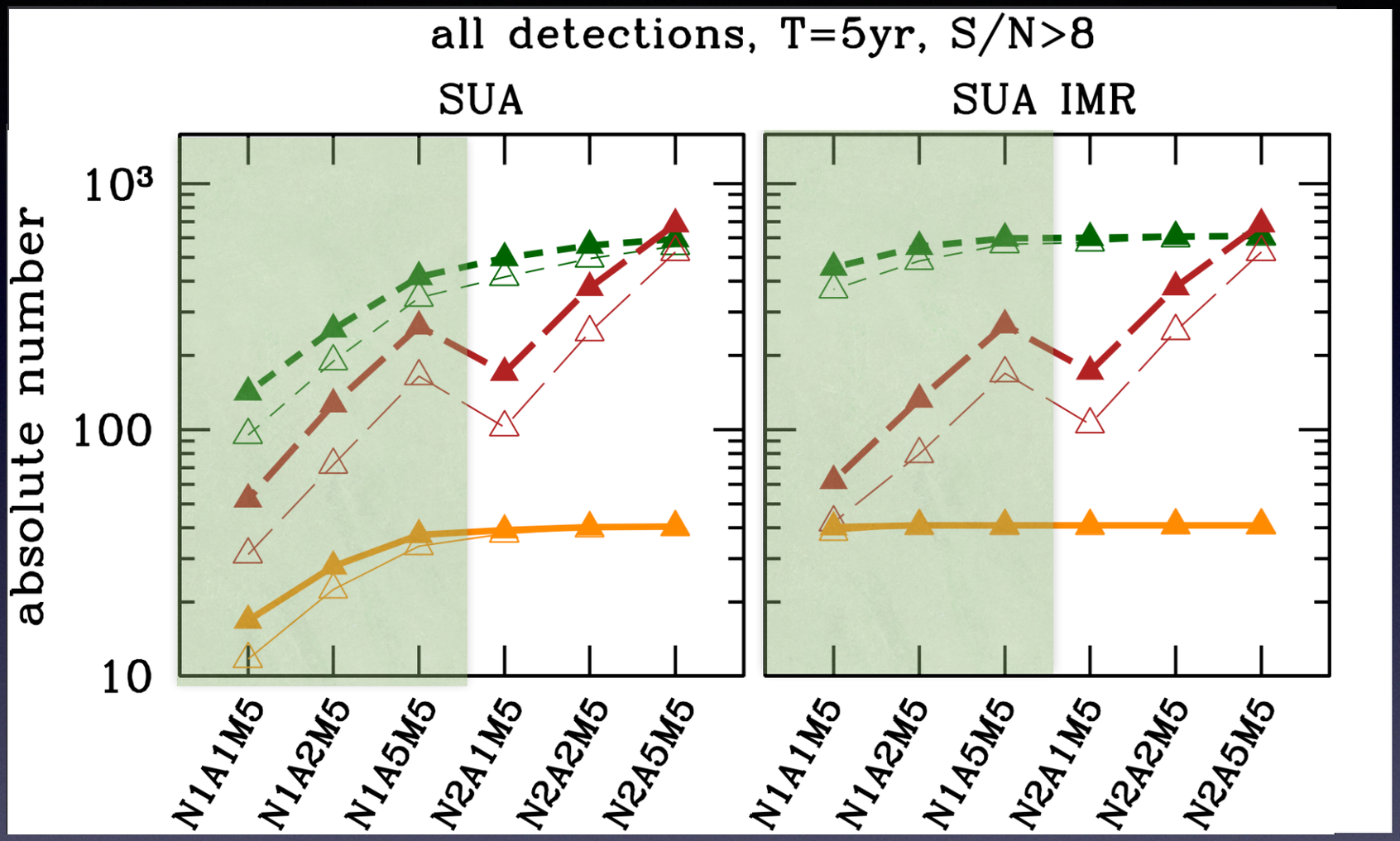

From Klein EB et al 2015

Red = popIII, orange = Q3-d, green = Q3-nod
thick = six links (L6), thin = four links (L4)

- Armlength L= 1, 2, 5 Gm (A1, A2, A5)
- Low-frequency (acceleration) noise at the LISA requirement level of LISA Pathfinder (N2) or 10 times worse (N1): we know it's N2!
- 4 or 6 links (L4, L6), 2 or 5 year mission (M2, M5)

The effect of BH spins: frame-dragging in isolated BHs

- Mass behaves qualitatively like in Newtonian gravity
- Spin affects motion around BHs (“frame dragging”):

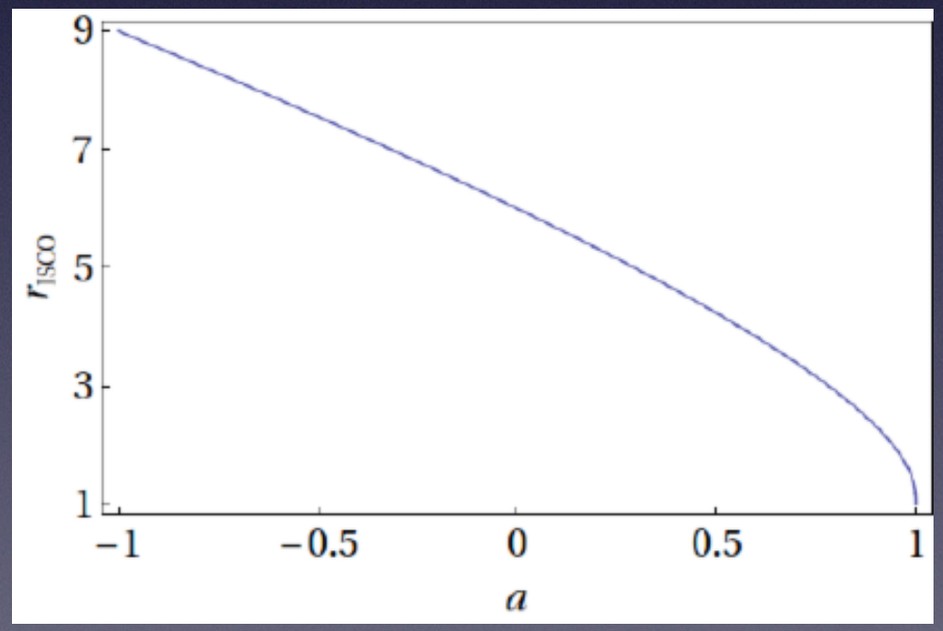

Innermost Stable Circular Orbit
(i.e. inner edge of thin disks)

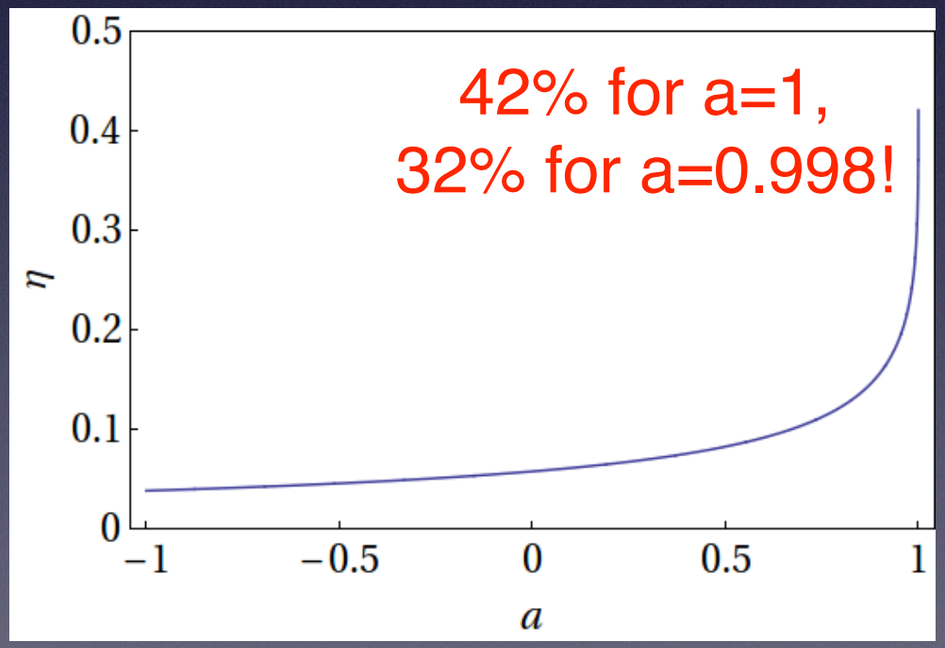

Efficiency of EM
emission from thin disks

The effect of BH spins: frame-dragging in binaries

- For large spins aligned with L, effective ISCO moves inward …

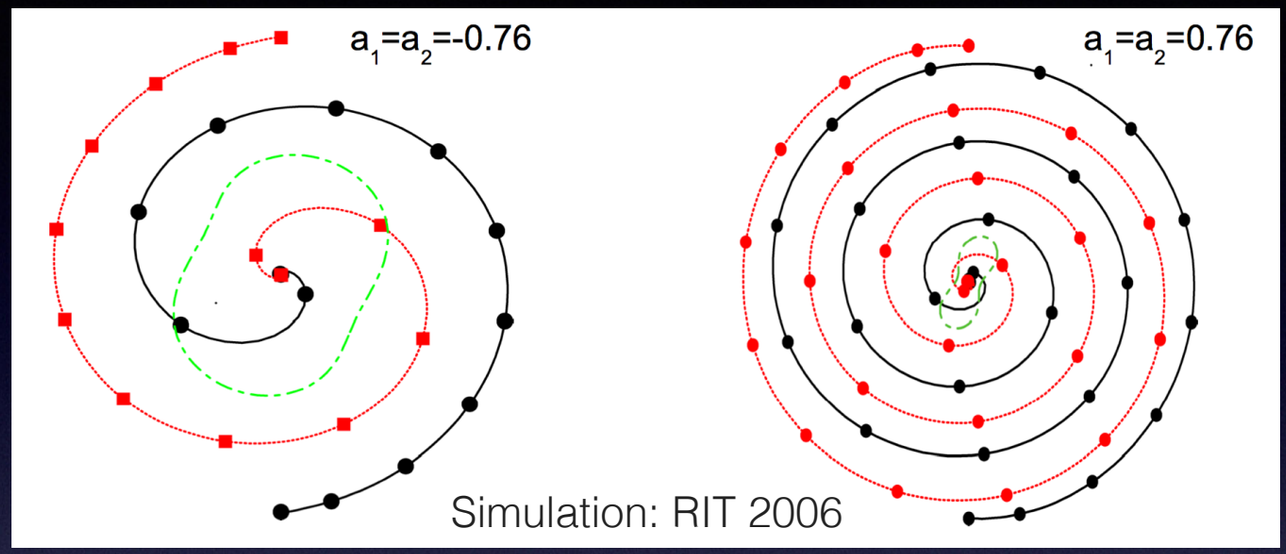

- ... and GW “efficiency” gets larger

Spins increase GW amplitudes

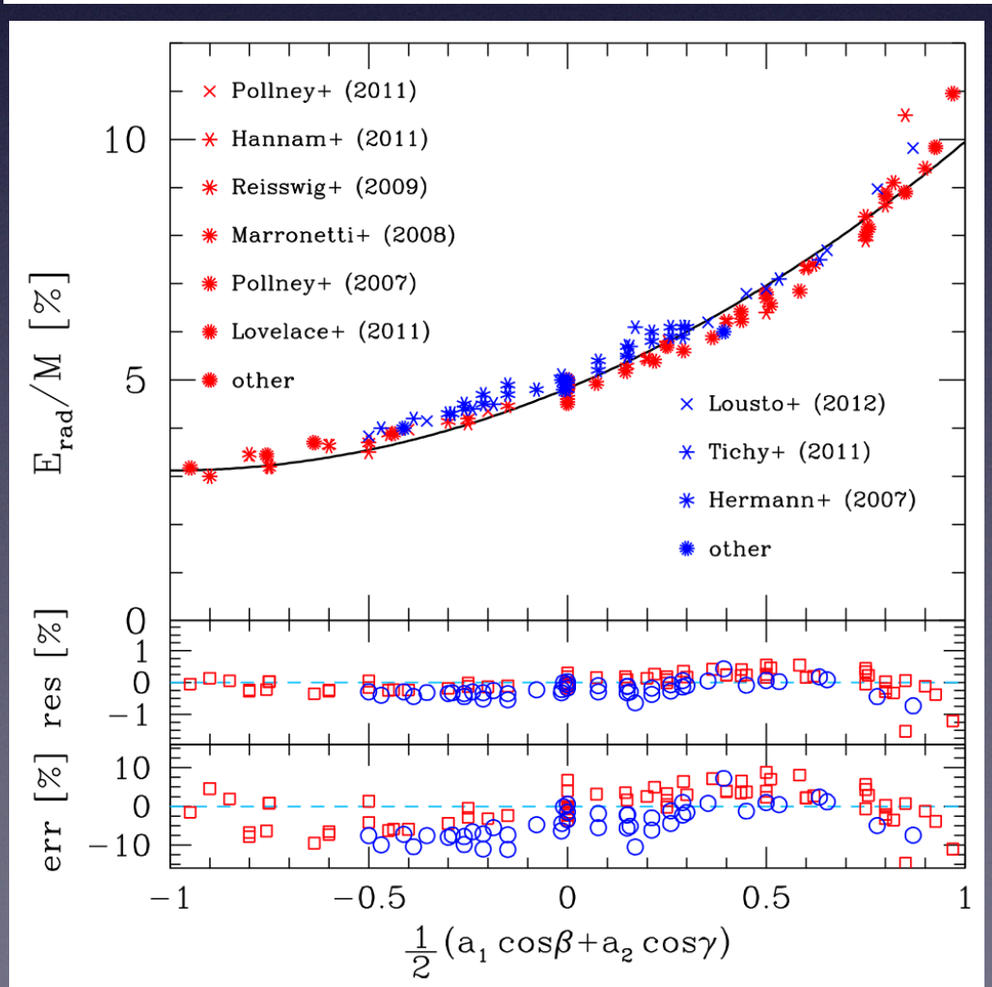

EB, Morozova & Rezzolla (2012)

The effect of BH spins on the waveforms

- Spin precesses around total angular momentum $J=L+S_1+S_2$
- Precession-induced modulations observable with GW detectors:

  - Increase SNR and improve measurements of binary parameters (e.g. luminosity distance and sky localization)

  - Allow measurements of angle between spins

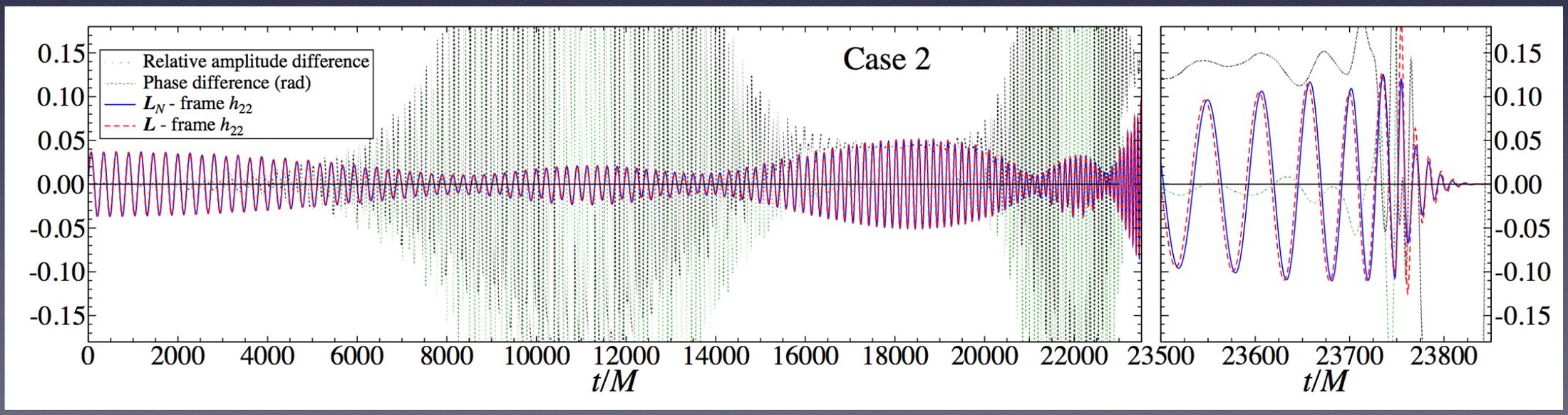

EOB waveforms for BH binary with mass ratio 1:6 and spins 0.6 and 0.8, from Pan et al (2013) [using spin-EOB model of EB & Buonanno 2010, 2011]

Errors on individual masses/spins

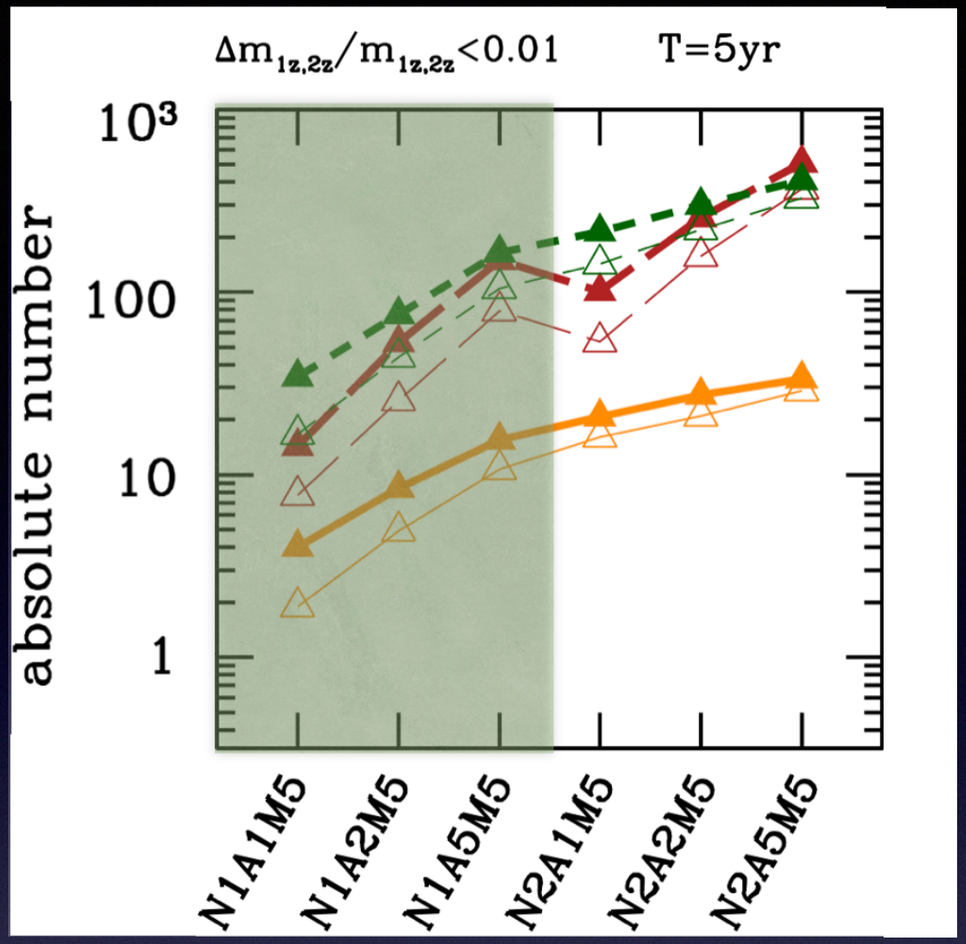

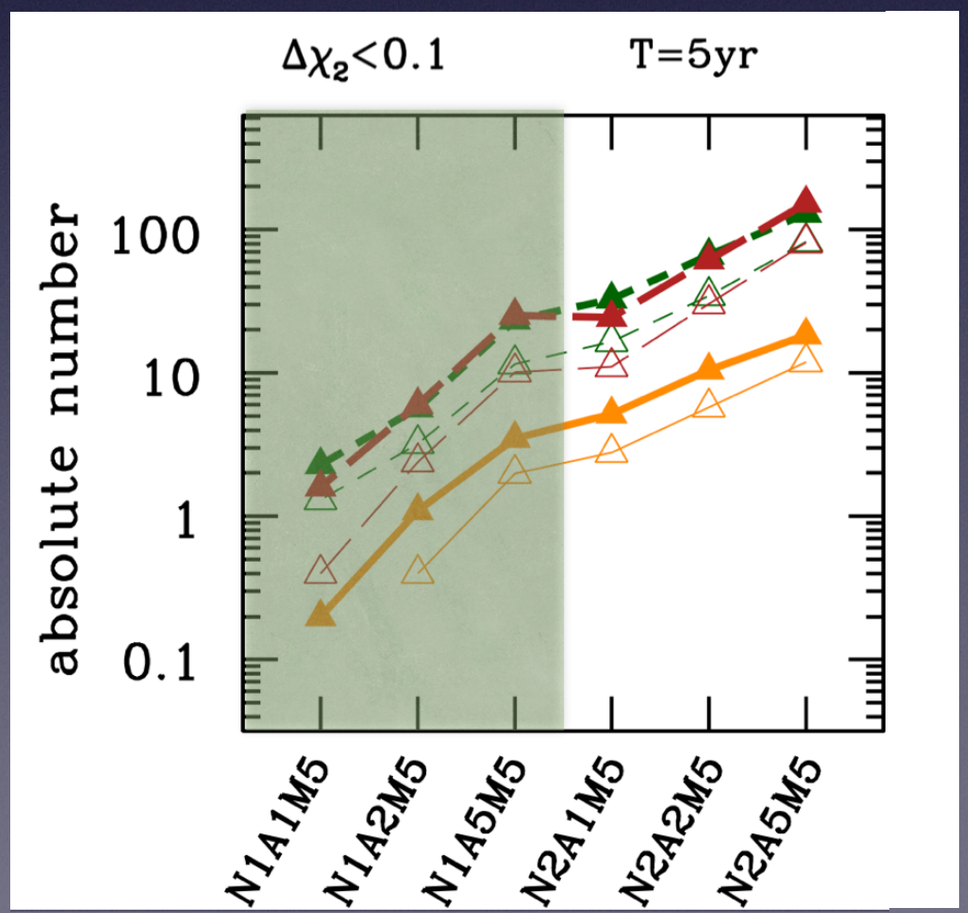

Red = popIII, orange = Q3-d, green = Q3-nod
thick = six links (L6), thin = four links (L4)

Errors on spin inclinations and final spin

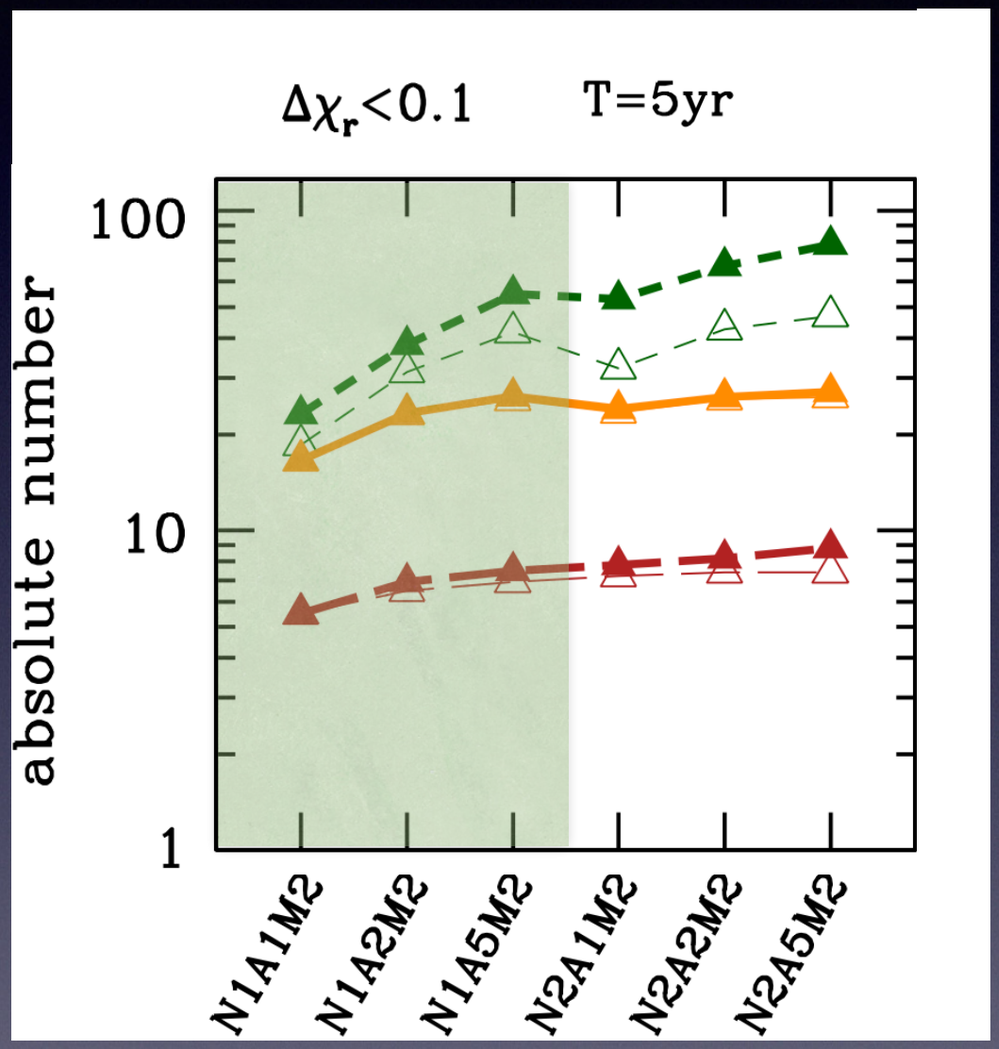

Red = popIII, orange = Q3-d, green = Q3-nod
thick = six links (L6), thin = four links (L4)

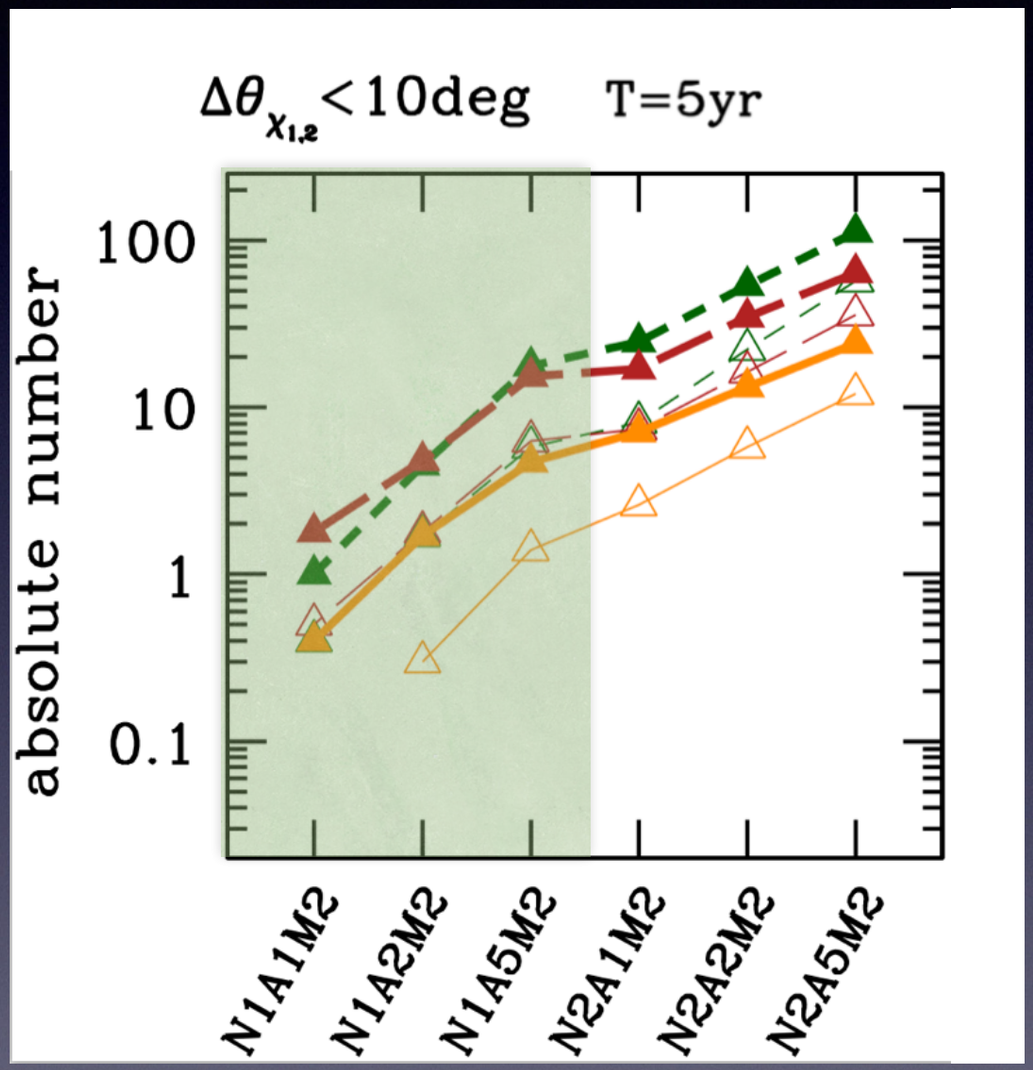

Provides information about interactions with gas (Bardeen-Petterson effect) and ringdown tests of GR

The Bardeen Petterson effect

- Coupling between BH spin S and angular momentum L of misaligned accretion disk + dissipation
- Either aligns or anti-aligns S and L in ~10^5 yrs (for MBHs) << accretion timescale
- Anti-alignment only if disk carries little angular momentum (L < 2S) and is initially counterrotating

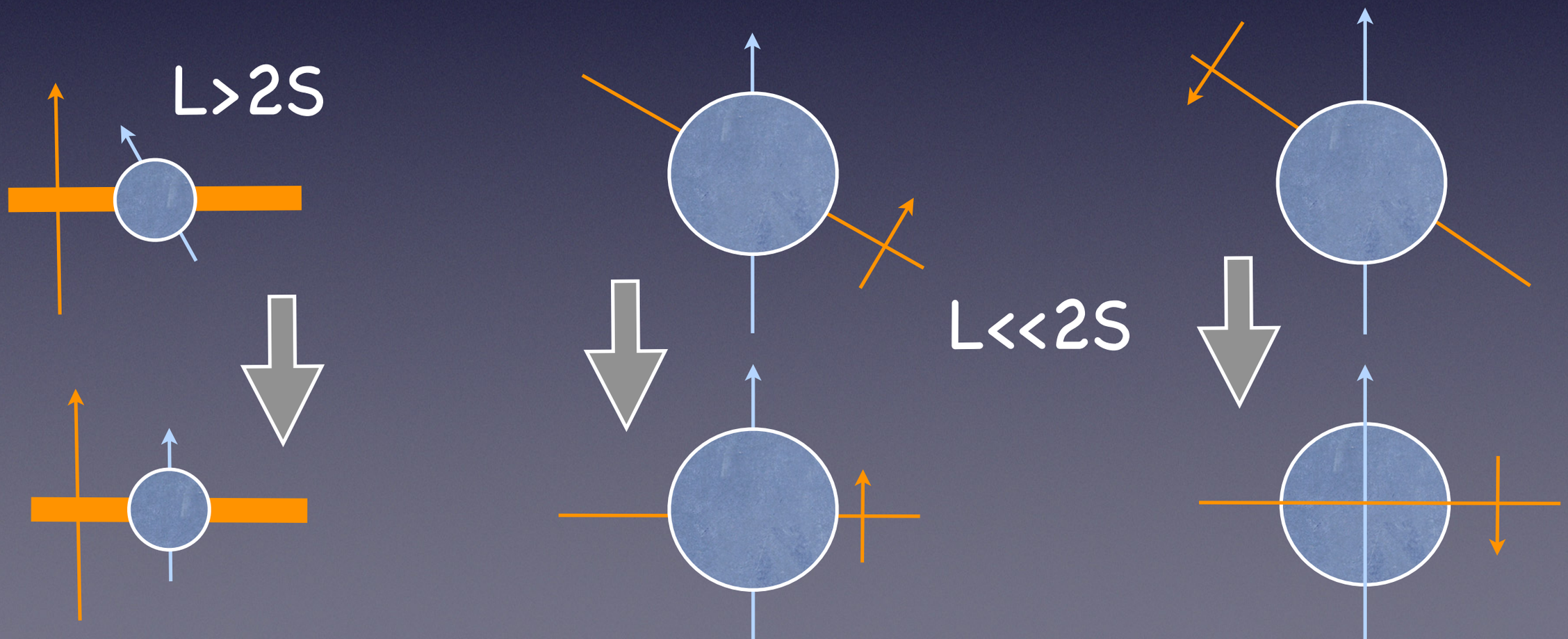

Cosmography (“standard sirens”) and probes of massive BH formation

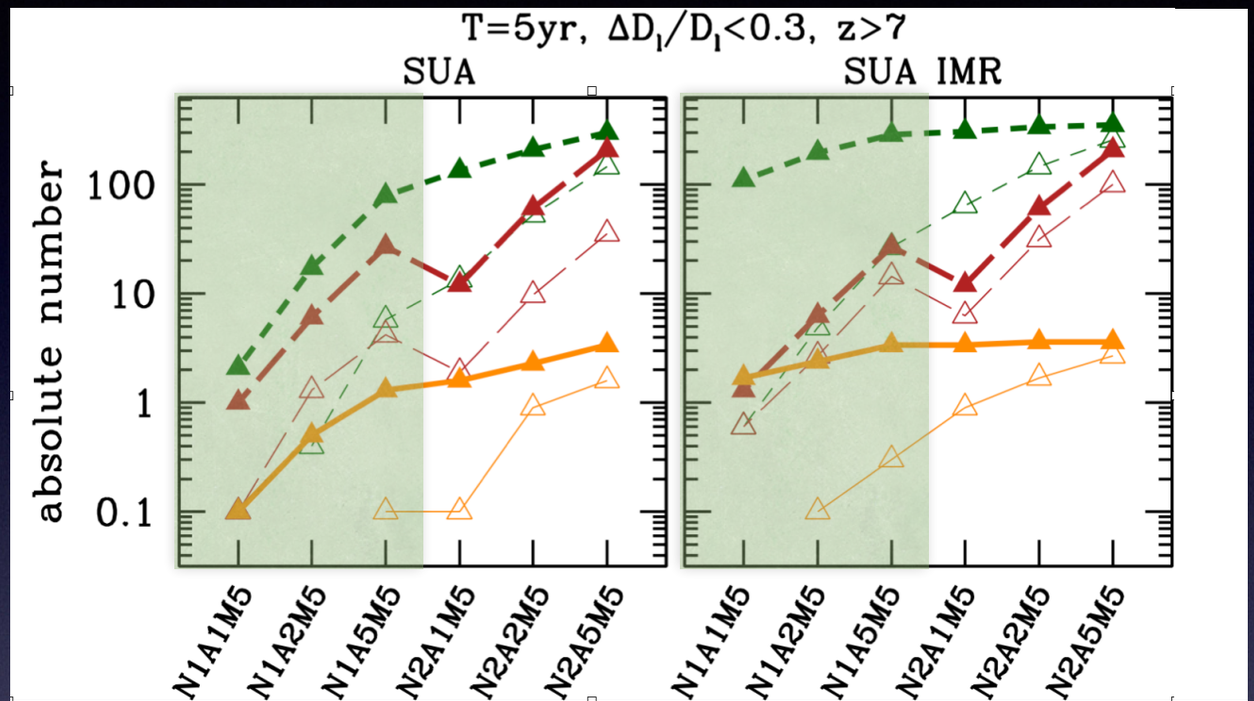

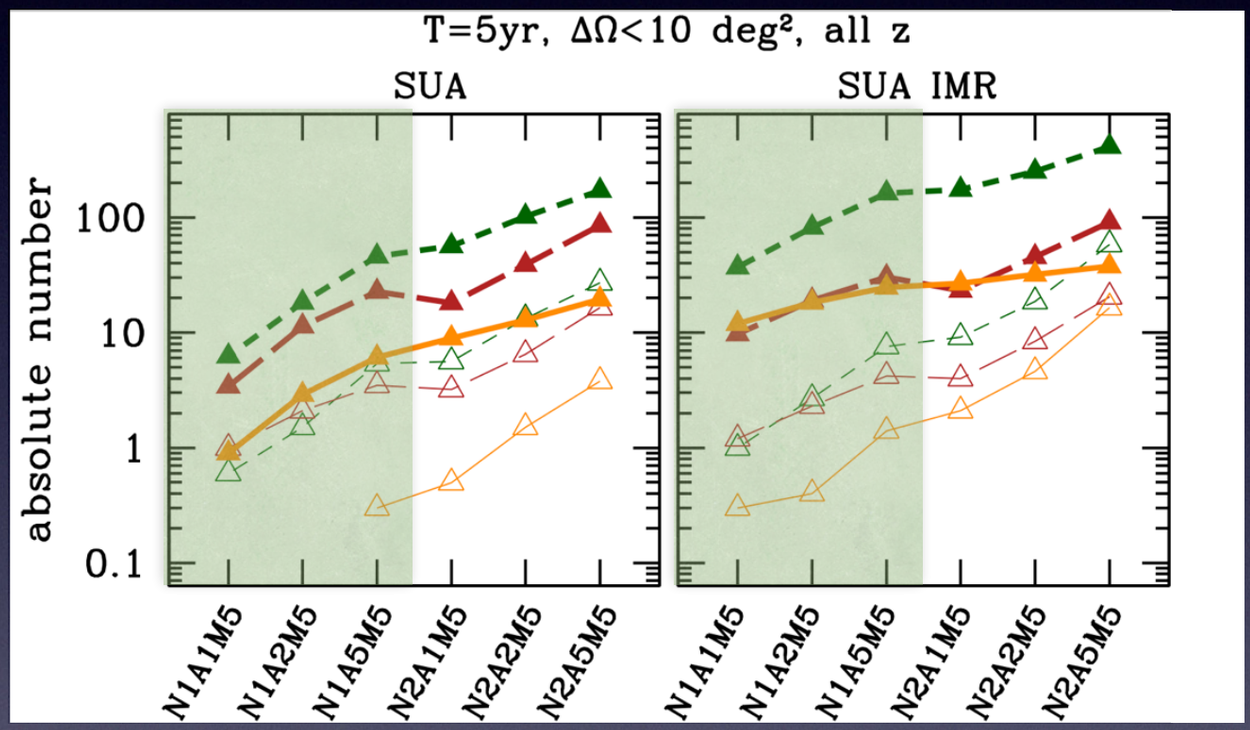

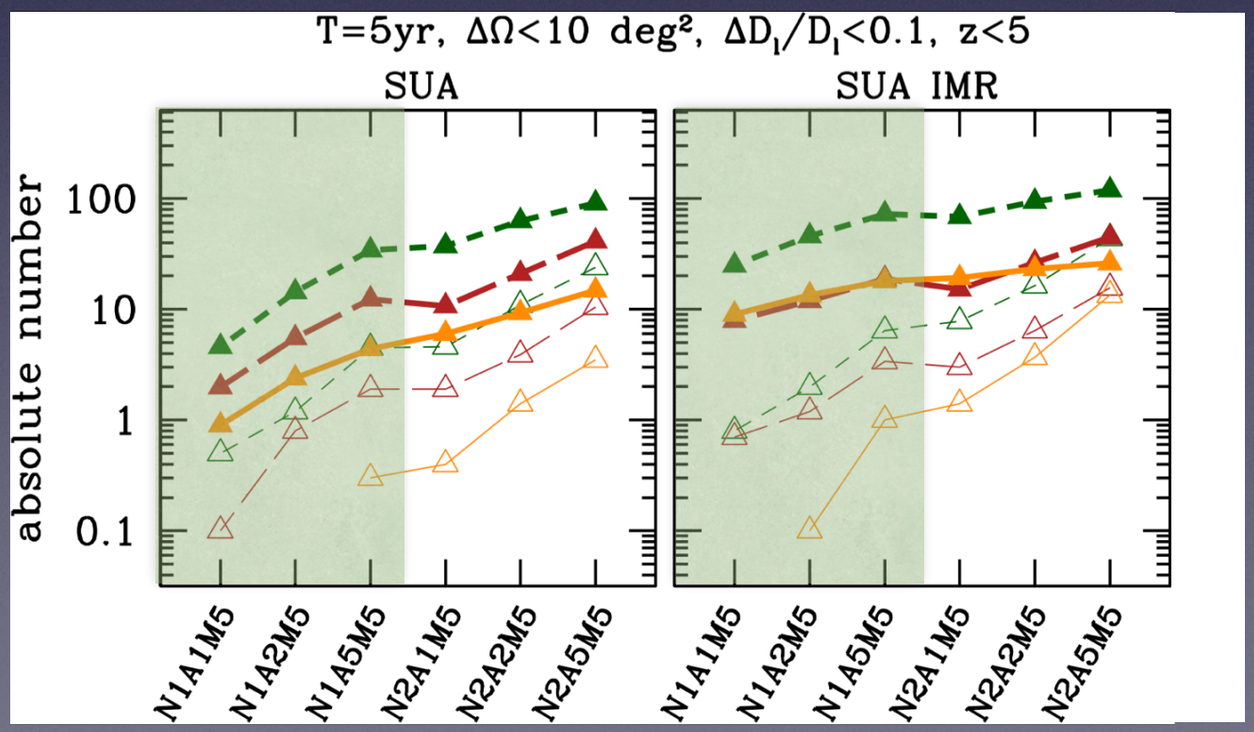

brown = popIII, orange = Q3-d, green = Q3-nod
thick = six links (L6), thin = four links (L4)

From Klein EB et al 2015; see also Tamanini EB et al 2016

Electromagnetic counterparts

- GWs provide measurement of luminosity distance (though degraded by weak lensing) but not redshift
- In order to do cosmography in a non-statistical way, we need redshift
- Electromagnetic (spectroscopic or photometric) redshift measurement needs presence of gas, e.g. radio jet+ follow-up optical emission

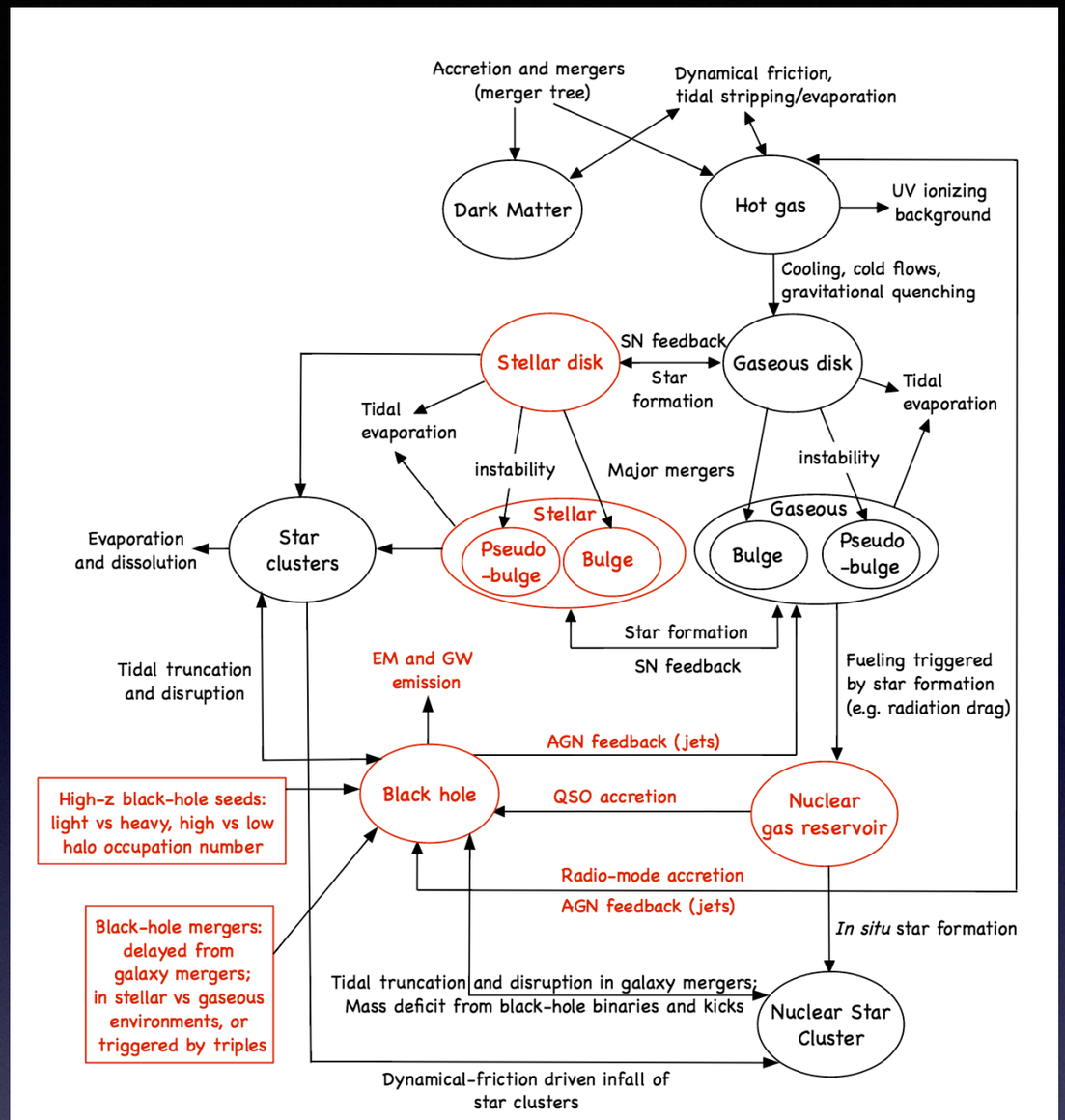

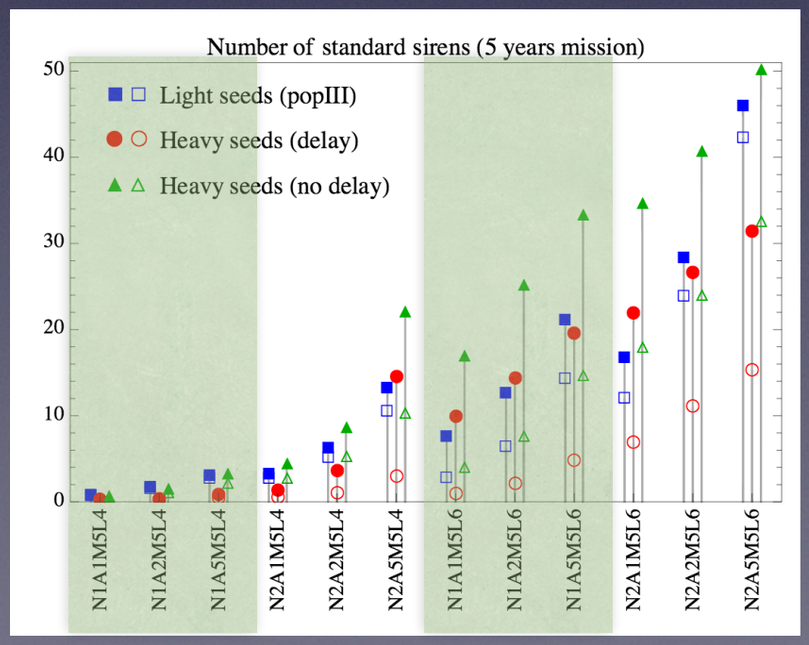

From Tamanini et al 2016

Cosmography with LISA

Model	N2A5M5L6						N2A2M5L4					
	$P(\%)$	$\Delta\Omega_M$	$\Delta\Omega_\Lambda$	Δh	Δw_0	Δw_a	$P(\%)$	$\Delta\Omega_M$	$\Delta\Omega_\Lambda$	Δh	Δw_0	Δw_a
5 param.	100	4.31	7.16	1.58	13.2	92.3	67.8	320	799	47.7	344	5530
	100	18.0	24.9	9.95	88.6	392	2.54	$\gg 10^4$	$\gg 10^4$	$\gg 10^4$	$\gg 10^4$	$\gg 10^4$
	100	2.80	5.15	0.681	4.66	55.7	68.6	138	306	13.3	127	2400
ΛCDM + curv.	100	0.0819	0.281	0.0521			91.5	0.471	2.66	0.429		
	100	0.220	0.541	0.136			12.7	$\gg 10^4$	$\gg 10^4$	$\gg 10^4$		
	100	0.0473	0.207	0.0316			90.7	0.174	1.26	0.145		
ΛCDM	100	0.0473	0.0473	0.0210			97.5	0.275	0.275	0.0910		
	100	0.0917	0.0917	0.0480			32.2	0.543	0.543	0.220		
	100	0.0371	0.0371	0.0146			99.2	0.126	0.126	0.0400		
DDE	100				0.253	1.32	97.5				1.03	6.36
	100				0.584	2.78	37.3				4.96	26.1
	100				0.176	1.00	95.8				0.427	2.87
Accel. & curv. test	100	0.0190	0.0735				99.2	0.211	0.396			
	100	0.0280	0.105				37.3	0.977	1.30			
	100	0.0213	0.0631				94.1	0.116	0.202			
Error on Ω_M	100	0.0173					100	0.0670				
	100	0.0238					53.4	0.0755				
	100	0.0172					100	0.0437				
Error on h	100			0.00712			100			0.0146		
	100			0.00996			53.4			0.0175		
	100			0.00531			100			0.00853		
Error on w_0	100				0.0590		100				0.121	
	100				0.0786		53.4				0.146	
	100				0.0467		100				0.0734	

sky-location by inspiral only

Model	N2A5M5L6						N2A2M5L4					
	$P(\%)$	$\Delta\Omega_M$	$\Delta\Omega_\Lambda$	Δh	Δw_0	Δw_a	$P(\%)$	$\Delta\Omega_M$	$\Delta\Omega_\Lambda$	Δh	Δw_0	Δw_a
5 param.	100	2.51	4.40	0.951	8.01	55.2	80.5	120	253	24.8	177	2230
	100	4.64	6.90	2.58	22.4	103	44.1	1480	3250	371	2350	$\gg 10^4$
	100	1.05	1.97	0.265	2.07	21.2	93.2	12.6	27.8	2.08	15.9	227
ΛCDM + curv.	100	0.0467	0.155	0.0299			96.6	0.315	1.51	0.228		
	100	0.0875	0.209	0.0527			77.1	0.396	1.61	0.306		
	100	0.0265	0.0914	0.0161			99.2	0.0610	0.342	0.0520		
ΛCDM	100	0.0267	0.0267	0.0121			99.2	0.121	0.121	0.0445		
	100	0.0368	0.0368	0.0199			90.7	0.151	0.151	0.0681		
	100	0.0186	0.0186	0.00803			100	0.0464	0.0464	0.0159		
DDE	100				0.149	0.798	98.3				0.507	3.09
	100				0.241	1.14	89.0				0.777	4.06
	100				0.101	0.544	99.2				0.201	1.20
Accel. & curv. test	100	0.0105	0.0412				99.2	0.0660	0.174			
	100	0.00972	0.0429				84.7	0.0544	0.161			
	100	0.00887	0.0310				99.2	0.0381	0.0804			
Error on Ω_M	100	0.00966					100	0.0319				
	100	0.00935					94.1	0.0283				
	100	0.00788					100	0.0199				
Error on h	100			0.00412			100			0.00850		
	100			0.00446			94.1			0.00937		
	100			0.00307			100			0.00485		
Error on w_0	100				0.0342		100				0.0678	
	100				0.0368		94.1				0.0729	
	100				0.0254		100				0.0416	

From Tamanini et al 2016

sky-location by IMR

- Better LISA configurations provide measurements of h under different systematics than present probes
- Measurement of Ω_m slightly better than SNIa with best designs
- Measurement of combination of Ω_m and Ω_Λ different from SNIa/CMB (i.e. potential to break degeneracy)
- Discovery space: LISA sensitive to cosmological evolution at z ~ 1 - 8

Cosmography with LISA

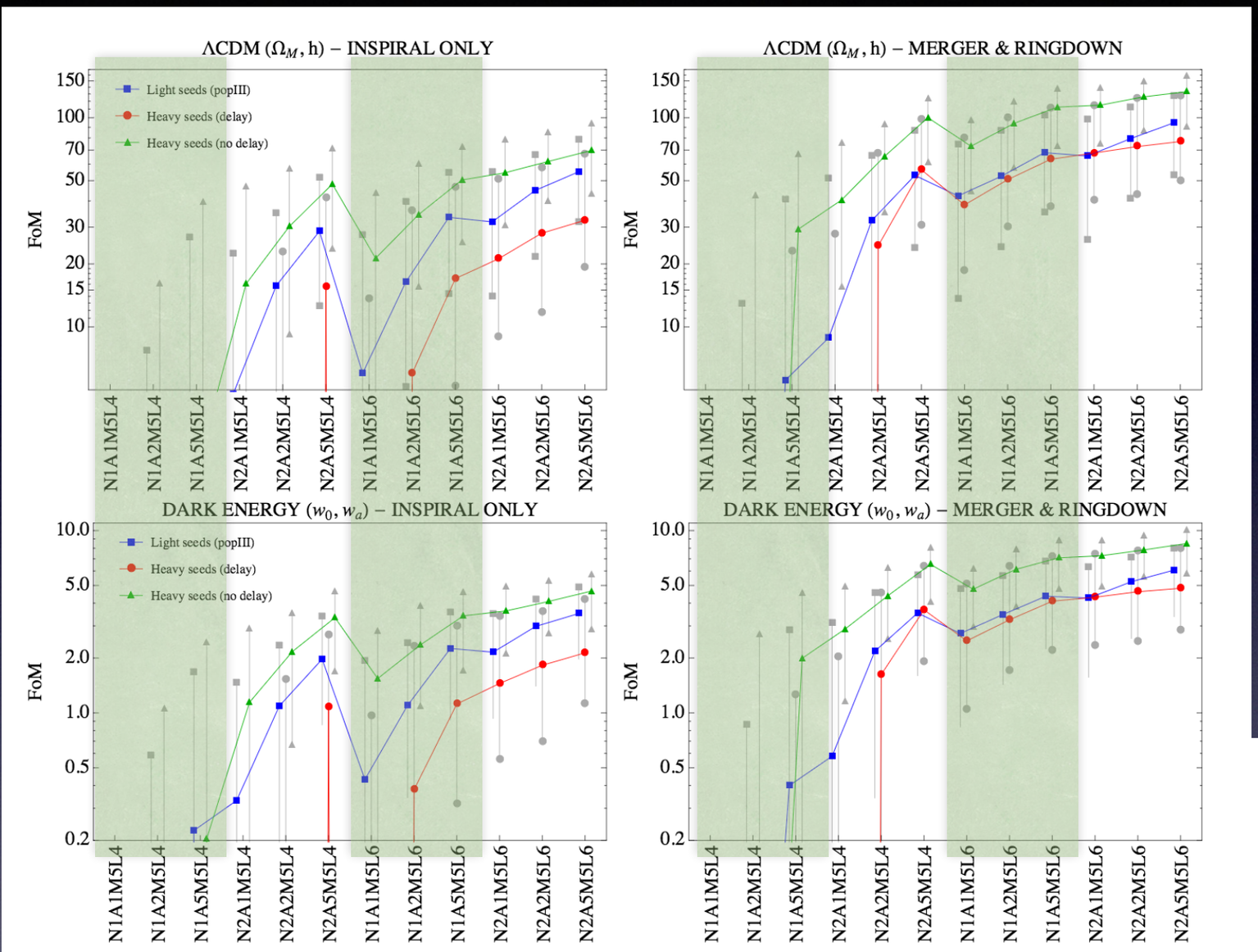

From Tamanini et al 2016

N2A5M5L6 N2A2M5L6 N2A1M5L6 N1A5M5L6 N2A5M5L4	Constraints comparable to or slightly worse than N2A5M5L6
N1A2M5L6	Constraints worse than N2A5M5L6, but better than N2A2M5L4.
N1A1M5L6 N2A2M5L4	Constraints comparable to or slightly better than N2A2M5L4
N2A1M5L4 N1A5M5L4 N1A2M5L4 N1A1M5L4	Constraints worse than N2A2M5L4 or no constraints at all.

FoM ~ 1/error

What can we learn from PTA limits?

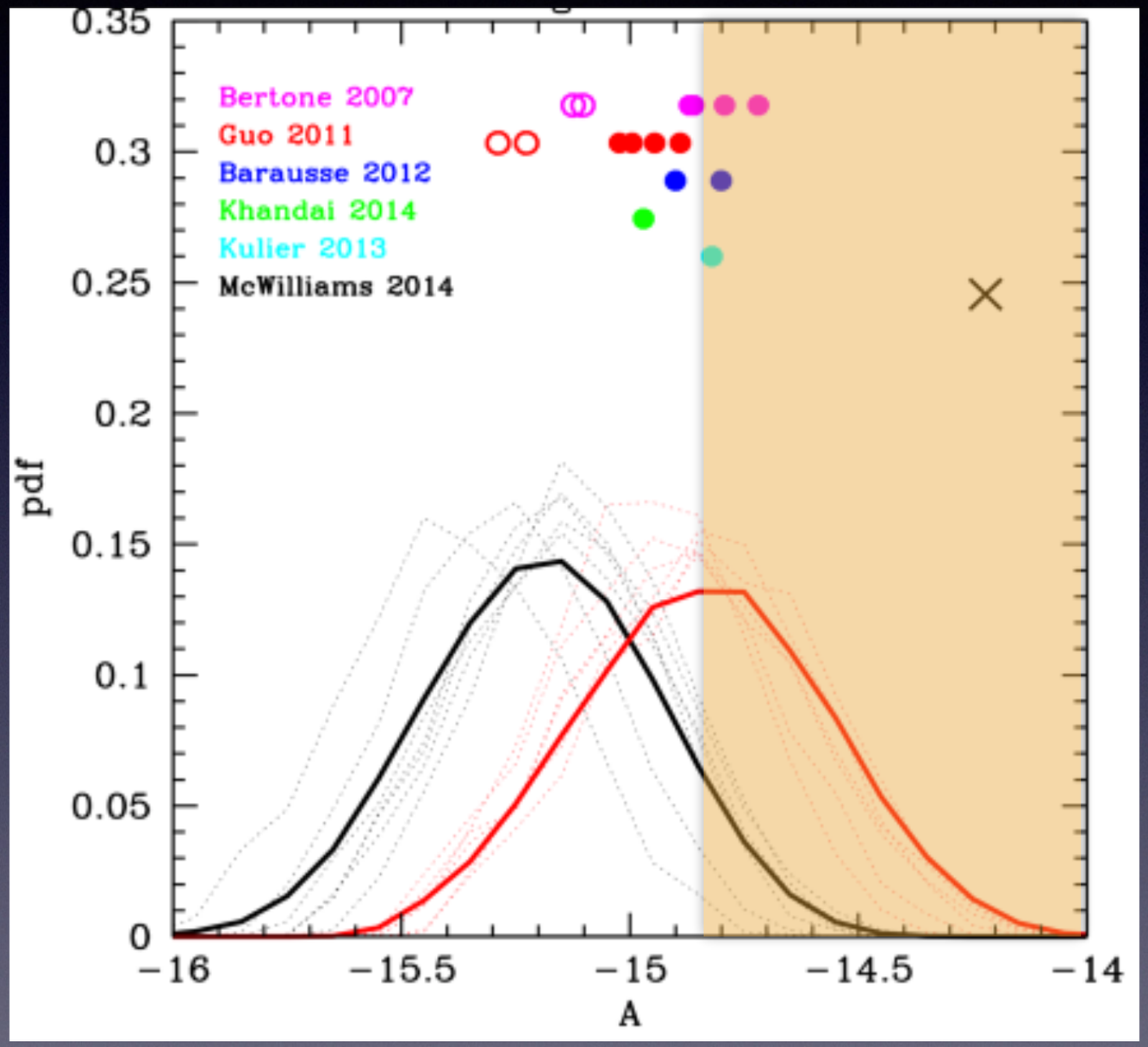

Background characteristic strain at f=1/yr is $A<1.45 \times 10^{-15}$ (Nanograv 2018)

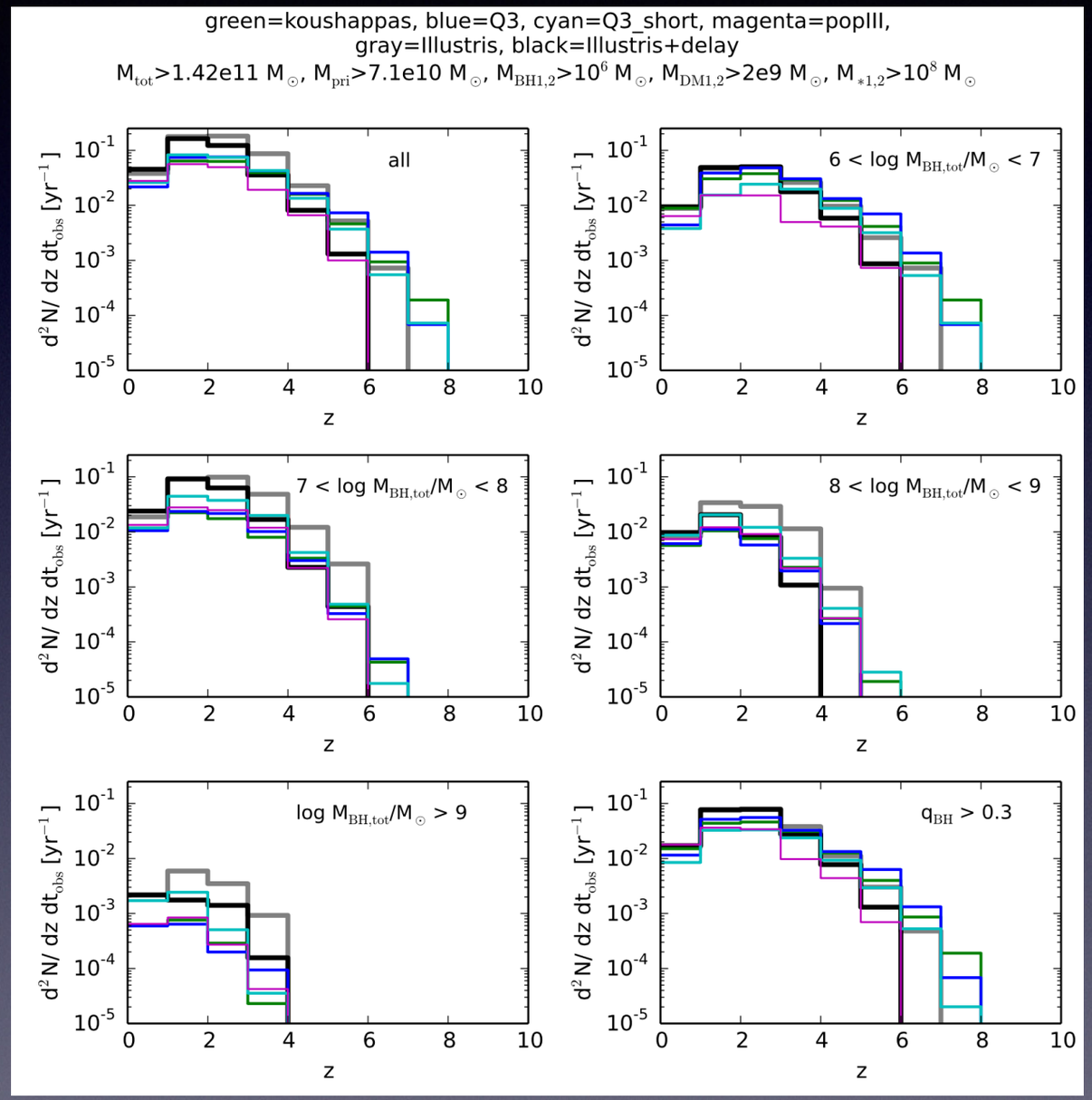

SAM vs simulations
(EB 2012 vs Illustris)

Why are we seeing nothing?

Predictions assume:

- GW driven binaries
- Circular orbits
- Efficient formation of bound massive BH binaries after galaxy mergers
- M-σ relation

Loopholes:

- Binaries may merge faster than expected based on GW emission alone (hence less time in band)
- Eccentric binaries (more power at high frequencies) due e.g. to strong environmental effects/triple systems
- Last pc problem (binaries stall)
- M-σ relation may be biased

The final parsec “problem”

- If BH binaries stall and do not merge, triple systems naturally form as a result of later galaxy mergers
- Merger induced by Kozai-Lidov resonances (secular exchange between eccentricity and orbital inclination)

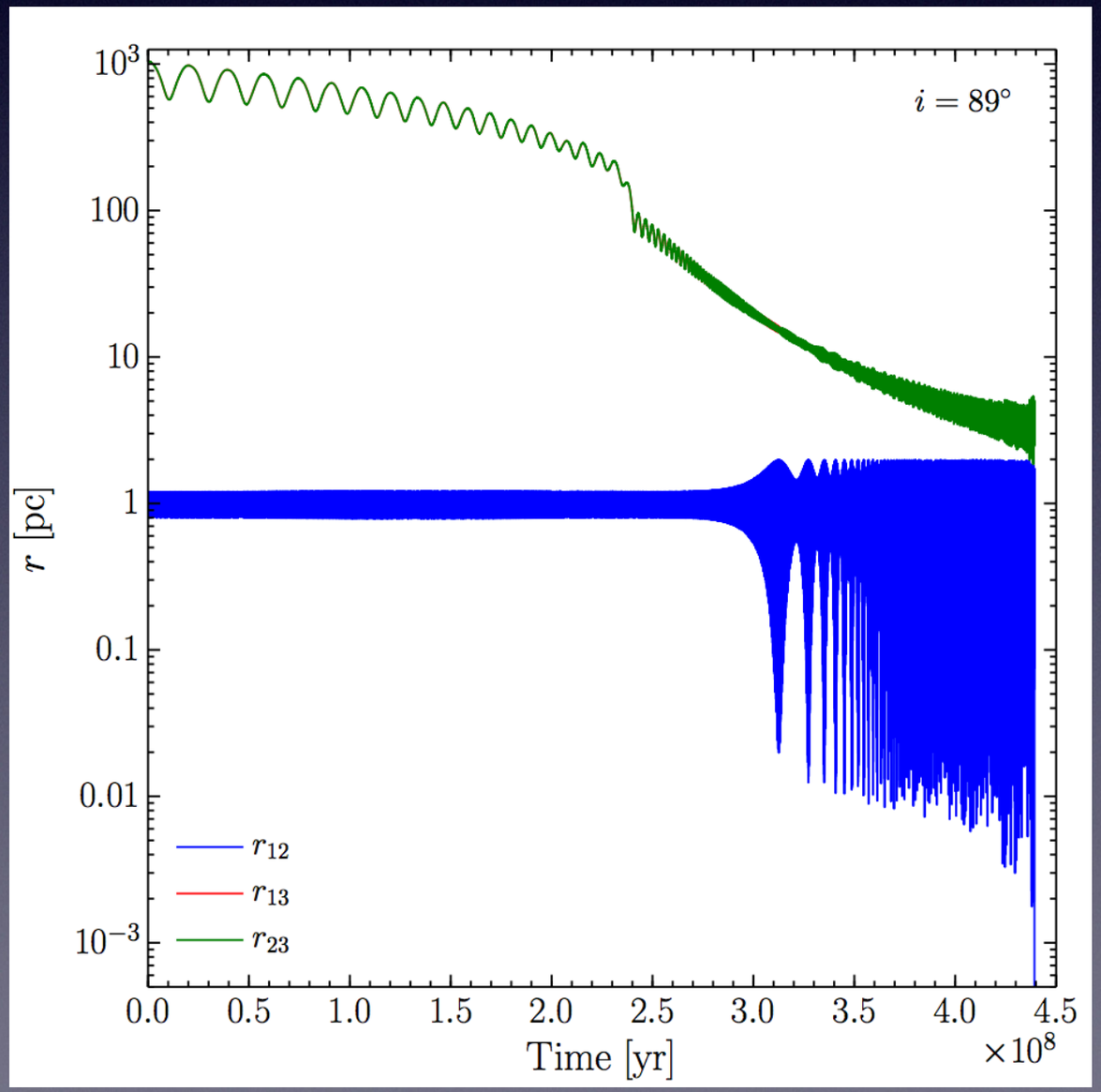

$$t_{\rm KL} \sim \frac{a_{\rm out}^3(1-e_{\rm out}^2)^{3/2}\sqrt{m_1+m_2}}{G^{1/2}a_{\rm in}^{3/2}m_3} \simeq 2\times 10^6 \ \ {\rm yrs},$$

$m_1 = m_2 = m_3 = 10^8$ M$_\odot$, $a_{\rm in} = 1$ pc, $a_{\rm out} = 10$ pc, and $e_{\rm out} = 0$.

PN 3-body simulation in a stellar environment, with m_1=10^8 M_{sun}, m_2=3 x 10^7 M_{sun}, m_3=5 x 10^7 M_{sun} (Bonetti, Haardt, Sesana & EB 2016)

Triple-induced BH mergers: PTA and LISA

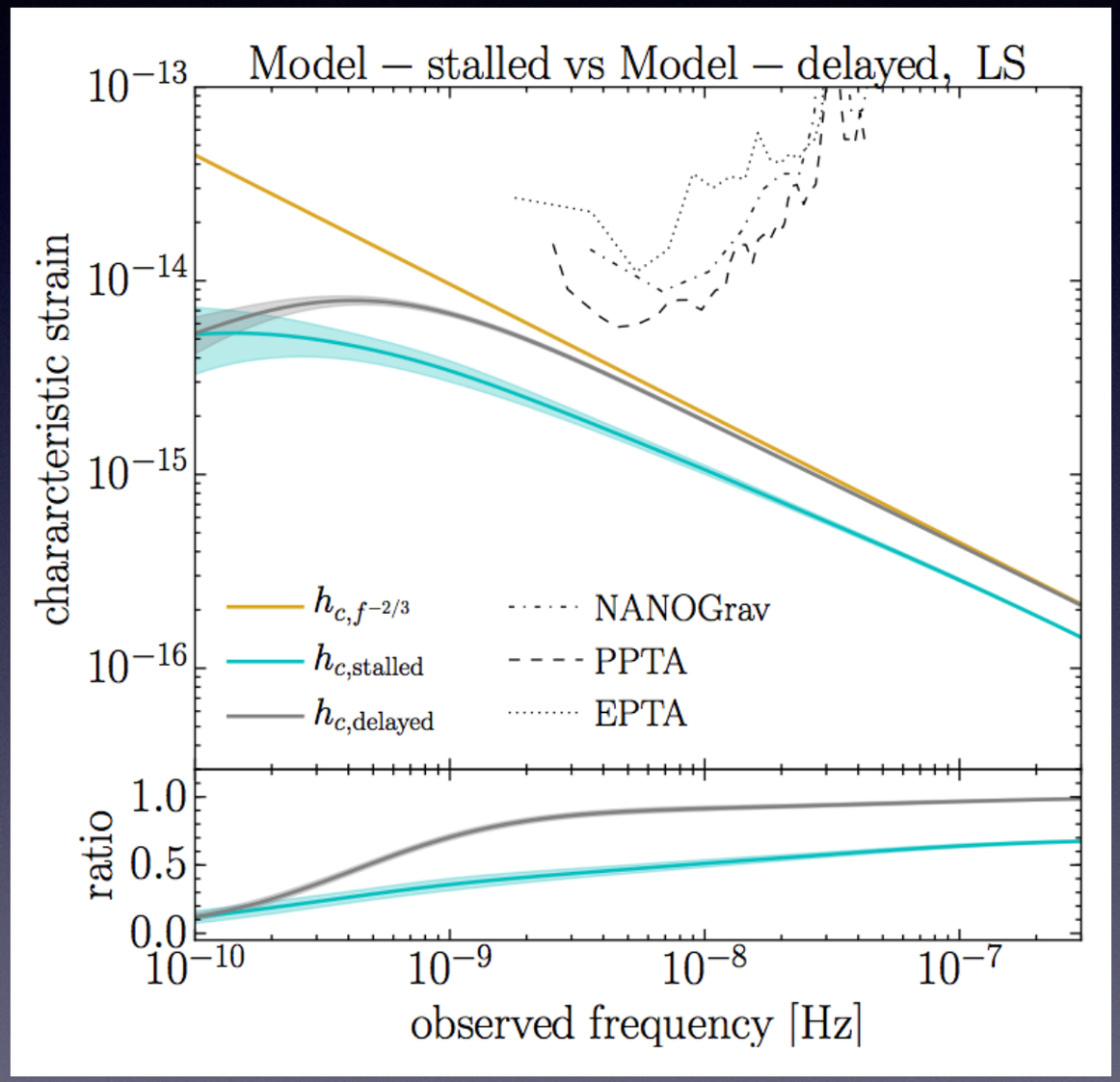

Bonetti, Sesana, EB, Haardt 2018

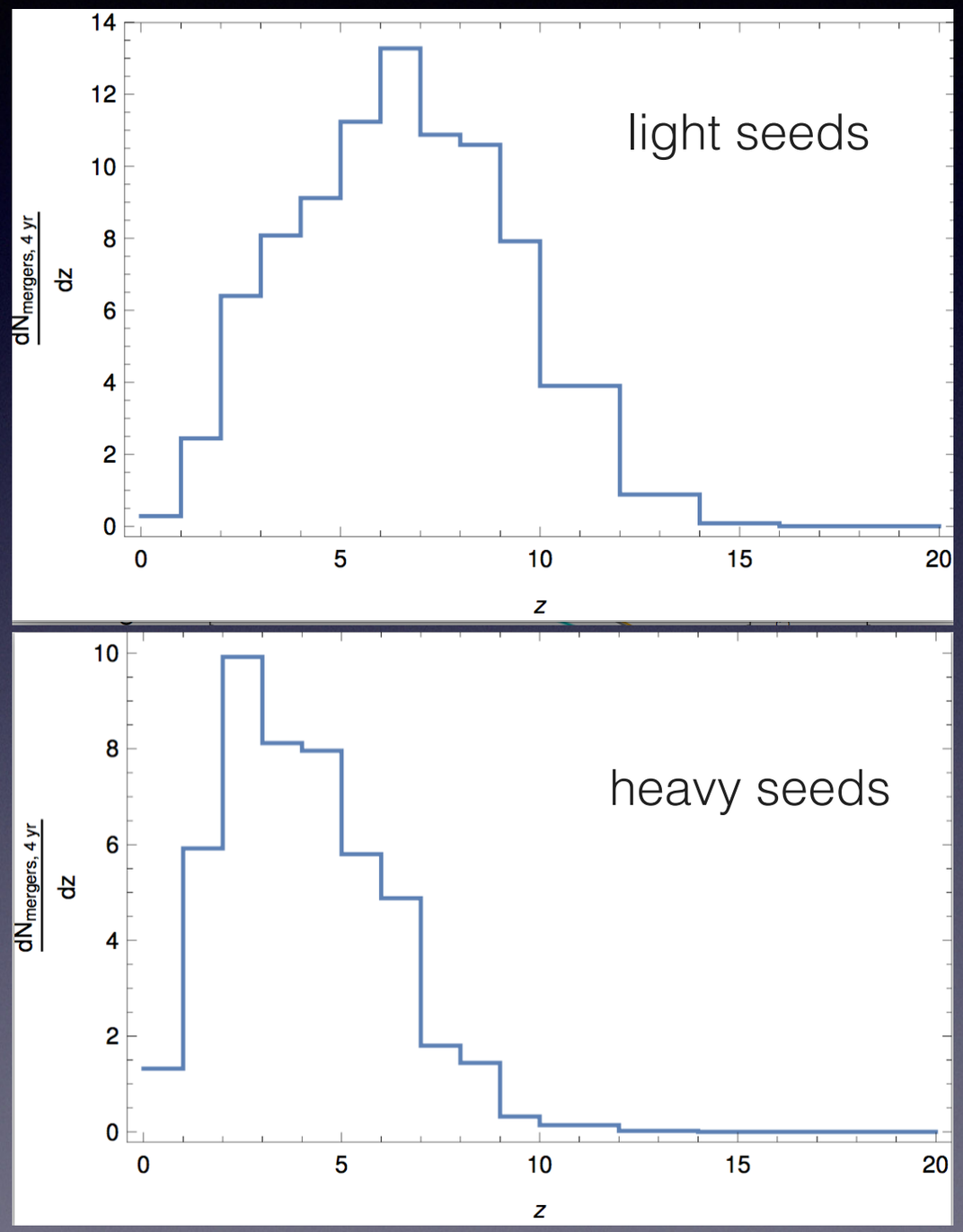

Bonetti, Sesana, EB & Haardt, in preparation

Eccentric inspirals and bursts?

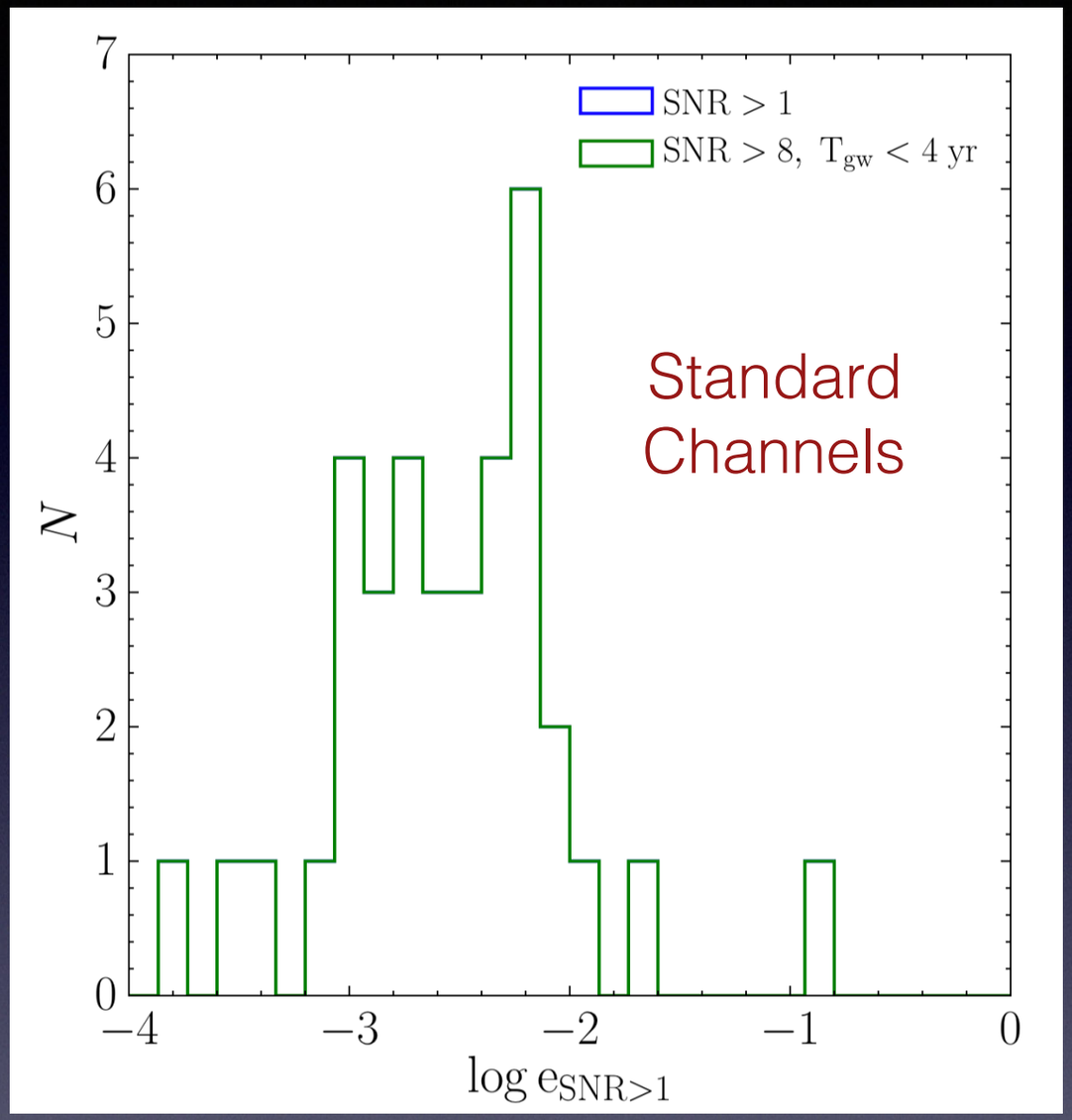

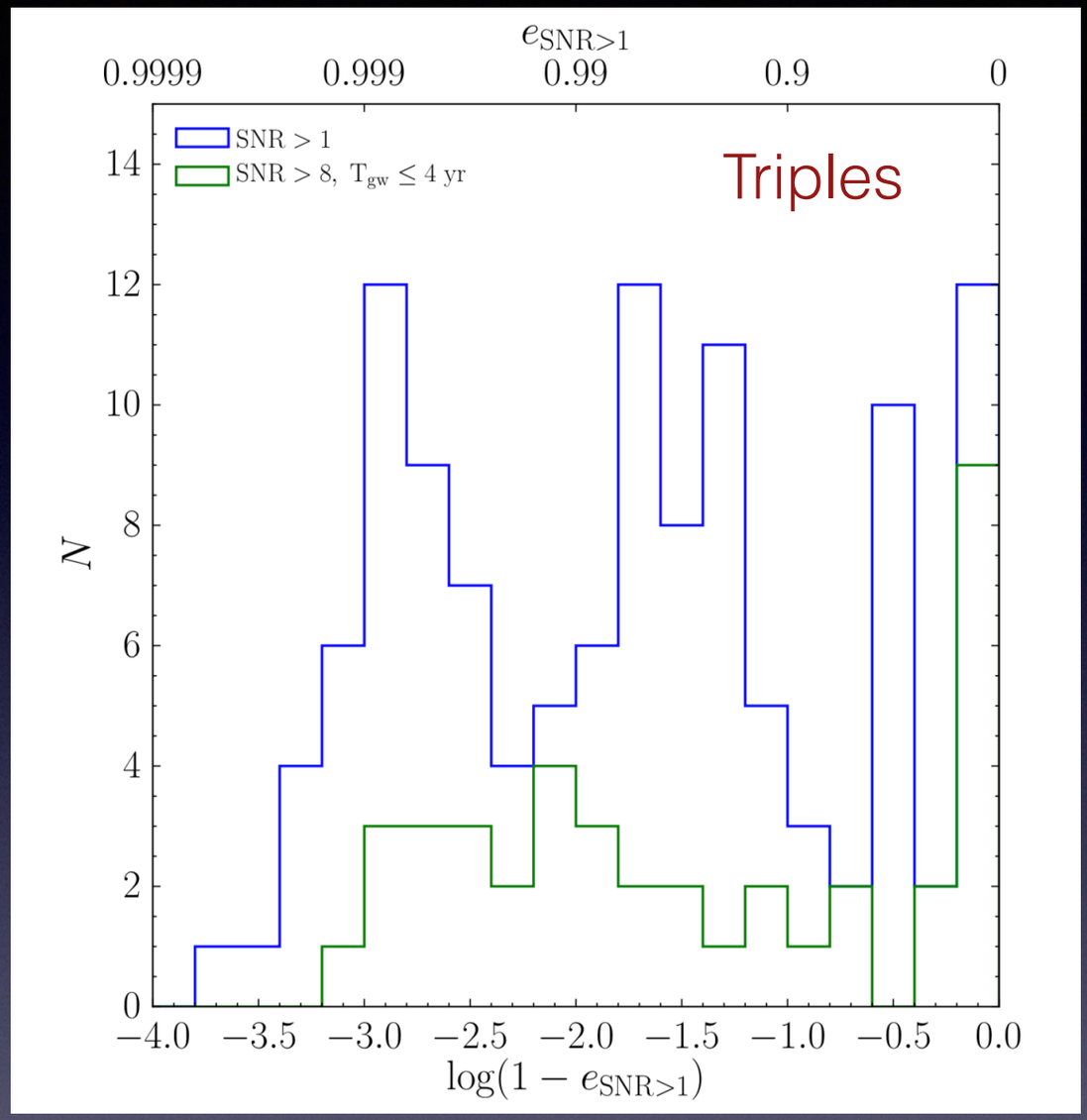

Bonetti, Sesana, EB & Haardt, in preparation

- Standard MBHB have small eccentricity by the time they get into band
- Triple driven systems can display eccentricities >0.99!
- Possibility to see eccentric non-merging sources (bursts)
- Possibility of an unresolved signal?

Multi-band gravitational-wave astronomy

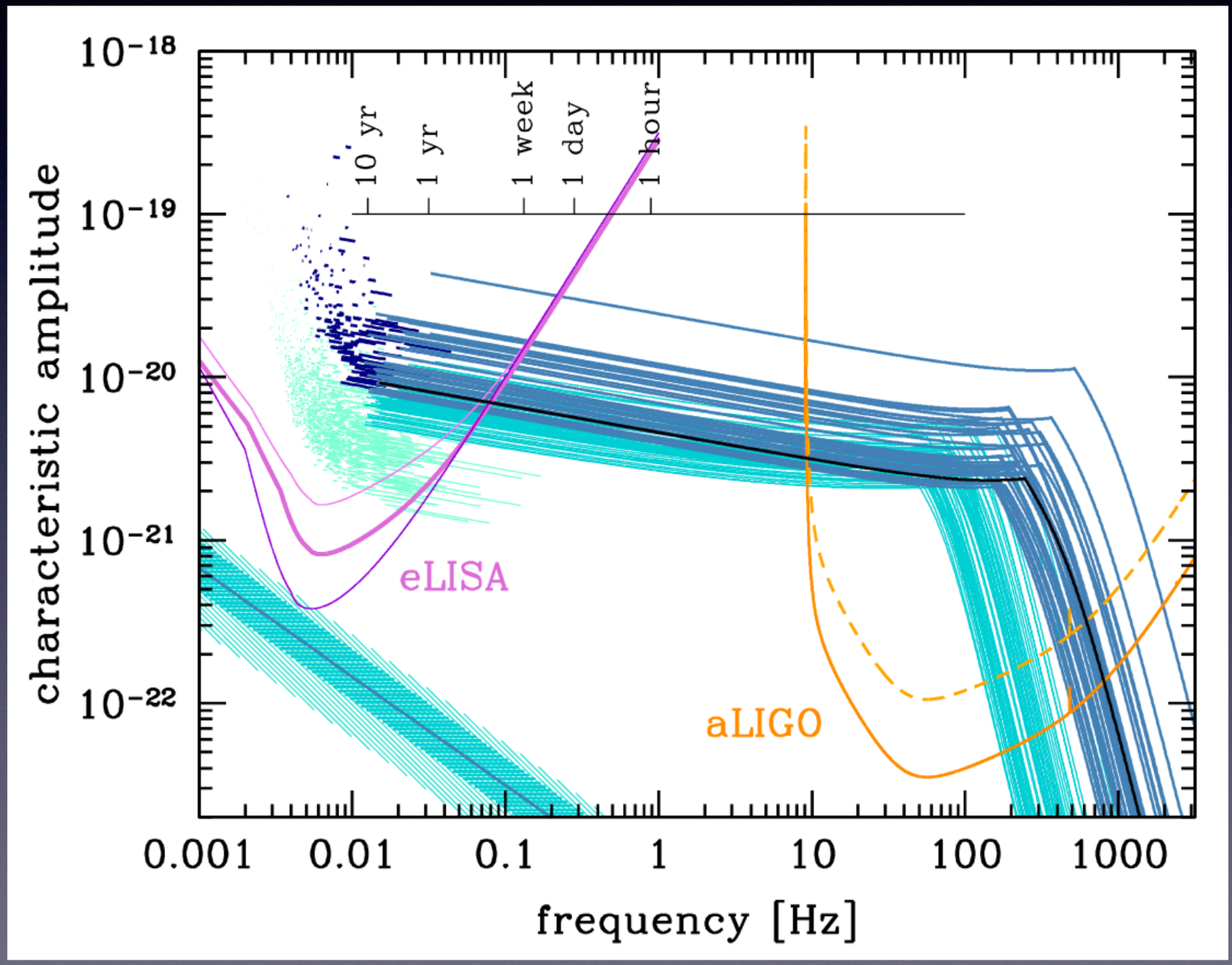

Sesana 2016

Multi-band gravitational-wave astronomy

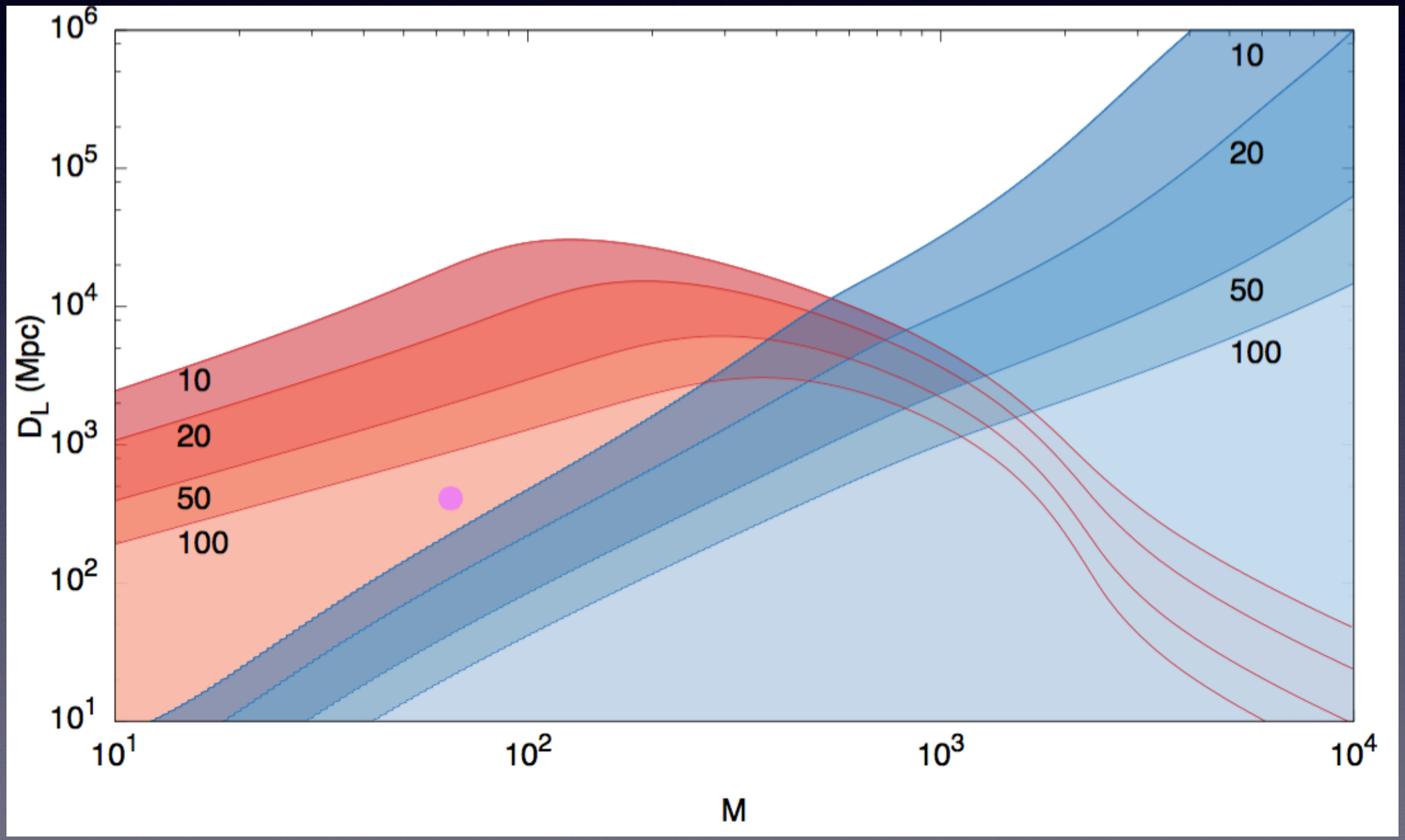

Tests of the equivalence principle with multi-band observations

- Smoking-gun sign of deviation from GR/BH "hairs" would be BH-BH dipole emission (-1PN term in phase/flux)

$$\dot{E}_{\rm GW} = \dot{E}_{\rm GR}\left[1 + B\left(\frac{Gm}{r_{12}c^2}\right)^{-1}\right]$$

- Pulsar constrain |B| $\lesssim 10^{-7}$, GW150914-like systems + LISA will constrain same dipole term in BH-BH systems to comparable accuracy

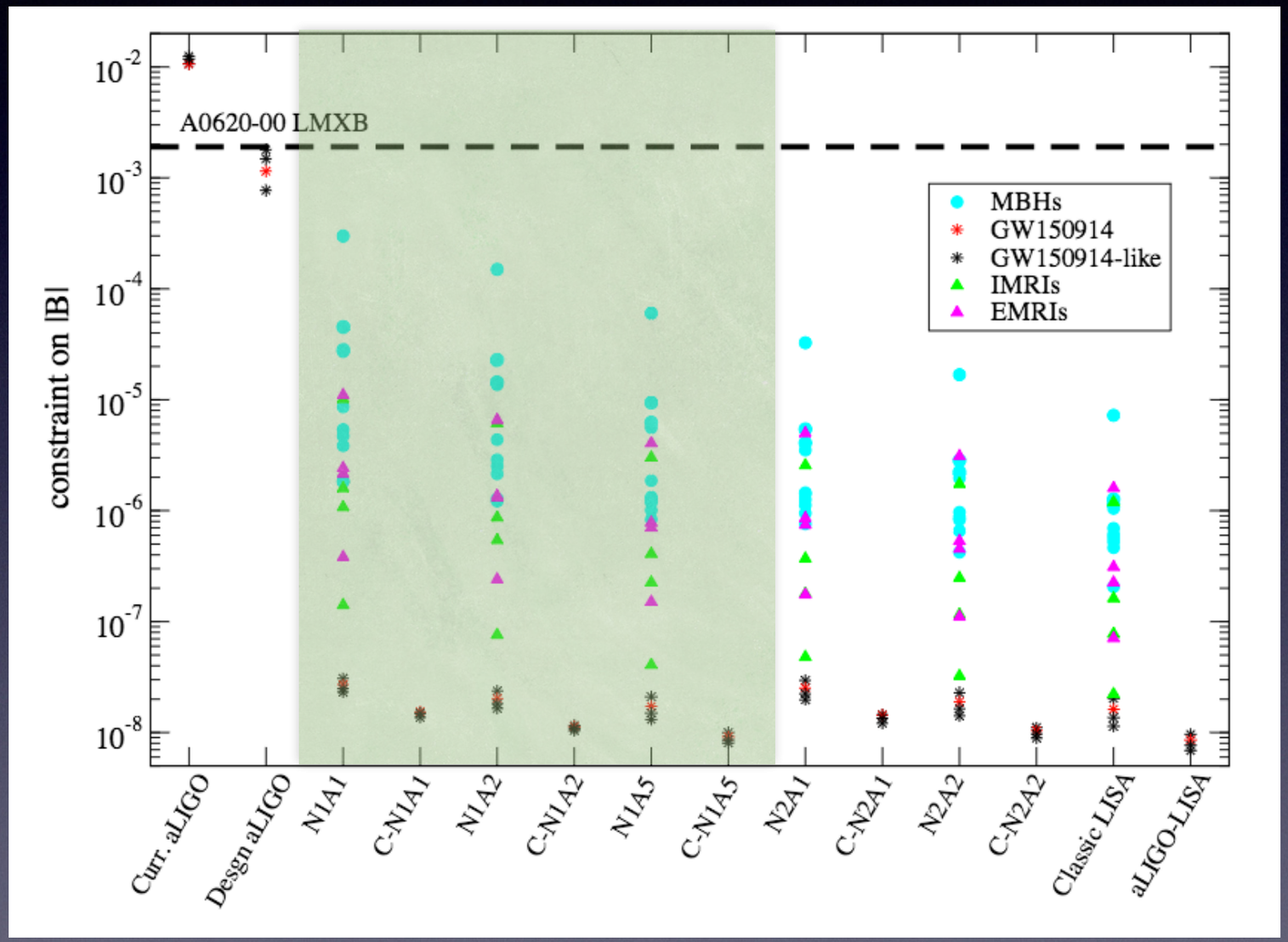

From EB, Yunes & Chamberlain 2016

Ringdown tests of the no-hair theorem

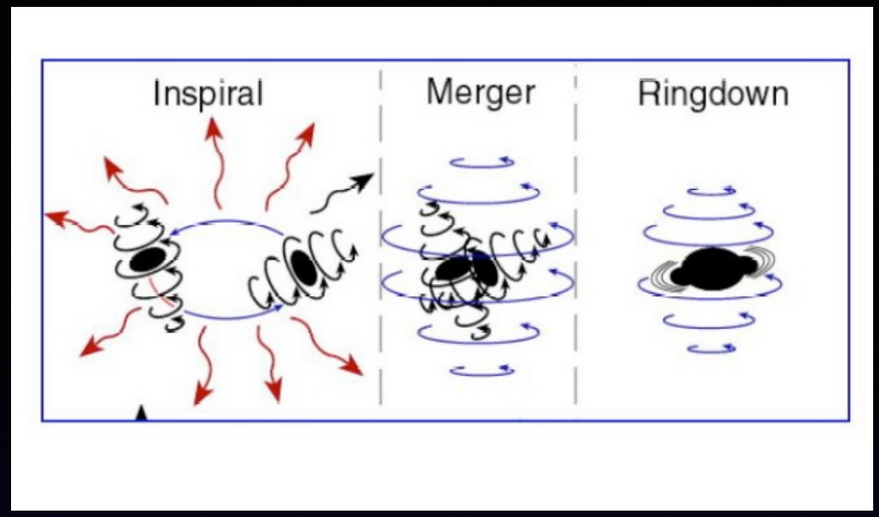

In GR, BHs have two hairs (mass and spin)

$$\omega_{\ell m} = \omega^{GR}_{\ell m}(M,J)(1+\delta\omega_{\ell m}) \qquad \tau_{\ell m} = \tau^{GR}_{\ell m}(M,J)(1+\delta\tau_{\ell m})$$

Tests impossible in ground-based detectors because little SNR in ringdown

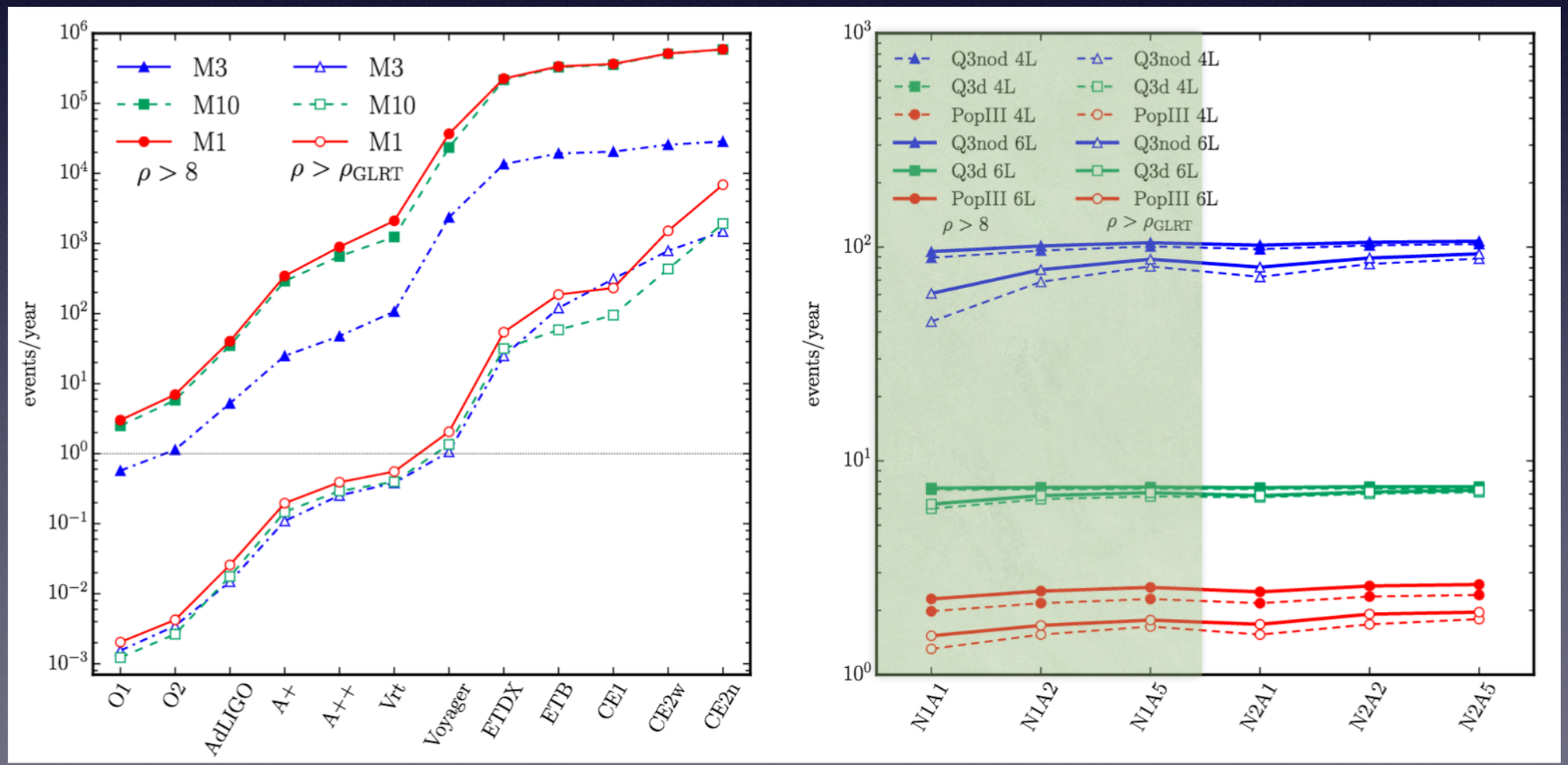

Berti, Sesana, EB, Cardoso, Belczynski, 2016

$$\rho_{\rm GLRT} \equiv \min(\rho^{2,3}_{\rm GLRT}, \rho^{2,4}_{\rm GLRT})$$

Bounds on BH mimickers

- Spinning objects (eg BHs) possess ergoregion, i.e. region where free falling observers cannot be static and need to coronate with BH due to frame dragging
- In ergoregion, negative energy modes can be produced but are confined within ergoregion (only positive energy modes can travel to infinity)
- By energy conservation, more and more negative energy modes can be produced, which would cause instability save for the existence of BH horizon (which acts as sink)
- BH mimickers with no horizon are unstable (ergoregion or super-radiance instability)

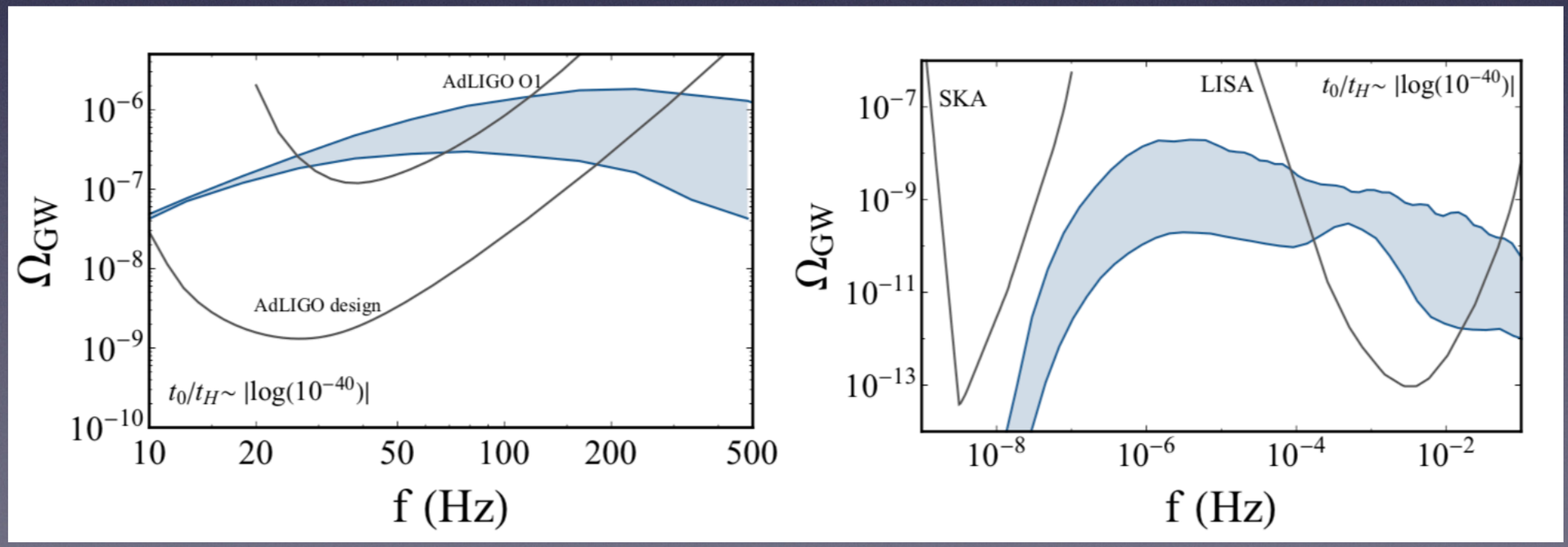

EB, Brito, Cardoso, Dvorkin, Pani 2018

Constraints on axions/fuzzy DM

- Isolated spinning BH + massive scalar fields with Compton wavelength comparable to event horizon radius are unstable under super-radiance
- Mass and (mostly) angular momentum are transferred from BH to scalar condensate surrounding BH on instability timescale; condensate then emits almost monochromatic waves on timescale
- Observable by LIGO/LISA as stochastic background and resolved sources

$$\tau_{\rm inst} \sim 0.07\,\chi^{-1}\left(\frac{M}{10\,M_\odot}\right)\left(\frac{0.1}{M\mu}\right)^{9}\ {\rm yr}\,,$$

$$\tau_{\rm GW} \sim 6\times 10^{4}\,\chi^{-1}\left(\frac{M}{10\,M_\odot}\right)\left(\frac{0.1}{M\mu}\right)^{15}\ {\rm yr}\,.$$

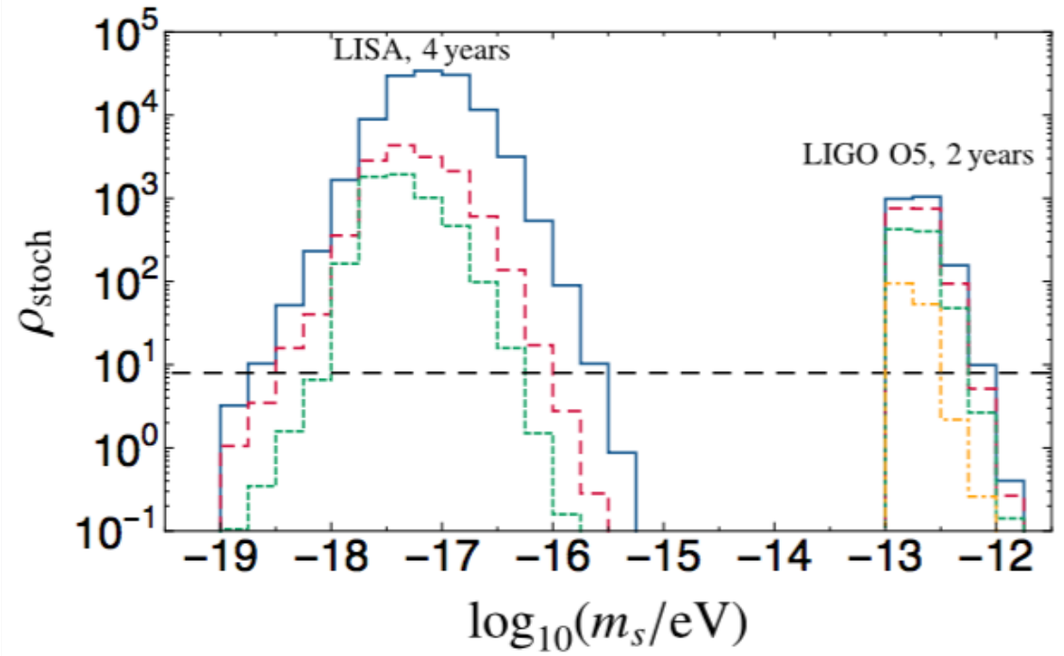

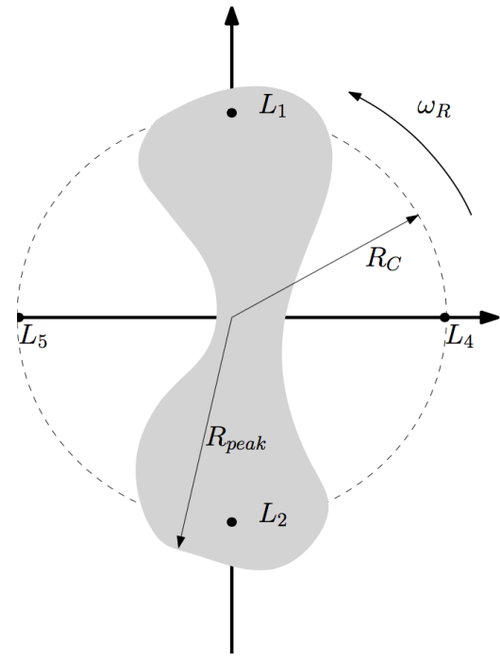

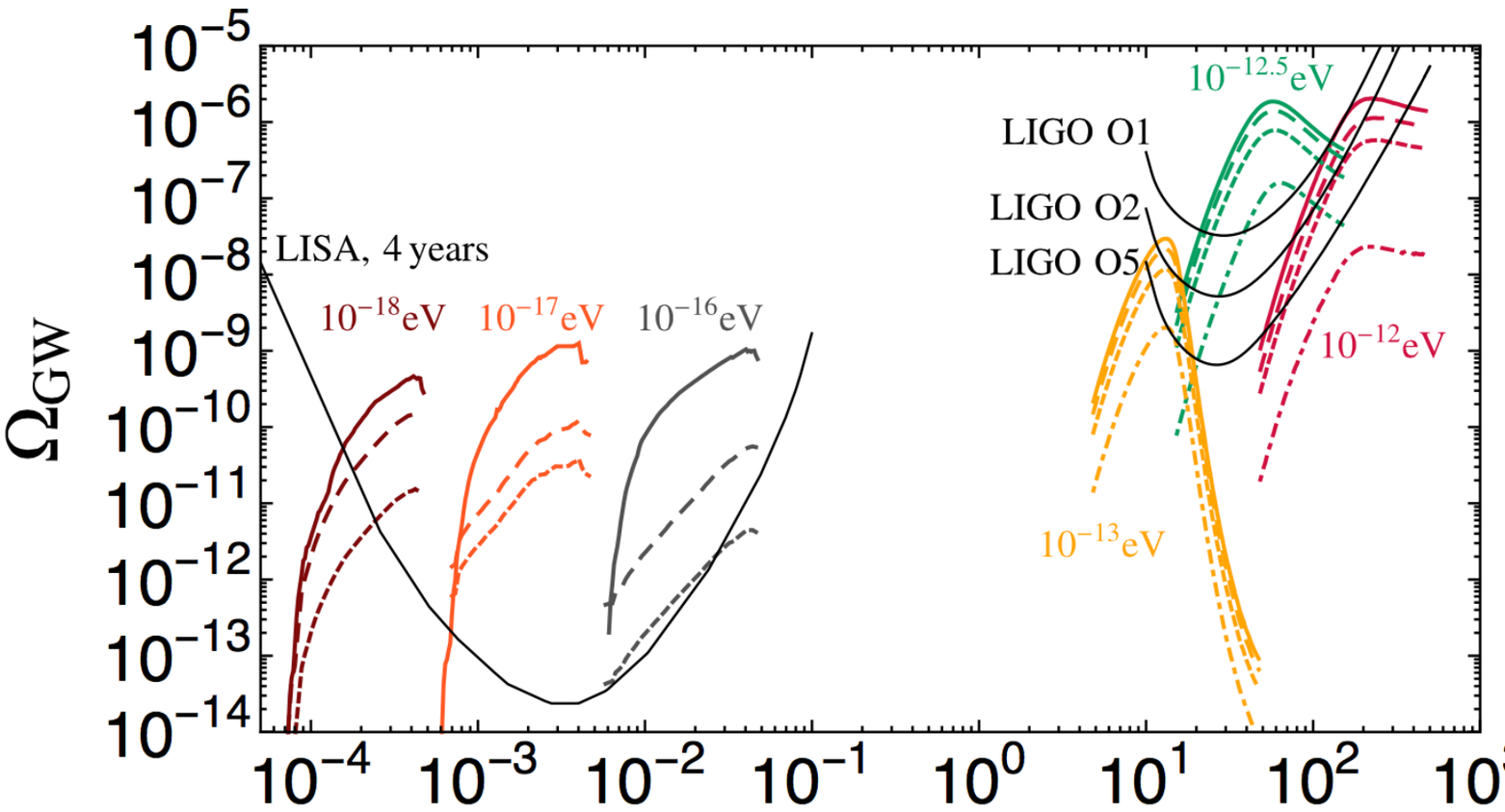

Brito, Ghosh, EB et al, PRL+PRD 2017

https://signup.lisamission.org/

The LISA Data Challenge and the enchilada problem

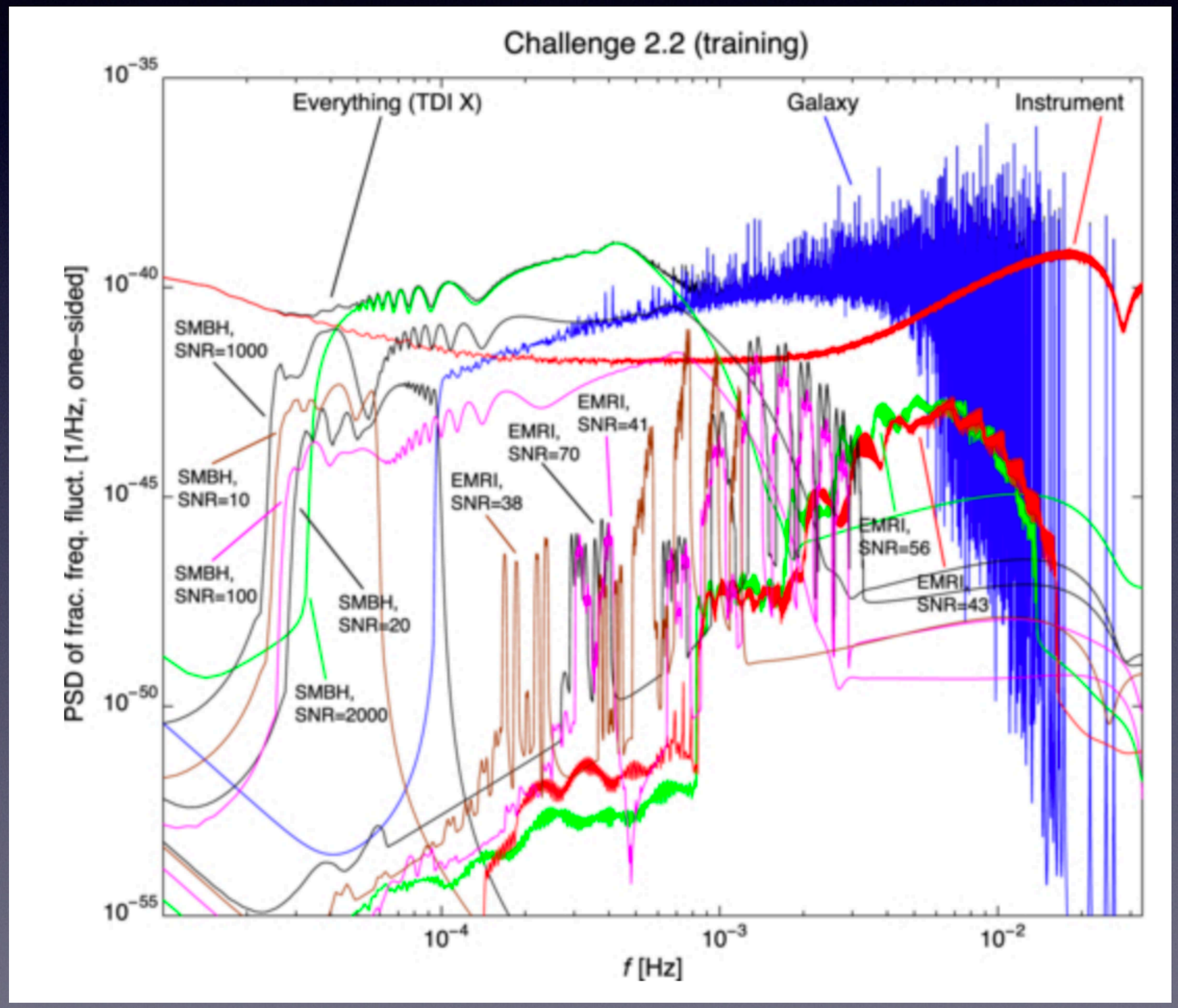

Conclusion

Gravitational waves have opened a new window on the Universe, and the LIGO detection is just the beginning…

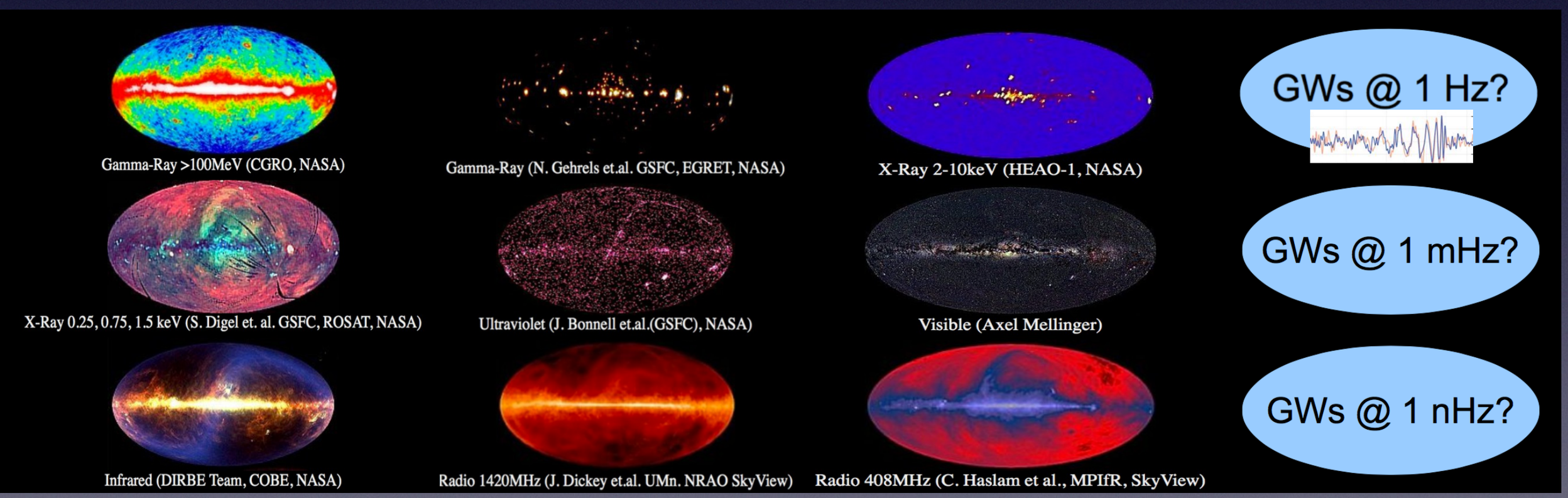

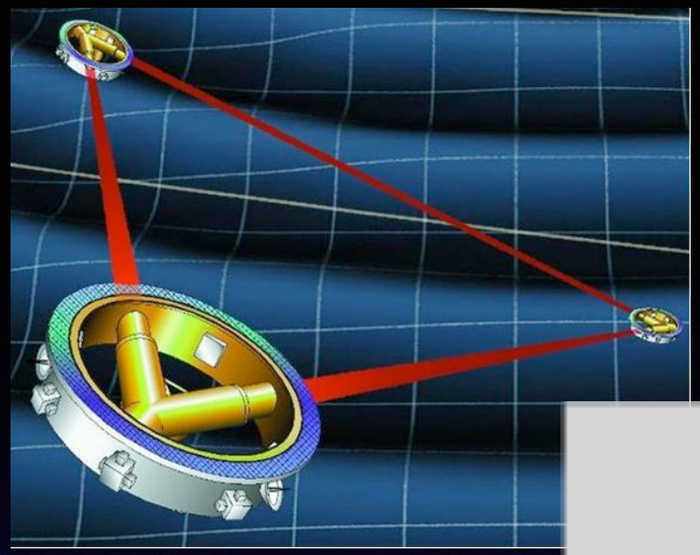

STAY TUNED!


Green Bank Telescope, WV, US
Arecibo Observatory, PR, US
LOFAR, Exloo, Netherlands
Parkes Observatory, Parkes, Australia
GMRT, Pune, India
WSRT, Westerbork, Netherlands
Effelsberg 100-m Radio Telescope, Effelsberg, Germany